# The Effects of IgA Deficiency and Maternal Dysbiosis on Type I Diabetes Incidence

by Erin Strachan

A thesis submitted in partial fulfillment of the requirements for the degree of

Master of Science

in

Immunology

Department of Medical Microbiology and Immunology

University of Alberta

## Abstract

There is a growing appreciation for the role of gastrointestinal (GI) health in promoting whole body wellbeing. Key features of a healthy gut include a balanced microbiota and their interaction with host immune defense mechanisms such as the production of Immunoglobulin A (IgA). Synergistically, the microbiota and IgA work to preserve the integrity of the gut barrier and regulate immune responses both locally and systemically. During infancy, both the microbiota and immune system undergo rapid development and are strongly influenced by maternal factors, conveyed largely via events in the neonatal GI tract. When these events fail to occur at appropriate times, the long term detrimental effects resulting from suboptimal immune development can contribute to subsequent development of pathologies such as Type 1 Diabetes (T1D), where the erroneous activation of autoreactive lymphocytes leads to the destruction of the pancreatic beta cells. Despite the well-documented importance of maternal factors on infant immune development, whether maternal immune dysregulation and dysbiosis can perpetuate the same in offspring remains largely unknown. To gain an understanding of how these maternal factors impact infant disease development, I used IgA-deficiency induced maternal dysbiosis in Non-Obese Diabetic (NOD) dams to study T1D development in their offspring. I found that maternal dysbiosis arising from IgA deficiency results in numerous neonatal changes in IgA-sufficient offspring, including increased GI immune cell numbers and cytokine production, increased gut inflammation, altered gut microbiome composition and a modified GI metabolomic profile. In adulthood, IgA-sufficient offspring born to IgA-deficient dams show lessened insulitis and a lower incidence of T1D overall as compared to those reared by IgA-sufficient dams. Cross-fostering experiments indicate this protective effect is mediated post-natally, leading me to hypothesize that maternal microbiome transfer plays a

significant role. I am currently exploring various characteristics of breast milk from IgA-deficient dams as well as conducting fecal microbiota transfer experiments to explore how this protective effect may be mediated.

## Preface

This thesis is composed of original work by Erin Strachan. The introduction contains work published in Strachan E, Clemente-Casares X, Tsai S. Maternal provisions in type 1 diabetes: Evidence for both protective & pathogenic potential. *Frontiers in Immunology*. 2023;14.

Analysis of microbiome data was performed with the help of Dr. Tingting Ju (laboratory of Dr. Ben Willing) in the Faculty of Agricultural, Life and Environmental Sciences at the University of Alberta. Metabolomic analysis of fecal samples was conducted by The Metabolomics Innovation Center (TMIC) at the University of Alberta Chemistry Department. Proteomic analysis of milk samples was conducted by Henry Wang in the laboratory of Dr. Julien Olivier, Department of Biochemistry at the University of Alberta.

The research project, of which this thesis is a part, received research ethics approval from the University of Alberta Research Ethics Board, Project Name “T1D Gut Study”, No. AUP00003665, approved October 6, 2020.

## Acknowledgements

This thesis is the culmination of three years of graduate student work built upon a lifetime of dreaming. Not many people get a second chance at pursuing higher education once they've chosen an alternate path in life. I am one of the fortunate, one who has been given the opportunity to pursue a dream while enjoying the blessings that come from having chosen the alternate path. Indeed, this opportunity has become a reality because of my family.

Scott, without your supportive attitude and your willingness to share me with science, this would not have been a possibility. You have continually and without complaint stepped up to fill both parental roles, all the while supporting this endeavor financially. Thank you.

To my kids, who have continued to live their lives and pursue their goals despite having only a part-time mom, you have excelled these past few years without a lot of help from me, and I am proud of you all for your independence, your perseverance and your selflessness.

To my Mom and Dad, thank you for your mental and practical support. You've listened to more scientific presentations than anyone should have to, fed my kids more meals than I can count, and lent me your vehicle more times than I care to admit. A thank you to my in-laws, who have offered support in the form of pizza & movie nights, summer baby-sitting and a place to crash on long days. Thank you to you all for encouraging me to take this journey.

Thank you to my supervisor, Sue, for your patience and guidance throughout this project. Thank you for taking a chance on me three years ago, when I contacted you out of the blue as a potential volunteer, then again two months later when you agreed to take me as a student. Your optimistic, encouraging nature makes the lab a good place to be.

My labmates have been a large part of the joy of these past three years. Thank you for the lunches and coffee dates that I've enjoyed so much, for the conversations and complaining sessions that always feel so necessary, and for making 'work' feel a lot more like a second home.

Finally, I am thankful to a Heavenly Father who has walked each and every day alongside me. I am grateful for the ups and the downs of this journey, always knowing I walk on a solid foundation.

# Table of Contents

**Abstract** ..... ii

**Preface** ..... iv

**Acknowledgement** ..... v

**List of Tables** ..... x

**List of Figures** ..... xi

**List of Abbreviations** ..... xii

**Chapter 1: Introduction** ..... 1

**1.1 T1D, an autoimmune disease** ..... 1

**1.1.1** T1D, in the world and in the clinic ..... 1

**1.1.2** Pathophysiology of T1D ..... 3

**1.1.3** Experimental models of T1D ..... 4

**1.2 Determinants of T1D** ..... 5

**1.2.1** Genetic determinants ..... 6

**1.2.2** Environmental determinants ..... 6

**1.2.3** Maternal factors in familial T1D ..... 7

**1.3 GI Involvement in T1D** ..... 8

**1.3.1** Microbiome & dysbiosis ..... 8

**1.3.2** IgA in gut immunity & homeostasis ..... 10

**1.4 Neonatal Immune Development** ..... 12

**1.4.1** Weaning reaction & immune regulation ..... 13

**1.4.2** Contributions of the microbiota ..... 14

**1.4.3** Maternal contributions ..... 15

**1.5 Theories of T1D onset** ..... 18

**1.6 Hypotheses & study objectives** ..... 23

**Chapter 2: Study Design, Methods & Materials** ..... 25

**2.1 Generation of the NOD.IgA colony** ..... 25

**2.1.1** Introduction of IgA KO allele ..... 25

**2.1.2** Breeding schemes ..... 27

**2.2 Methods & materials** ..... 31

**2.2.1** Mating, weaning & fostering ..... 31

**2.2.2** Disease monitoring ..... 31

**2.2.3** Collection and processing of tissue and blood ..... 31

**2.2.4** ELISA ..... 33

**2.2.5** Gut permeability assays ..... 33

**2.2.6** Quantitative PCR (qPCR) ..... 33

**2.2.7** Histology & scoring of pancreata ..... 34

**2.2.8** Histology & scoring of bowel sections ..... 35

**2.2.9** Microbiota analysis ..... 36

**2.2.10** Metabolomic analysis ..... 36

**2.2.11** Breast milk collection & proteomic analysis ..... 36

**2.2.12** Breast milk antibody specificity assays ..... 37

**2.2.13** FMT procedure ..... 38

**2.2.14** Tables of antibodies, reagents & software ..... 39

**Chapter 3: Results – Characterization of the Novel NOD.IgA Mouse Strain** ..... 43

**3.1 Introduction** ..... 43

**3.2 Results** ..... 44

**3.2.1** Effect of IgA deficiency on T1D incidence ..... 44

**3.2.1.1** T1D incidence is largely unaffected by IgA deficiency ..... 44

**3.2.2** Exploring early and later life immunity in the novel IgA-deficient NOD strain ..... 47

**3.2.2.1** NOD.IgA HET and KO animals exhibit heightened GI immunity ..... 47

**3.2.2.2** Gut permeability is delayed in NOD.IgA HET and KO cohorts ..... 54

**3.2.2.3** Serum immunoglobulin levels indicate both disease- and genotype-dependent systemic humoral responses ..... 58

**3.2.3** Exploring the effect of IgA deficiency on the NOD microbiome ..... 62

**3.2.3.1** IgA deficiency affects the presence of specific members of the early microbiome 62

**3.3 Discussion** ..... 67

**Chapter 4: Results – Maternal Dysbiosis as an Influencer of Disease in Offspring** ..... 70

**4.1 Introduction** ..... 70

**4.2 Results** ..... 71

**4.2.1** Effect of maternal IgA deficiency on T1D incidence in offspring ..... 71

**4.2.1.1** Maternal IgA deficiency alters disease susceptibility in the next generation ..... 71

**4.2.2** Maternal IgA deficiency-induced microbiome changes in IgA-sufficient offspring ..... 74

**4.2.2.1** Multi-generational IgA deficiency promotes a highly diverse microbiome ..... 74

**4.2.2.2** Early microbiome composition is heavily influenced by maternal IgA status ..... 78

**4.2.2.3** Maternal IgA deficiency contributes to an altered metabolome in offspring ..... 84

**4.2.3** Early life immunity in NOD.IgA HET offspring from IgA-sufficient and -deficient dams ..... 89

**4.2.3.1** Maternal IgA deficiency yields offspring with signs of increased gut inflammation early in life ..... 89

**4.2.3.2** Offspring of IgA-deficient dams show evidence of a stronger weaning reaction . 92

**4.2.3.3** Maternal IgA deficiency promotes a heightened systemic immune response at weaning with no evidence of islet autoimmunity ..... 100

**4.2.4** Effects of maternal IgA deficiency on adult NOD.IgA HET immunity & disease pathogenesis ..... 103

**4.2.4.1** Maternal IgA deficiency leads to elevated systemic and GI antibody responses in adulthood ..... 103

**4.2.4.2** Maternal IgA deficiency regulates gut barrier function later in life ..... 106

**4.2.4.3** Offspring of IgA-deficient dams exhibit signs of reduced autoimmunity at 12 weeks ..... 110

**4.2.5** Postnatal Maternal Influences ..... 114

**4.2.5.1** Heightened disease susceptibility in offspring of IgA-sufficient dams is attenuated by fostering to IgA-deficient dams ..... 114

**4.2.5.2** IgA-deficient dams compensate for loss of breast milk IgA with increased levels of IgG and IgM ..... 117

**4.2.5.3** Breast milk from IgA-sufficient and -deficient dams differ substantially in protein composition ..... 118

**4.3 Discussion** ..... 124

**Chapter 5: Discussion, Conclusion & Future work** ..... 127

**5.1 Discussion** ..... 127

**5.2 Future work** ..... 130

**5.2.1** Continuing cross-fostering experiments ..... 130

**5.2.2** Maternal microbiome manipulation (Fecal Microbiota Transfer) ..... 131

**5.2.3** Further exploration of breast milk ..... 132

**5.3 Conclusion** ..... 133

**Bibliography** ..... 136

## List of Tables

**Table 2.1** List of antibodies for flow cytometry ..... 39

**Table 2.2** List of reagents ..... 40

**Table 2.3** List of commercial kits ..... 41

**Table 2.4** List of hardware & software ..... 42

**Table 4.2.3.2** Immune cell population comparisons in NOD.IgA HET cohorts ..... 95

## List of Figures

**Figure 1.5** Proposed mechanisms of autoimmune activation leading to insulitis ..... 22

**Figure 2.1.1** Introduction of IgA knockout allele to the immunoglobulin heavy chain gene ..... 26

**Figure 2.1.2** Breeding schemes used to generate experimental NOD.IgA mice ..... 29

**Figure 3.2.1.1** Incidence of T1D in the novel NOD.IgA colony ..... 46

**Figure 3.2.2.1** GI immune responses in the NOD.IgA colony ..... 51

**Figure 3.2.2.2** Gut permeability in the NOD.IgA colony ..... 56

**Figure 3.2.2.3** Serum antibody levels in pre-diabetic and diabetic animals in the NOD.IgA colony ..... 60

**Figure 3.2.3.1** Analysis of the early microbiota in NOD.IgA WT, HET & KO mice ..... 65

**Figure 4.2.1.1** Incidence of T1D in offspring from IgA-sufficient vs -deficient dams ..... 73

**Figure 4.2.2.1** Microbiome analysis of NOD and NOD.IgA KO adult females ..... 76

**Figure 4.2.2.2** Microbiome analysis of NOD.IgA HET cohorts ..... 80

**Figure 4.2.2.3** Metabolomic profile comparison between NOD.IgA HET cohorts ..... 87

**Figure 4.2.3.1** GI immune responses in NOD.IgA HET cohorts at 5 weeks of age ..... 91

**Figure 4.2.3.2** GI Immune cell population in NOD.IgA HET cohorts at 3-4 weeks of age ..... 97

**Figure 4.2.3.3** Non-GI immunity in NOD.IgA HET cohorts in early life ..... 102

**Figure 4.2.4.1** Serum and fecal antibody levels in adult NOD.IgA HET mice ..... 105

**Figure 4.2.4.2** Gut barrier properties in adult NOD.IgA HET mice ..... 108

**Figure 4.2.4.3** Insulitis and PLN T cell populations in 12 week NOD.IgA HET cohorts ..... 112

**Figure 4.2.5.1** T1D incidence in IgA-sufficient offspring fostered at birth ..... 116

**Figure 4.2.5.2** Antibody concentrations in breast milk from NOD & NOD.IgA KO dams ..... 118

**Figure 4.2.5.3** Protein composition of breast milk from NOD & NOD.IgA KO dams ..... 122

**Figure 5.3** The effects of maternal IgA deficiency on T1D incidence in offspring ..... 132

## List of Abbreviations

| | |
|---|---|
| AA | Autoantibodies |
| Ab-Ag | Antibody-antigen complex |
| ACUC | Animal Care and Use Committee |
| AhR | Aryl hydrocarbon receptor |
| AID | Activation induced cytidine deaminase |
| APC | Antigen presenting cells |
| APRIL | A proliferation inducing ligand |
| ASA | American Diabetes Association |
| BAFF | B cell activating factor |
| BBDP | Biobreeding diabetes-prone rats |
| CCAC | Canadian Council for Animal Care |
| CD5L | CD5 antigen-like |
| CXCL17 | Chemokine (C-X-C motif) ligand 17 |
| DC | Dendritic cells |
| EGF | Epidermal growth factor |
| ELISA | Enzyme linked immunosorbent assay |
| Fab | Fragment, antigen-binding |
| FcRn | Neonatal Fc receptor |
| $F^{KO}$ mIgA+ HET | NOD.IgA HET offspring born to NOD dam, fostered to NOD.IgA KO dam |
| $F^{WT}$ mIgA- HET | NOD.IgA HET offspring born to NOD.IgA KO dam, fostered to NOD dam |
| GAD | Glutamic acid decarboxylase |
| GAPs | Goblet cell associated antigen passages |
| GC | Germinal center |
| GI | Gastrointestinal |

| | |
|---|---|
| IA-2 | Tyrosine phosphatase-related insulinoma-associated 2 molecule |
| IDDM | Insulin dependent diabetes mellitus |
| IEC | Intestinal epithelial cells |
| IGRP | Islet-specific glucose-6-phosphatase catalytic subunit-related protein |
| IL- | Interleukin- |
| ILF | Isolated lymphoid follicles |
| INS-VNTR | Insulin gene variable number of tandem repeats |
| JDRF | Juvenile Diabetes Research Foundation |
| Lcn-2 | Lipocalin-2 |
| LPS | Lipopolysaccharide |
| M cells | Microfold cells |
| MDGF | Myeloid-derived growth factor |
| MFI | Mean fluorescence intensity |
| MHC I | Major histocompatiblity complex class I |
| mIgA- HET | NOD.IgA HET progeny from NOD.IgA KO dams |
| mIgA+ HET | NOD.IgA HET progeny from NOD WT dams |
| MLN | MMesenteric lymph node |
| NK | Natural Killer cell |
| NOD | Non-obese diabetic mouse |
| NOD.IgA HET | Non-obese diabetic mouse, heterozygous for functional alpha constant region |
| NOD.IgA KO | Non-obese diabetic mouse, negative for functional alpha constant region |
| NOD.IgA WT | Non-obese diabetic mouse, wild type for functional alpha constant region |
| PC | Plasma cell |
| pIgR | Polymeric Ig Receptor |
| PLN | Pancreatic lymph node |

| | |
|---|---|
| PP | Peyer's patches |
| PRR | Pattern recognition receptors |
| PCA | Principal component analysis |
| qPCR | Quantitative polymerase chain reaction |
| SC | Secretory component |
| SCFA | Short chain fatty acids |
| sIgA | Secretory immunoglobulin A |
| SPF | Specific pathogen free |
| T1D | Type I Diabetes |
| $T_{fh}$ | Follicular helper T lymphocytes |
| TGFβ | Tumor growth factor β |
| TRA | Tissue restricted antigen |
| Treg | Regulatory T lymphocytes |
| TRIGR | Trial to Reduce IDDM in the Genetically At Risk |
| ZnT8 | Zinc transporter 8 |

# Chapter 1: Introduction

Immunity is a balancing act that relies on accurate assessment and precise management of contrasting, often opposing factors. The effectiveness of our immune system is contingent on its ability to assess a threat correctly, respond appropriately, and resolve the threat without undue harm to the host. Thus, poor immune regulation leaves an individual vulnerable to self-mediated destruction. During development, T and B lymphocytes are subjected first to the process of central tolerance followed by tight regulation via various mechanisms of peripheral tolerance. Errors and malfunctions in tolerance education and regulation can give rise to autoimmune diseases, as is the case with Type 1 diabetes (T1D). Research over the last decades has expanded our understanding of the various events involved in onset and pathogenesis of T1D. Furthermore, it has illuminated the numerous factors contributing to disease, among them genetic, environmental, dietary and microbiome contributions, as well as early life events and conditions.

## 1.1 T1D, an autoimmune disease

Given the complexities of immune development and regulation, errors and malfunctions can give rise to a myriad of autoimmune diseases, such as T1D. T1D arises due to defective tolerance that culminates in the inappropriate activation of self-reactive lymphocytes that attack the insulin producing beta cells of the pancreas. Symptoms of T1D are varied and often go undetected until the beta cells have been destroyed, leaving the individual without the capacity to produce insulin and regulate blood sugar levels. The bulk of the beta cell damage is carried out by autoreactive $CD8^+$ T lymphocytes with help from immune populations of both lymphoid and myeloid lineage[1]. Research over the last decades has led to an improved understanding of the various factors involved in onset and pathogenesis of T1D and has helped uncover many of the predisposing events and elements that contribute to one's susceptibility to the disease.

### 1.1.1 T1D, in the world and in the clinic

Though the prevalence of T1D varies between geographical regions, there is no evidence of any country or people group left untouched by the disease. Putting an absolute figure on the number of people affected has been problematic for various reasons, but recent estimates

suggest 8.42 million individuals suffer from T1D worldwide[2]. Historically, T1D has largely been considered a disease diagnosed during childhood or adolescence, but the most recent figures indicate that this may be changing. Indeed, the mean age at diagnosis is 32 years of age, and 62% of new diagnoses occur in individuals over 20 years of age. T1D does still affect the young, however, with a substantial peak in disease incidence in children aged 10-14 years. Geographically, North America encompasses the region of highest incidence, while south and east Asia show lowest incidence[2]. Interestingly, an individual endemic to regions of low incidence has a marginally increased risk of T1D upon emigrating to a region of higher incidence, and children born to immigrant parents largely assume the disease risk of their country of birth[3]. Thus, the disease risk is a sum of both genetic and environmental factors, which will be discussed in further detail in Section 1.2.

Working together, the Juvenile Diabetes Research Foundation (JDRF), American Diabetes Association (ASA) and the Endocrine Society have developed a staging classification system for T1D progression and diagnosis[4]. This system reflects both the heterogeneity of disease progression as well as some of the key pathologies driving the disease. One of the earliest detectable signs of pre-clinical disease is the presence of circulating autoantibodies (AA), commonly those reactive to insulin, glutamic acid decarboxylase (GAD), zinc transporter 8 (ZnT8) and tyrosine phosphatase-related insulinoma-associated 2 molecule (IA-2)[5,6]. Despite their prevalence, the role of these AA in disease pathogenesis is largely unknown[7]. Stage 1 is defined by the presence of two or more AA in the blood, indicating autoimmunity has developed, but blood sugar levels remain normal. An individual advances from Stage 1 to Stage 2 when blood sugar levels become dysregulated, detected as elevated glucose levels, either after fasting (110-125 mg/dL) or following an oral glucose tolerance test. Pathologically, this is indicative of beta cell dysfunction although the individual is still considered asymptomatic. Within five years, 75% of individuals at Stage 2 will progress to Stage 3, characterized by the presentation of various symptoms including persistent blood sugar dysregulation, weight loss, fatigue, glucose in the urine (glucosuria), excessive urination (polyuria), and excessive thirst (polydipsia). By Stage 3, an individual is insulin dependent and clinically diagnosed with T1D.

### 1.1.2 Pathophysiology of T1D

Despite the dominant role AA play in clinical detection of T1D, their role in disease progression and pathogenesis remains a topic of debate. They are certainly one of the early signs indicating the development of autoimmunity, but they are dispensable for development of the disease and the presence of a single AA yields only low probability of progressing to T1D[7]. Rather, it may be autoreactive B cells themselves, apart from AA production, that promote disease onset or facilitate islet damage, as B cell depletion therapy was shown to delay T1D progression in patients[8]. Moreover, it is $CD8^+$ T lymphocytes that are the primary culprits of the immune-mediated damage to beta cells, aided by autoreactive $CD4^+$ T lymphocytes. These autoreactive T lymphocytes can be detected in circulation in low numbers, but are found in considerable proportions in pancreatic lesions of patients[9,10] and, when recovered from patient tissue, show capabilities of beta cell killing *ex vivo*[11]. Furthermore, pancreatic lesions frequently show infiltration by B lymphocytes, Natural Killer (NK) cells and macrophages[3,12], reflecting the cooperative nature of immunity. Somewhat surprisingly, the detection of autoreactive $CD4^+$ and $CD8^+$ T lymphocytes is not uncommon in healthy individuals without circulating AA[12], but those identified in T1D patients tend to be enriched for activated and memory phenotypes[3].

The antigens recognized by autoreactive T lymphocytes vary between individuals, and frequently show some diversity from those bound by AA. Some autoantigens are peptides from unmodified, tissue specific proteins such as insulin and islet-specific glucose-6-phosphatase catalytic subunit-related protein (IGRP). There is also evidence of autoantigens arising from post-translationally modified proteins, or erroneously-produced fusion peptides, possibly as a result of beta cell stress[3]. Moreover, beta cells from patients have been shown to be complicit in the immune-mediated destruction via hyper-expression of major histocompatibility complex class I (MHC I), allowing for robust presentation of antigen to infiltrating lymphocytes, and through localized type I interferon production[13].

The etiology and pathophysiology of T1D is complex, highly variant between individuals, and still not completely understood. It involves genetic predisposition, environmental influences, and life events thought to trigger autoimmune initiation, all topics which will be discussed in more detail in the following sections. Moreover, these complexities and persistent unknowns

underscore the need for animal models of T1D, where scientists can manipulate and control variables in an effort to answer specific questions and contribute to the understanding of a disease that spans the globe.

### 1.1.3 Experimental models of T1D

Several animal models are available to study T1D under controlled conditions and with measures too invasive for study on human patients. Most animal models utilize rodents, specifically rats and mice. Disease models can be broadly categorized as chemically-induced models, spontaneous (genetic) models, and virally-induced models. Generally speaking, the choice of model depends on what aspect of the disease one wants to study, and what stage of the disease is most relevant to the research question. In chemically-induced models, where disease processes begin at the point of chemical administration, one has the advantage of a controlled timeline, allowing for treatment comparisons at similar stages of disease progression. The disadvantages in these models are prominent, however, and include a lack of genetic contribution, non-immune mediated beta cell destruction, and an artificial mode of initiation. Some models of viral induction of T1D use viral infection, or immunization with viral protein, to initiate disease in transgenic animals expressing a viral protein in beta cells[14]. Others take advantage of viral infection of beta cells to induce pancreatic inflammation and initiate lymphocyte infiltration, while still others use an enteroviral infection to accelerate disease onset in diabetes-prone mice[14]. Each of these models mimics aspects of human disease thought to be triggers for autoimmune development or promoters of disease progression (see Section 1.5). Spontaneous models, though not perfect, most closely resemble human T1D. They rely on a disease-promoting genetic environment, allowing for similar immune and non-immune processes to progress disease following initiation of autoimmunity via similar trigger events.

Two spontaneous rat models have been used to study T1D over the last half century. Biobreeding diabetes-prone (BBDP) rats are a spontaneous model of T1D, where approximately 90% of male and female rats develop insulitis following puberty, leading to immune-mediated destruction of beta cells and overt diabetes from 8-16 weeks of age[15]. Many of the pathologies of human T1D are reflected in this model, including the hyper-expression of MHC I and enhanced IFNα production by beta cells[13]. One major drawback to this model is

an additional phenotype of lymphopenia from birth, marked by severely diminished numbers of $CD4^+$ T lymphocytes and almost no $CD8^+$ T lymphocytes. The LEW 1AR1/-iddm is a second strain of rat available for T1D study. Similar to the BBDP rat, this strain shows spontaneous development of disease with equivalent incidence between male and female animals, from 20%-60% depending on the degree of inbreeding. Early innate immune cell infiltration into islets is followed by T and B lymphocyte infiltration, mimicking insulitis development in human patients. These rats survive well following overt disease, making them an ideal model to study disease-related complications[15].

The most commonly used rodent model of T1D currently is the non-obese diabetic (NOD) mouse model[15,16]. This strain of mouse shares many commonalities with T1D in human patients, including the presence of a T1D genetic susceptibility locus encompassing the MHC region, located on chromosome 6 in humans and chromosome 17 in mice. Additionally, the two share several other non-MHC susceptibility genes. T1D in NOD mice have several autoantigens in common with the human disease, and they exhibit similar biomarkers such as the presence of circulating AA. Furthermore, symptoms such as hypoinsulinemia, hyperglycemia, glucosuria, polyurea and polydipsia are prominent in both NOD mice and human T1D patients. Pathologically, disease processes are similar, with islet infiltration by macrophages, dendritic cells (DC), NK cells, and B and T lymphocytes, followed by $CD8^+$ T lymphocyte-mediated damage to the beta cells. NOD mice exhibit insulitis approaching 100%, whereas human patients show infiltration of approximately 23%-33% of islets in the first year following diagnosis[3], making this a significant difference between disease in NOD mice vs humans. Another difference is the disease sex disparity observed in NOD colonies. Whereas human T1D preferentially affects males over females[17], NOD colonies show the opposite trend, with 70-90% of females and 40-60% of males affected[15]. Despite these two differences, the NOD mouse model has enabled a deeper understanding of many aspects of T1D and has allowed for the development and testing of numerous therapies that may one day make the current global epidemic of T1D a part of history.

### 1.2 Determinants of T1D

Much research has been devoted to the elucidation of factors that contribute to the development of T1D. Some are straightforward to study, such as the contribution of genetics.

Others are more subtle, requiring large study populations and a deep delve into the data. Interestingly, some of these factors show a dependency on one another and contribute increased risk only when present concurrently[18], making this a complicated but compelling area of study.

### 1.2.1 Genetic determinants

A child who has a first degree relative with T1D has a 10-fold higher risk of being diagnosed with the disease than does a child with no affected family member, evidence of a considerable genetic component of disease susceptibility[19]. Half of the known genetic disease association involves alleles of the MHC II genes. Studies have identified high risk haplotypes referred to as DR3-DQ2 (*DRB1*03:01-DQA1*05:01-DQB1*02:01*) and DR4-DQ8 (*DRB1*04-DQA1*03:01DQB1*03:02* ) that can increase the odds of a T1D diagnosis by 16-fold[20]. Conversely, some MHC II alleles confer protection. It has been shown that anti-diabetogenic MHC II alleles confer protective effects by presenting autoantigenic peptides in a way that promotes the thymic negative selection of diabetogenic T lymphocytes and by enhancing regulatory T lymphocyte (Treg) development and function[21–23]. Multiple additional genetic defects in immune pathways have been associated with T1D, including genes involved in immune cell activation, signalling, function, and regulation[24–26]. Insulin is commonly an autoantigen in T1D in both humans and mouse models, and certain aspects of the insulin gene are associated with either disease susceptibility or protection, including the insulin gene variable number of tandem repeats (INS-VNTR) minisatellite region. Certain VNTR alleles correlate with increased insulin mRNA expression in the thymus during gestational development and are thought to promote clonal deletion of insulin-reactive T lymphocytes[27]. Taken together, these findings provide support for the theory of impaired central tolerance and defective immune regulation as a driving force in T1D development.

### 1.2.2 Environmental determinants

With genetic factors accounting for only a fraction of T1D susceptibility[24,25,28] and a substantial rise in T1D prevalence that can't be explained by genetics alone, considerable effort has been put into exploring the non-genetic factors that play a role in modulating T1D development[19]. Numerous environmental factors have been elucidated, many of which involve

events occurring along the gastrointestinal (GI) tract. Broad spectrum antibiotic use during infancy and early childhood has been linked to increased incidence of T1D, with its modus operandi attributed to microbiome remodeling. Notably, this association is seen primarily among children delivered by cesarean section[29], another factor known to influence microbiome composition[30]. Additionally, maternal diet during pregnancy and breastfeeding, as well as age at which certain foods are introduced to the child have been shown to affect risk of developing T1D[19]. Other environmental factors include infections experienced by mom and/or child, most of which increase chances of T1D development[19,31], although there is evidence of protective effects being conferred by gestational respiratory infections[18]. Maternal gestational enteroviral infections, as well as those in the neonate, have been strongly correlated with T1D in various human studies[32]. Increased birth weight and childhood obesity have also been linked with increased T1D incidence later in life[31]. Considerable effort has been invested into determining how these various environmental factors influence disease susceptibility, and some of these findings will be discussed in further detail in the following sections.

### 1.2.3 Maternal factors in familial T1D

Studies on familial T1D have found that among children with a parent with T1D, those with an affected mother show up to 4-fold lower incidence of disease than those with an affected father[33–43] while few reports support the opposite[44]. The most thoroughly studied T1D-associated attribute shared between mom and babe is the transfer of maternal AA both during gestation and at birth. The German BABY-DIAB study[45] analyzed blood samples from more than 1000 children born to a parent with T1D. Of the children with affected fathers, all were negative for AA at birth. In contrast, >75% of the neonates born to affected mothers harbored circulating AA, which were deemed to be of maternal origin since they were of the same specificity and isotype as those detected in the mothers at delivery. Indeed, a consistent finding in many human studies is a positive correlation between maternal AA levels and those measured in cord blood or neonatal circulation at birth, indicating significant transplacental transfer of T1D-associated AA. Furthermore, most studies report the elimination of maternal AA by 9 months of age[5,44–46]. In the German BABY-DIAB study[45], only 12 children remained positive for T1D-associated AA by 2 years of age. Interestingly, these same 12 children had exhibited amongst the lowest cord blood AA levels at birth. The 'Trial to Reduce IDDM in the

Genetically At Risk' (TRIGR) study in Finland also noted a positive correlation between maternal and neonatal AA levels in their study of 74 T1D mothers and their newborns, although they found no evidence of induction of beta cell autoimmunity during fetal development[46]. Thus, in spite of significant AA transfer, a causal link between maternal AA and infant T1D development has not been established. Attempts to ascertain the effect of maternal AA transfer using animal models has yielded contradictory results[47,48].

The potential transfer of disease-associated maternal factors such as AA and autoreactive lymphocytes via breast milk has raised questions about the effects of breastfeeding a newborn when the mother is diabetic. Interestingly, the majority of studies looking at the effects of breastfeeding on T1D development support a protective role for long-term breastfeeding[49,50], although very few take into account the T1D status of the mother. Of those looking specifically at breastfeeding by affected mothers, we were unable to find any that supported a positive correlation between breastfeeding and disease development in offspring, and some evidence that supports an inverse relationship. The German BABY-DIAB study found no correlation between breastfeeding duration by affected mothers and AA levels in their infants[6], and reported a protective effect of breastfeeding for >3 months[33]. Because of the lack of evidence linking breastfeeding by affected mothers to any deleterious effects in their infants, exclusive breastfeeding remains the recommendation of most health authorities[51–53].

### 1.3 Gastrointestinal involvement in T1D

The changing epidemiology of T1D has been observed throughout the world, with an increasing incidence seen amongst individuals with low to moderate genetic risk. Many scientists view this as an indication that environmental determinants are more important in determining T1D susceptibility now than they have been historically[1]. The volume of studies exploring numerous aspects of environmental influences has expanded substantially over the last couple of decades, with many of the identified factors, life events and lifestyle determinants pointing to the involvement of the GI tract in T1D onset[31].

#### 1.3.1 The microbiome & dysbiosis

The intestinal microbiota is a facet that has been widely investigated for both its role and response to T1D onset and pathogenesis. Human studies, as well as animal models, have

consistently demonstrated changes in microbiome diversity, composition and activity in affected individuals both prior to and after diagnosis[54]. The microbiome plays a significant role in immune system activities, influencing immune responses both in the gut as well as throughout the body. This is particularly true during the neonatal period, when it has the capacity to influence immune education, development and regulation with lifelong impact. The generally accepted view is that babies are sterile *in utero* and encounter microorganisms for the first time during delivery. There are many factors that influence the microbial composition of an infant's microbiome for the first year of life, foremost among them mode of delivery and the receipt of breast milk[55], but generally by the age of 2-3 years the child's gut microbial community has stabilized and strongly resembles that of his or her mother. There is an amazing degree of bi-direction communication between the microbiota and intestinal immune cells occurring through a variety of mechanisms, including direct microbial recognition, production of microbial metabolites, and secretion of cytokines, chemokines and growth factors. Although there is no clear microbial 'signature' that has been linked to T1D, patients often exhibit deviations in their microbiota that distinguish them from healthy individuals, including increased microbial diversity and altered representation of certain microbial phyla[55–61]. Characteristics of a balanced microbiota include the ability to maintain an anti-inflammatory environment, inhibit the growth of pathogenic microorganisms in the gut lumen, promote sufficient gut barrier integrity, and impede the migration of microbes across the intestinal barrier. The production of short chain fatty acids (SCFA), especially butyrate, by the microbiota is a key contributor to these gut functions; butyrate is both an energy source for the intestinal epithelial cells (IEC) that make up the gut lining and a promoter of anti-inflammatory immune responses. Importantly, a decline in gut barrier function is frequently seen in individuals experiencing dysregulated immunity[62–65] and decreased abundance of butyrate-producing bacteria has been reported in children at various stages of T1D progression[56,59,60]. These findings support a model of disease initiation whereby dysbiosis leads to diminished gut barrier integrity, allowing for microbial translocation and thus promoting inflammatory responses both in the gut and systemically.

### 1.3.2 IgA in gut immunity & homeostasis

Of the numerous mechanisms employed by the host GI tract to maintain a balance between tolerance of foreign entities and protection against infection, the production and secretion of immunoglobulin A (IgA) is arguably one of the most complex. IgA is the most abundant antibody produced in the mammalian body and is found in serum, saliva, tears, breast milk and in the oral, GI, respiratory and genital-urinary mucosa. With the exception of serum IgA, secreted IgA is predominately found as a dimer and is referred to as secretory IgA (sIgA). The two monomers are linked via a J chain, which helps facilitate binding to the polymeric Ig Receptor (pIgR) expressed on IEC, allowing for its transport across the epithelial barrier. Once in the lumen, the sIgA molecule is cleaved from the pIgR such that a peptide fragment from the receptor, referred to as the secretory component (SC), remains covalently attached to the IgA dimer. The IgA monomer units, J chain and SC are all heavily glycosylated, helping to protect the molecule from proteolytic activity in the gut lumen and facilitating its adherence to the mucus layer[66,67].

In the GI tract, the journey from naive B lymphocyte to IgA-secreting plasma cell (PC) is complex and can proceed via numerous routes. The naive B lymphocyte can originate from either B1 or B2 lymphocyte pools, it can be activated via T-dependent or T-independent pathways, and activation can occur in a number of different lymphoid structures, or none at all. The canonical pathway of B lymphocyte activation occurs primarily in Peyer's Patches (PP), organized lymphoid structures underlying the epithelial barrier found predominantly in the small intestine. The process involves delivery of luminal antigen by Microfold (M) cells, found in the overlying epithelial tissue, to DC in the PP. The antigen is acquired by the B lymphocyte, and after direct interaction with PP T lymphocytes, the activated B lymphocyte undergoes somatic hypermutation and class switching in a germinal center (GC). This process of generating high affinity IgA-producing B lymphocytes requires tumor growth factor β (TGFβ)[68], interleukin (IL) -21, IL-6 and retinoic acid[69] expressed by various cell types in the gut[66,67].

Naive B lymphocytes along the GI tract can also undergo T-independent activation[70]. Generally, these are thought to be B1 cells that associate with DC and M cells in either isolated lymphoid follicles (ILF), another organized lymphoid structure found associated with

the epithelial layer, or possibly in the lamina propria itself . Although T lymphocytes are present, they do not interact directly with the B lymphocytes. Rather, activation occurs by interaction with luminal antigen in the presence of B cell activating factor (BAFF), TGFβ, and a proliferation inducing ligand (APRIL). The ability of these lymphocytes to class switch indicates expression of activation induced cytidine deaminase (AID), although the IgA antibodies produced remain of low affinity[71]. In each of these scenarios, full differentiation to $IgA^+$ PC involves migration to and from the mesenteric lymph node (MLN) in the presence of IL-10, IL-6, BAFF and APRIL[66].

Low affinity sIgA produced by PC arising from both T-dependent and -independent activation make up a considerable pool of sIgA along the GI tract[71]. These antibodies tend to recognize microbial cell surface structures that are conserved across several species, such as lipopolysaccharide (LPS). sIgA can bind these microbial targets via canonical fragment, antigen-binding (Fab) affinity, or by non-canonical means involving binding of sIgA-linked glycans to microbial surfaces[72]. Similarly, high affinity sIgA can bind conserved microbial targets through its glycan components, but is renowned for its ability to target and neutralize invasive or pathogenic microorganisms through highly specific canonical Fab recognition[66,72]. The effect of both low and high affinity sIgA binding to microbial cells is impressive. Through lumenal sIgA binding, microbial cells can be immobilized in the mucus layer. Agglutination can inhibit their adherence to epithelial surfaces and their ability to function, colonize, and proliferate. Targeting of structures such as flagella and secretion systems make it difficult for mobility and cellular processes. sIgA can also neutralize toxins or microbial secretions that threaten host homeostasis[66]. All of these functions are conducted in a non-inflammatory manner, ensuring that host GI homeostasis is maintained.

A recent study added another layer of complexity to the story while at the same time revealing insights into neonatal GI immune development. This study showed that, at least in mice, an early postnatal pool of B1 cells gives rise to a significant proportion of adult $IgA^+$ PC in the small intestine. These memory-like $IgA^+$ B lymphocytes are both long-lived and self-sustaining, owing to their persistence in chronic GC in PP, and give rise to related but distinct clones of $IgA^+$ PC in the small intestine[73].

Abnormal IgA responses in individuals affected by T1D have been widely observed. In newly diagnosed pediatric T1D patients, increased proportions of IgA-bound stool microbes have been noted[61], perhaps indicative of heighted GI immune responses and increased IgA production in general, or possibly a response to the presence of specific microbial species. On the other hand, T1D patients exhibit decreased commensal-reactive IgA serum levels[74]. Furthermore, amongst T1D populations worldwide there is an elevated incidence of selective IgA deficiencies, defined as serum IgA levels below 7 mg/dL with normal levels of serum IgG and IgM[75]. Thus, although the role of IgA in T1D-related events remains elusive, it is clear that such a role does exist.

### 1.4 Neonatal Immune Development

The immune environment in a newborn is distinctly different from that of an older child or adult. Although all components of the innate and adaptive systems are present by the third trimester of gestation, many are present in lower concentrations or exhibit weak responses to stimuli, diminished chemotaxis, impaired cytotoxicity, or reduced expression of activation receptors[76]. During this phase of development, B and T lymphocytes have limited receptor repertoires, and when challenged with foreign antigen, display a strong propensity towards a regulatory phenotype. In general, the neonatal immune environment can be characterized as anti-inflammatory, highly tolerogenic and amazingly malleable to external influences and manipulation[76].

Due to the largely sterile environment *in utero*, antigenic stimulation prior to birth is dominated by maternal alloantigens and autoantigens. Upon delivery, the neonate is bombarded by antigenic challenge primarily through respiratory and gastrointestinal avenues[77,78]. The challenge of this particular period of time is the need to balance an emerging functional immune system with the exponential growth and colonization of the gut microbiota, while at the same time providing sufficient immune protection for the infant. Furthermore, both the innate and adaptive arms of the immune system require maturation, education and expansion. This is a tall order, but one that is amply met via both maternal and endogenous mechanisms. Research into various avenues of immunity and disease have established that within childhood there exists a critical window of time, one that is vital to the successful development and education of one's immune system. Immunological events that

occur, or fail to occur, during this timeframe have the ability to shape one's health in a lifelong fashion.

### 1.4.1 The weaning reaction & immune regulation

Insights into the neonatal period have been largely ascertained through animal studies in recent years. In mice, this window of time encompasses postpartum weeks 1-3 and the immunological events that occur have been termed the 'weaning reaction'[79]. The weaning reaction occurs in the GI tract, largely in the distal ileum and colon[79–81]. From birth to approximately 10 days postpartum (D10), endogenous immune activity along the GI tract appears subdued, owing in part to low microbial presence, fewer mucosal immune cells, and indirect suppression by factors such as epidermal growth factor (EGF) in breast milk[81]. However, GI changes begin to occur around D14, ultimately reaching their peak around D21 which coincides with the time of weaning. The microbial load in the colon increases exponentially during this time, particularly with respect to *Clostridia* and *Bacteroides* members[79]. Hitherto, the ability of mucosal antigen presenting cells (APC) to sample and present luminal microbial antigen is inhibited due to the low permeability of the epithelial barrier and lack of trans-epithelial dendrites[81], but decreasing levels of murine breast milk EGF around D14 allows for the spontaneous formation of goblet cell associated antigen passages (GAPs). GAPs produce a transient permeability in the murine small intestine and colon, enabling mucosal APC to acquire and present microbial antigen which results in antigen-specific mucosal $CD4^+$ T lymphocyte activation and proliferation. When these events occur from D14-D21 in mice, clonotypic expansion results in a population of $CD4^+$ $Foxp3^+$ regulatory T lymphocytes (Tregs)[79,81], a subset of T lymphocytes that promotes antigen-specific tolerance. This tolerance appears to be maintained into adulthood. At the same time, the increase in microbial antigen exposure, concomitant with the reduction of inhibiting breast milk factors, induces significant changes in the transcriptional profile of the murine GI tract[79,80]. Upregulated expression of genes involved in barrier integrity, mucosal defense, chemotaxis, and inflammation are observed at D21, although they quickly revert to baseline levels by 4 weeks of age[79]. Similarly, by 4 weeks of age colonic GAPs are largely gone and the impermeability of the epithelial barrier is restored[81].

Particularly enlightening is what ensues when the weaning reaction fails to occur, or occurs outside the D14-21 window of time. If microbial stimulation is unavailable prior to D21 (for instance, germ-free mice colonized post D21) or breast milk EGF remains elevated up until weaning, a phenomenon referred to as "pathological imprinting" occurs, such that mice become highly susceptible to inflammatory diseases in adulthood, showing dysregulation of a broad range of immune responses[79,81]. Pathological imprinting also occurs if mice are unable to respond to microbial stimulation due to genetic manipulation[81], are experimentally prevented from inducing $CD4^+Foxp3^+$ Tregs[79], or are weaned outside the D14-21 window[79]. Each of these scenarios yields clonotypic expansion of $CD4^+$ T lymphocytes that are pro-inflammatory in nature and tolerance is not established. Thus, a successful weaning reaction is reliant on a consortium of factors that include microbial presence prior to weaning, receding levels of breast milk EGF allowing for formation of colonic GAPs, the ability to induce $CD4^+Foxp3^+$ Tregs, and a significant dynamic induction of immune-associated gene expression around D21. Deviations from this protocol result in pathological imprinting that promotes dysregulated immune responses later in life[79,81]. Importantly, a suboptimal weaning reaction may not leave an obvious signature in adulthood; in the cited studies, no differences were observed in the microbiota or $CD4^+Foxp3^+$ Treg numbers of adult mice despite a suboptimal weaning reaction and subsequent immune dysregulation[79,81].

### 1.4.2 Contributions of the microbiota

Microbiome colonization plays a critical role in stimulating the neonatal immune system[82–84]. Studies using germfree mice have provided a glimpse into the molecular and functional immune changes prompted by microbial colonization. Compared to pups born to germfree mice, those born to dams colonized with a complex microbiota show upregulated ileal expression of genes involved in lymphocyte activation (CD45, *Nfkb*), microbial sensing (*Tlr2, Tlr4*) and cytokine production (*Tslp, Tnf*)[85]. This is followed by decreased expression of several chemokines (*Ccl2, Ccl3, Cxcl1, Cxcl2*) in the terminal ileum, while the MLN show downregulated expression of genes involved in antigen presentation (CD80, *H2-Ea*) and lymphocyte activation (CD40)[85]. Using mice colonized postnatally, El Aidy *et al.*[80] showed that introduction of a complex microbiota resulted in expression of innate immune associated genes (*Reg3g, Reg3b, Retnlb*) and increased expression of cytokines (IFNγ, TNFα, IL-10) and

antigen presentation elements (*Tap1, Tap2, Psmb8, Psmb9*)[80]. Furthermore, pups born to colonized dams show evidence of improved gut integrity[86].

Microbial exposure has been shown to expand B and T lymphocyte repertoires, promoting lymphocyte proliferation and influencing their differentiation[73,79,87–91]. Trafficking of microbial antigen from the intestine to the thymus via DC results in the stimulation and proliferation of populations of microbe-specific T lymphocytes[88], including microbiota-specific Tregs that develop and differentiate in the thymus, subsequently migrating to the intestine[89]. Additionally, upon early life exposure to the microbiota, peripheral T lymphocytes can be induced to a regulatory phenoytpe referred to as inducible Tregs (iTregs) which express the transcription factors Foxp3 and RORγt[92]. Peri-natal exposure to broad-spectrum antibiotics, which induces a state of dysbiosis, has been shown to significantly decrease the numbers of iTregs in the colon and contribute to dysregulated intestinal immune responses later in life[93], further demonstrating the ability of the microbiota to influence the adaptive immune response.

Overall, colonization stimulates both pro- and anti-inflammatory signals that together drive a balanced tolerogenic response in a time-specific manner, allowing for continued microbial presence and microbiome establishment while simultaneously promoting the maturation and expansion of the neonatal immune system. Perturbations of these microbially-influenced immune signals often result in irreparable impairment of the developing immune system.

### 1.4.3 Maternal contributions

The contributions made by a mother to the lifelong immune health of her child are diverse and extensive. Some of these contributions are involuntary, such as genetic contributions of risk alleles for diseases such as T1D. Other contributions are related to choice, such as breastfeeding and age at introduction of certain dietary components. Maternal infections and antibiotic use will influence the health of her neonate, as will her own diet and lifestyle choices. By and large, the mechanisms by which these factors influence long-term immune health in the neonate are via establishment of a healthy microbiota, and through development and education of the neonatal immune system[94].

Although actively debated, it is generally accepted that babies *in utero* are largely sterile, resulting in a GI tract that is extremely vulnerable to microbial colonization at birth[95]. Amidst the numerous factors that influence the development of the infant microbiota, mode of delivery and breastfeeding are amongst the most influential[30,96]. During a natural birth, microorganisms from the vaginal tract act as pioneer colonizers of this highly hospitable niche, resulting in an early infant microbiome that resembles the maternal vaginal microbiome. For infants born via Caesarean section, the early microbiome resembles the maternal skin flora and as a group, show significant differences from vaginally delivered neonates[30,97]. However, by 6 months of age these differences have largely disappeared and infant diet (breastfed or formula-fed) emerges as the main stratifier of microbiome composition[98–100]. Breast milk harbors its own unique microbiome which includes viable microorganisms from both *Lactobacillus* and *Bifidobacteria* genera in humans[101]. Both vaginally-acquired and breast milk provided microorganisms aid in the early development of a healthy microbiome and diminish opportunity for pathogenic microbes to establish colonization[82–84]. Human milk oligosaccharides aid in this endeavor by selectively promoting the growth of commensal bacteria such as *Lactobacillus* and *Bifidobacterium* species, both of which have been shown to promote infant health through inhibition of enteric infections[102,103], cross-feeding contributions to the colonization of other commensal species[104,105], and bolstering production of the immunomodulatory SCFA[4,106,107]. The importance of early establishment of a healthy, balanced microbiota has become increasingly evident. Correlative studies in humans consistently show increased prevalence of immunodysregulatory diseases amongst individuals exposed to dysbiosis-promoting events during infancy and early childhood[108]. Similarly, studies in animals have demonstrated the deleterious effects of early dysbiosis on health status later in life and have provided substantial evidence for the health-promoting effects of SCFA-producing commensal microorganisms such as *Bifidobacterium* and *Lactobacillus* particularly during the gestational and neonatal periods[106]. In older individuals affected with T1D, an altered gut environment is frequently seen both prior to and following diagnosis. An aberrant microbiome has been observed to precede or coincide with disease onset[55–60,109–111] and is believed to be a contributor to disease development. Notably, a decreased abundance of SCFA-producing bacteria has been reported in children at various

stages of T1D progression[56,59,60,109,112] and a decline in gut barrier function, as evidenced by increased permeability and microbial translocation, has been observed in patients[62–65,109].

Beyond microbiome remodeling, maternal factors are a significant driver of early immune system development. For the first month of life, maternally derived antibodies in breast milk provide the bulk of gut immunoglobulin as the infant has yet to produce sufficient amounts of his or her own[113,114]. Even beyond this period, breast milk antibodies supplement gut immunoglobulin to a substantial degree[114]. Breast milk contains antibodies of all isotypes but is particularly high in IgA, IgM and IgG[83]. Pathogen-reactive IgG can act in the gut lumen to coat enteric pathogens such as *Citrobacter rodentium* and enterotoxigenic *E. coli*, protecting the infant from infection[115,116]. Similarly, IgA and IgM accomplish their function in the gut lumen but tend to show less specificity for their targets, instead binding to microbial cell surface structures that are common between a number of microorganisms[87]. Together, luminal antibodies protect against pathogen overgrowth and coat toxins and commensal microbes, keeping them away from the intestinal lining and establishing the spatial gradient of microbial density indicative of a healthy gut environment[117]. Furthermore, breast milk antibodies have been implicated in the maintenance of a tolerogenic environment unique to the neonatal intestine, helping to suppress $CD4^+$ T lymphocyte maturation[118] and inhibit development of GC[119]. Moreover, maternal IgA acts as an opsonin, promoting the phagocytosis of IgA-bound microorganisms by colostrum/breast milk phagocytes and activating their various immunological functions[120]. This particular role for IgA may be species-dependent, as murine phagocytes do not express an Fc receptor for IgA[121].

The functional importance of maternal IgG extends far beyond its capacity to bind enteric pathogens in the infant gut lumen. Its active transport, or transcytosis, from mom to infant during both the gestational and breastfeeding periods provides a source of systemic passive immunity against pathogens and is highly effective in protecting the neonate against infection and disease[122,123]. Transcytosis is carried out by a specialized immunoglobulin transporter called the neonatal Fc receptor (FcRn), which is expressed by a number of cell types. In mice, FcRn expression is found on yolk sac epithelial cells during gestation[124,125] and on IEC during the postpartum period[115,126]. In humans, placental endothelial cells and syncytiotrophoblasts express FcRn[125,127–131], allowing for significant transfer of maternal antibodies particularly

during the third trimester[132–134]. Similar to mice, human FcRn is also expressed by IEC to allow for breast milk IgG uptake. Moreover, the presence of FcRn on the surface of both human and murine hematopoietic cells[125,135–137] provides a mechanistic role for maternal IgG in fetal and neonatal immune development. FcRn expression on the surface of phagocytes and APC facilitates the capture of maternal IgG-antigen (Ab-Ag) complexes and subsequent presentation of maternally-derived antigen to naive T lymphocytes[138,139]. Maternal IgG has been detected in the MLN, PP, and thymus of murine offspring[119,140] and its presence allows for the uptake of commensal antigen by way of Ab-Ag complexes binding to the FcRn on immune cells, thereby increasing microbial antigen sampling and presentation[119]. By and large, this mode of antigen transfer induces a tolerogenic response in the neonate by promoting the proliferation of $CD4^+$ Treg populations[119,140–142].

To further add to the complexities of maternal contributions to infant development, studies have demonstrated that the maternal microbiome can directly influence the humoral immune repertoire in breast milk[143]. The presence of certain immunogenic commensal microorganisms within the maternal microbiome can elicit strong humoral responses in the PP of lactating mice. The resulting $IgA^+$ PC migrate to the mammary glands, where their commensal-specific sIgA production can contribute significantly to the milk antibody content. In this way, the infant is provided with maternal antibodies that are uniquely capable of modulating relevant microbial populations present within their own microbiome.

### 1.5 Theories of T1D onset

Blame can be, and has been, laid on impairments in immune regulation at several stages of the process for its involvement in T1D development. During the process of central tolerance, immature T lymphocytes in the thymus must prove their ability to be mediocre; that is, they must be able to bind self-peptide in the context of MHC presentation, but displaying too strong a propensity for autoantigen will invariably result in their demise. During this testing phase, various tissue restricted antigen (TRA) are displayed by thymic epithelial cells in order to assess the candidate T lymphocyte's affinity for each. However, expression levels of TRA can vary between individuals, as the process is subject to regulatory mechanisms such as alternative splicing, allelic variation, and epigenetic or transcriptional regulation[1]. These mechanisms can result in inadequate TRA expression in the thymus and allow for the escape

of autoreactive T lymphocytes. As discussed earlier, this may be the case for some VNTR alleles of the insulin gene. Furthermore, various MHC alleles can present self-antigen in a manner that obstructs negative selection of autoreactive lymphocytes. For example, human MCH I allele *HLA-A2* has been shown to present preproinsulin peptide such that the affinity of binding by a candidate $CD8^+$ T lymphocyte is low, avoiding its negative selection[144]. These loop holes in the process of central tolerance may also be the cause of decreased Treg populations observed in T1D patients[145]. Fortunately, peripheral tolerance mechanisms exist outside the thymus to regulate lymphocyte activation and prohibit autoimmunity. These include the activities of Treg populations, which dampen inflammatory responses through a variety of mechanisms. T1D patients have reduced Treg proportions compared to healthy individuals[145] and some patients harbor Treg populations with impaired suppressive activity or autoreactive $CD8^+$ T lymphocytes that are resistant to Treg suppression[1]. Moreover, there is evidence of TRA expression in epithelial and immune cells in secondary lymphoid tissues, such as lymph nodes and spleen, which help maintain tolerance to self antigen[1,146,147]. Impairments in these peripheral tolerance mechanisms, such as loss of insulin expression in the pancreatic lymph node (PLN)[148] and by splenic DC[146], may be in part responsible for loss of tolerance to the common autoantigen insulin in T1D. Additionally, many immune genes associated with T1D susceptibility come into play here, where enhanced lymphocyte activation, amplified effector functions and impaired inhibitory signalling[1] can promote autoimmune responses.

Besides impaired central and peripheral tolerance, which are largely genetically-based phenomena, many environmental factors have been implicated in initiating or promoting T1D, including the role of infections. Perhaps the most frequently reviewed class of infection in T1D is enteroviral infections, including those by rotaviruses and Coxsackie B4 virus. Maternal infections during gestation are associated with increased T1D incidence in children, as are infections during infancy or early life[19]. Other circumstantial pieces of evidence include elevated levels of anti-Coxsackie B4 antibodies in T1D patients and a negative correlation between childhood rotavirus vaccination and T1D incidence[3]. Since enteroviruses can infect the thymus, it is possible this may lead to impaired central tolerance. Additionally, some enteroviruses have a tropism for beta cells[149]. Although active islet infection is seen very rarely, studies have frequently found Coxsackie B4 viral RNA in islets of T1D patients,

suggesting either an incomplete infection or the presence of infiltrating APC with prior viral encounter[3]. These observations have led to several postulations. Beta cell infection, even an incomplete one, will create inflammation and cell stress, leading to beta cell death, antigen shedding and increased autoantigen presentation. This, coupled with an inflammatory environment in the pancreas and associated PLN, could lead to the erroneous activation of naive autoreactive lymphocytes. Additionally, beta cell stress can promote the production of neo-antigen via post-translational modifications, protein misfolding, or erroneous transcript splicing[150].

Enteroviruses don't need to leave the GI mucosa in order to trigger autoimmune processes. Increased gut permeability is strongly associated with T1D, and enteroviral infections may initiate or exacerbate this[3,151], increasing risk of translocation of microbial cells and their products across the epithelial barrier. Microbial antigen presence in the lamina propria and MLN can trigger pro-inflammatory processes within and extending beyond the gut mucosa, leading to activation of naive autoreactive lymphocytes via mechanisms of molecular mimicry or bystander activation. Indeed, enterovirus-specific antibodies have been shown to cross-react with islet autoantigen[152], and one study reported rotavirus-induced activation of $CD4^+$ T lymphocytes with cross-reactivity to IA-2[153]. Enteroviral infections can also lead to remodeling of the microbiota community, contributing to the dysbiosis so frequently noted in T1D patients[54]. Dysbiosis itself also plays a role, albeit an incompletely understood one, in promoting the early events of autoimmune activation. Despite great variation within the field with respect to which species are protective versus diabetogenic, there is overwhelming agreement that SCFA-producing species, particularly those producing butyrate, are depleted in individuals at various stages of T1D[56,59,60,109,112]. SCFA are known to bolster gut barrier integrity, improve immune surveillance and promote an anti-inflammatory environment along the GI tract[154]. Indeed, the disease-modifying capabilities of the microbiome has been demonstrated via fecal microbiota transfer studies in mice[155,156] and in a human clinical trial with new onset T1D individuals[157].

Undoubtedly, it is a combination of many factors and events that tip the scale to initiate and progress T1D autoimmunity (**Fig 1.5**). Elements unrelated to immunity, such as the beta cells

themselves, can also contribute to T1D susceptibility, evidence that this is a complex, intriguing disease with much left to learn.

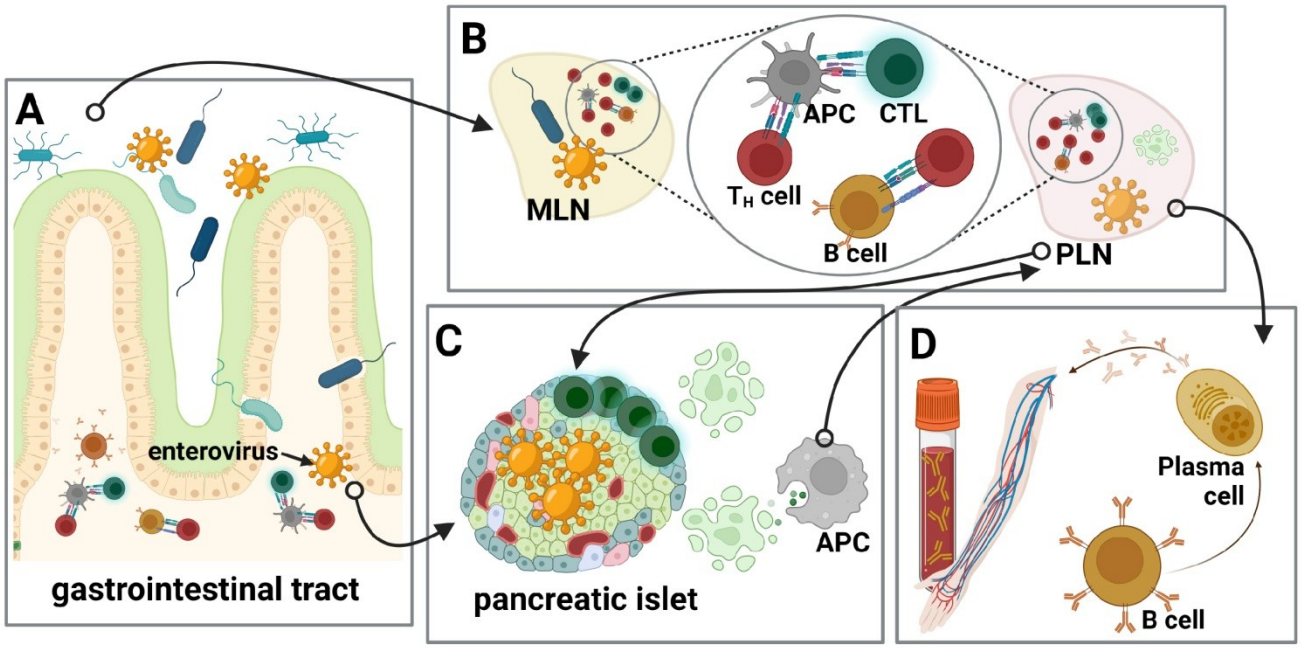


**Figure 1.5 Proposed mechanisms of autoimmune activation leading to insulitis**

**(A)** Gastrointestinal events such as infection or prolonged antibiotic use trigger changes in the GI tract, leading to dysbiosis, increased GI inflammation and impaired barrier integrity. Together, these changes promote microbial translocation across the IEC lining and increase pathogen-associated molecular pattern (PAMP) presence in secondary lymphoid organs such as the MLN and PLN. **(B)** Presentation of PAMPs to T lymphocytes in the MLN and PLN results in T and B lymphocyte activation and promotion of a pro-inflammatory environment. Impaired central and peripheral tolerance in genetically at-risk individuals can allow for the erroneous activation of autoreactive lymphocytes by multiple mechanisms, including molecular mimicry and bystander effects. **(C)** Decreased barrier integrity allows for enteroviral access to pancreatic islets, resulting in infection and death of beta cells. As infected cells die and release autoantigens, APC internalize these autoantigens and present them to lymphocytes in the PLN. Owing to ineffective peripheral tolerance, islet-reactive lymphocytes become activated and infiltrate the islets, promoting further beta cell destruction. **(D)** Activated islet-specific B lymphocytes undergo differentiation to plasma cells which enter systemic circulation and secrete islet-specific antibodies into the bloodstream. Detection of these autoantibodies is a clinical indicator preceding diagnosis of T1D.

Figure created with BioRender.com

## 1.6 Hypotheses & study objectives

As discussed above, several well-documented correlations exist between events along the GI tract and incidence of T1D. Increased risk of developing T1D is associated with selective IgA deficiencies[158–160], use of antibiotics during infancy[29], maternal gestational enteroviral infections, infant and childhood enteroviral infections, and age of introduction of certain foods[19,31]. T1D susceptibility is negatively associated with breastfeeding and rotavirus immunizations during childhood[3,19,31]. Furthermore, the GI environment in patients show evidence of disease involvement, likely as both an influencer of and response to disease, exhibiting increased gut permeability[58,64,109], altered GI microbial communities [55–60,109–111], decreased SCFA levels and SCFA-producing species[56,59–61,109,112], thinner mucus layer[161,162], increased IgA production[61] and altered immune cell populations[145,161,162]. Animal studies have corroborated these data, providing compelling evidence for the involvement of the GI environment in early events of T1D. IgA-mediated immunity along the GI tract is an important component of gut health, contributing to homeostasis, modulating the microbiome and preventing infection. This is supported by studies in both human populations and animal models[163,164]. Taking all of this together, we hypothesized that complete IgA deficiency would disrupt gut homeostasis and induce dysbiosis, leading to earlier onset and/or increased T1D incidence in a diabetes-prone animal model. Thus, this hypothesis constituted our first objective – to determine the effect of IgA deficiency on T1D development in a genetically conducive environment.

Furthermore, we proposed that complete IgA deficiency would affect disease in subsequent generations via maternal dysbiosis. Dysbiotic microbiomes associated with gestational and type II diabetes in women are conferred to their children, shaping infant microbiota and metabolite composition[165–168]. Somewhat surprisingly, we can find no study investigating a similar relationship between T1D-associated maternal dysbiosis and its effects on infant microbiome establishment, immune development, or T1D incidence. In fact, despite its importance, there is a paucity of studies that elucidate maternal-derived mechanisms of T1D resistance vs pathogenesis in offspring. T1D studies worldwide have consistently reported a bias in disease prevalence amongst children of a parent with diabetes, with decreased risk attributed to those with an affected mother [33–43]. This observation suggests that on top of

genetic predisposition, an affected mother may bestow a protective phenotype upon her children, an intriguing possibility that raises many questions about the role of maternal factors in autoimmune diseases. Furthermore, given the numerous maternal influences on neonatal immune development, coupled with the significance of the gestational and neonatal influences on lifelong immune function and resilience, the effects of maternal factors on the development of T1D cannot be over-emphasized. Thus, we endeavored to explore this unknown realm, with a focus on how maternal dysbiosis influences the early GI environment and T1D progression in genetically-susceptible offspring. In line with the first hypothesis, we proposed that maternal IgA deficiency-induced dysbiosis would be conferred to the offspring, contributing to a heightened inflammatory environment along the GI tract and worsening T1D incidence. Thus, this goal constituted our second objective.

# Chapter 2: Study Design, Methods & Materials

## 2.1 Generation of the NOD.IgA colony

In order to study the effect of IgA deficiency on T1D development, we chose to use the NOD mouse model. The spontaneous nature of T1D development in this model allowed us to study IgA deficiency without confounding variables associated with induced disease models, such as the effect of the inducing agent on microbiome remodelling and immune development. Furthermore, the NOD mouse model harbors a genetically-conducive environment for disease onset and progression, reflecting conditions present in human T1D patients. Thus, we anticipated that the disease related events set in motion by IgA deficiency-induced microbiome remodelling and loss of GI homeostasis more closely reflected those occurring in patients during the pre-diabetic stages. Importantly, the use of a spontaneous disease model allowed us to explore T1D development across multiple generations and at early time points without concerns regarding timing of disease initiation, toxicity, or mortality in neonatal mice. Animals were housed under specific pathogen free (SPF) conditions, allowing for development of a complex but controlled microbiome community. All animal use and experimentation was conducted with approval from relevant Animal Care and Use Committees (ACUC) and met Canadian Council on Animal Care (CCAC) guidelines.

### 2.1.1 Introduction of IgA KO allele

Male IgA deficient C57BL/6 mice were graciously donated by Dr. Margaret Conner, Scientific Director of the Gnotobiotics Core at Baylor College of Medicine in Houston, Texas. These were mated with female NOD mice to produce progeny with one immunoglobulin heavy chain gene baring a deletion encompassing the complete α switch region and a portion of the α constant region[169] (**Fig 2.1.1**). The result of this genetic deletion is the inability to undergo class switch recombination to IgA. Animals of the F1 generation, all heterozygous for the IgA deletion allele, were mated with the NOD strain to produce an F2 generation of mixed genotypes. Those carrying the IgA deletion allele were identified through polymerase chain reaction (PCR) and backcrossed with the NOD strain. This process was repeated for 10 generations to remove genetic contribution of the C57BL/6 ancestry before mating two heterozygous animals to produce progeny of three genotypes. These genotypes are denoted henceforth as NOD.IgA WT (those carrying two wild-type IgA alleles, therefore IgA

sufficient), NOD.IgA HET (those carrying one IgA deletion allele, therefore IgA sufficient), and NOD.IgA KO (those carrying two IgA deletion alleles, therefore IgA deficient). For experiments characterizing the NOD.IgA HET & KO animals, NOD.IgA WT were used as the comparison as this controlled for any residual C57BL/6 genetic contribution persisting in this novel strain and thus was a more suitable control than the NOD strain.

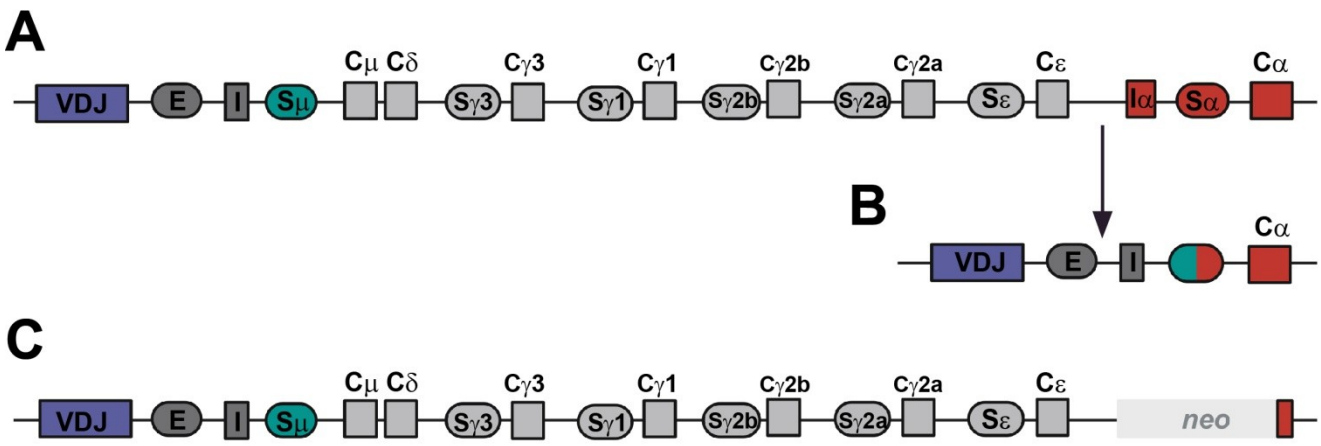


**Figure 2.1.1 Introduction of IgA knockout allele to the immunoglobulin heavy chain gene**

Schematic of the murine immunoglobulin heavy chain gene before (**A**) and after (**B**) class switch recombination in a wild-type mouse. The immunoglobulin heavy chain gene carrying the IgA deletion allele (**C**) no longer allows for class switch recombination to IgA, as the α initiator and α switch region (Iα & Sα, both required for the recombination reaction) and first exon of the α constant region (Cα) have been replaced with a neomycin resistance gene.
Figure created with BioRender.com

### 2.1.2 Breeding Schemes

The breeding pairings used to generate mice for experiments and disease monitoring were carefully considered for this project, as there were several important factors to take into account. First, although I needed progeny of all three genotypes, I didn't want to generate mixed litters due to the potential for sharing of gut microorganisms. In a disease model where susceptibility is driven by the microbiota, as we hypothesized, early sharing of microorganisms via mixed litter housing would likely eliminate the phenotype[170]. Thus, breeding pairs were set up to generate progeny of one genotype only. Secondly, I required progeny born to IgA-sufficient dams and to IgA-deficient dams in order to explore the effects of maternal dysbiosis, in line with our second objective. However, early results clearly showed that although the NOD.IgA WT and HET females were both IgA-sufficient, they were very different with respect to GI environment and immunity. Because of this, I chose to forgo the NOD.IgA HET females as dams in favor of using females that carried two wild-type IgA alleles. Furthermore, consistently using NOD.IgA WT females as IgA-sufficient dams would result in a heightened degree of inbreeding, which increases risk of incurring and perpetuating arbitrary genetic mutations within the colony. To avoid this, I chose to use NOD females as the IgA-sufficient dams when generating progeny to pursue the second objective. The various breeding schemes used throughout this study are outlined in **Figure 2.1.2**. Lastly, I considered the confounding variable of paternal factors on progeny disease. Although we cannot completely remove these factors, I sought to minimize them by removing the sire from the mating cage as soon as a litter was born. At the very least, this minimized the dispersion of his microbiome to progeny.

Several other variables arose throughout the project, mostly pertaining to the contribution of undesirable maternal factors. Harem breeding is commonly used in animal studies to reduce animal costs and is a breeding arrangement I frequently used. I have observed that when multiple litters are present in a cage, pups will breastfeed from both dams, so I ensured that all dams in a harem were of the same genotype. This also raised questions pertaining to milk composition as a variable of parturitional age, a variable that unfortunately may have influenced my data at some points. I also encountered situations where dams became diabetic at some point during the pre-weaning period. Hyperglycemia affects milk composition and

production[171,172], thereby introducing variables that undoubtedly influence progeny health and development. Indeed, I have noted that pups breastfeeding from hyperglycemic dams failed to grow as expected. In an attempt to control these variables, progeny from dams diagnosed with T1D either during pregnancy or the breastfeeding period were not included in the study.

In summary, I expended considerable effort on designing breeding schemes that allowed me to pursue the project objectives, while at the same time attempting to control for the numerous confounding variables present in my study.

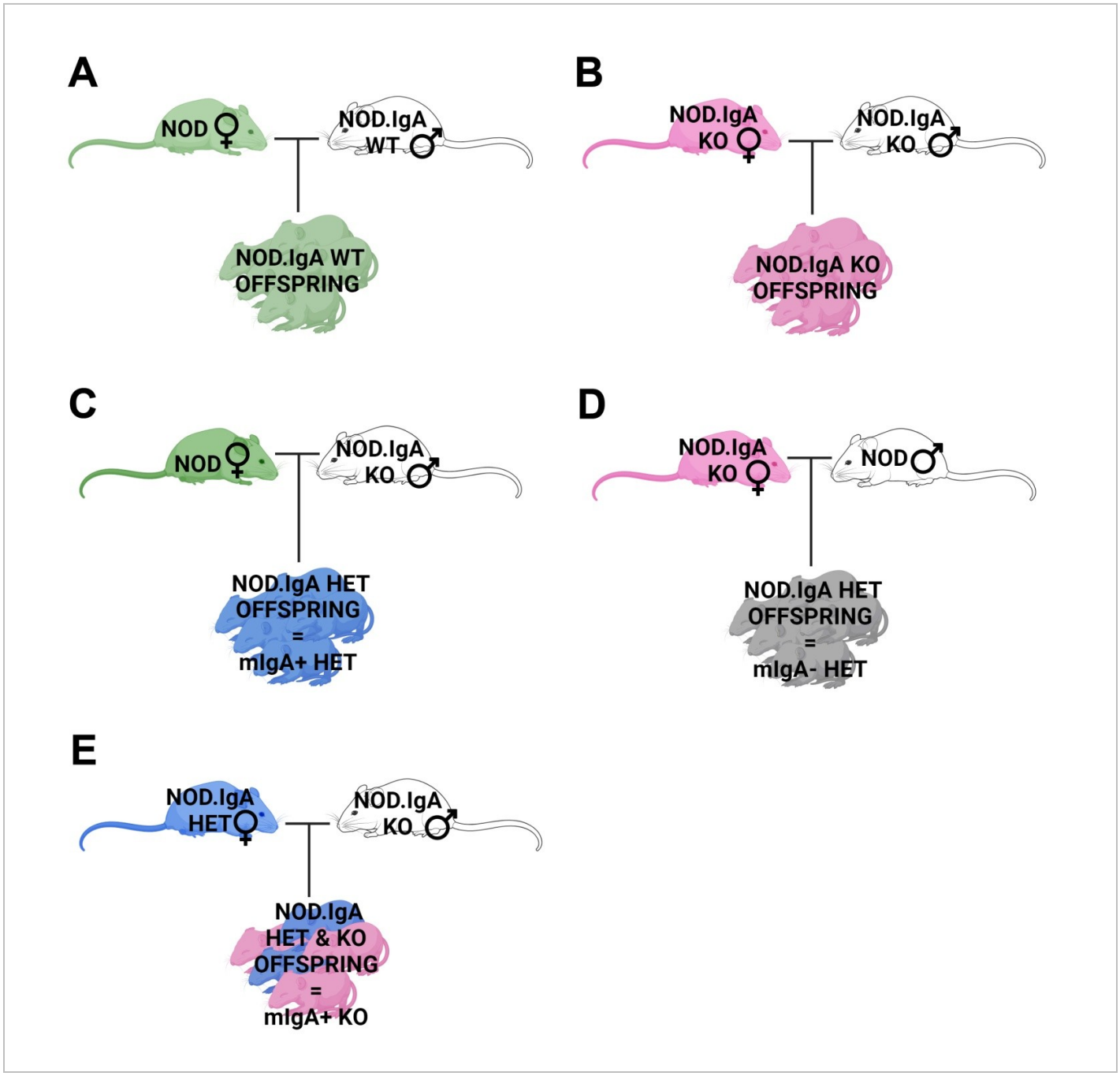
A
NOD ♀
NOD.IgA WT ♂
NOD.IgA WT OFFSPRING
B
NOD.IgA KO ♀
NOD.IgA KO ♂
NOD.IgA KO OFFSPRING
C
NOD ♀
NOD.IgA KO ♂
NOD.IgA HET OFFSPRING = mIgA+ HET
D
NOD.IgA KO ♀
NOD ♂
NOD.IgA HET OFFSPRING = mIgA- HET
E
NOD.IgA HET ♀
NOD.IgA KO ♂
NOD.IgA HET & KO OFFSPRING = mIgA+ KO

**Figure 2.1.2 Breeding schemes used to generate experimental NOD.IgA mice**

To generate NOD.IgA WT mice (**A**) breeding crosses consisted of NOD females and NOD.IgA WT males. To generate NOD.IgA KO mice (**B**) crosses consisted of NOD.IgA KO females and NOD.IgA KO males. Heterozygous mice were generated in two breeding schemes, depending on the desired maternal genotype. NOD.IgA HET offspring from IgA-sufficient dams, referred to as mIgA+ HET (**C**) were generated from NOD females crossed with NOD.IgA KO males. NOD.IgA HET offspring from IgA-deficient dams, referred to as mIgA- HET (**D**) were generated from NOD.IgA KO females crossed with NOD males. In order to generate NOD.IgA KO mice from IgA-sufficient dams, referred to as mIgA+ KO (**E**) NOD.IgA HET females were mated with NOD.IgA KO males and the resulting mIgA+ KO offspring separated from the NOD.IgA HET pups as early as possible. The indicated colors reflect the color scheme used to present data throughout this thesis.
Figure created with BioRender.com

## 2.2 Methods & materials

### 2.2.1 Mating, weaning & fostering

NOD.IgA WT mice were generated by mating NOD females with NOD.IgA WT males. This ensured that all offspring were NOD.IgA WT while seeking to minimize the problems associate with extensive inbreeding. NOD.IgA KO mice were generated via mating of NOD.IgA KO males and females. To generate NOD.IgA HET from IgA sufficient dams (mIgA+ HET), NOD females were mated with NOD.IgA KO males. NOD.IgA HET from IgA-deficient dams (mIgA- HET) were generated by mating NOD.IgA KO females with NOD males. All breeders were >10 weeks of age. Prior to mating, all mice were tested for glucosuria. Breeders that tested positive for glucosuria at any point during mating were retired. Litters arising from dams positive for glucosuria either during pregnancy or prior to weaning were not used for experiments. Within 24 hours of birth, sires were removed from the breeding cages in an effort to minimize paternal factors contributing to offspring disease development. All pups were weaned from the dam at 21-22 days of age.

For fostering experiments, mIgA+ HET were fostered to IgA-deficient dams and mIgA- HET to IgA-sufficient dams by dam exchange within 24 hours of birth. Fostered offspring were then weaned at 21-22 days of age and followed for disease for 30 weeks.

### 2.2.2 Disease monitoring

NOD.IgA WT, HET & KO female mice were monitored weekly for glucosuria using Diastix (Ascensia Diabetes Care). A urine glucose concentration >0.5 g/dL constituted a positive test, whereupon mice were euthanized. Mice were followed until 30 weeks of age.

### 2.2.3 Collection and processing of tissue and blood

At indicated age, mice were euthanized in a $CO_2$ chamber and relevant tissues and organs removed for processing. MLN and PLN were placed in cold PBS, then manually homogenized and passed through a 70 **µ**m filter to create a single cell suspension. Cells were washed in cold PBS, centrifuged at 1500 rpm for 5 min, resuspended in RPMI and stored on ice for cell counting. Large bowels were excised and measured for length, followed by manual removal of

fecal contents and mucus. They were weighed, cut longitudinally, sectioned into ~5 mm segments and stored in PBS on ice. A 10 cm section of the small bowel adjacent to the cecum was excised, relieved of its mucus layer and sectioned similar to the large bowel. Bowel segments were transferred to 50 ml conical tubes containing 10 ml stripping buffer (HBSS + 2% FBS, 5mM EDTA, 15mM HEPES) and incubated at 37$^{o}$C with shaking for 20 min (x2). Tissue was then rinsed in 10 ml of ice cold wash buffer (HBSS + 2% FBS, 15mM HEPES), minced with scissors to create a pulp, transferred into 10 ml digestion buffer (RPMI + 10%FBS, Penn/Strep, L-glutamine, 1 mM NaPyruvate, β-ME, 50 U/ml DNase, 0.5 mg/ml Collagenase IV) and incubated at 37$^{o}$C for 45 min with shaking. Digested tissue was then passed through a 70 **μ**m filter, rinsed with cold PBS, centrifuged at 1800 rpm for 5 min, resuspended in RPMI and cells were counted.

For each tissue, approximately 1x10$^{6}$ cells were transferred to a 96 well plate and centrifuged at 1800 rpm for 5 min. The supernatant was removed and cells were blocked with Fc-block in FACS buffer (1/100 dilution) for 10 min on ice. An additional aliquot of FACS buffer containing antibodies (1/250 dilution) directed against relevant extracellular markers was added, and incubated at 4$^{o}$C for 30 min. Cells were washed, centrifuged at 1800 rpm, resuspended in FoxP3 fix/perm buffer (eBiosciences), and incubated at 4$^{o}$C for 45 min. Cells were centrifuged and resuspended in kit Fixation buffer and left overnight at 4$^{o}$C. The next morning, cells were centrifuged and resuspended in kit Fixation buffer containing antibodies (1/250 dilution) directed against relevant intracellular targets. Samples were incubated at 4$^{o}$C for 30 min, washed, centrifuged, and resuspended in Fixation buffer, then analyzed by flow cytometry on a BD LSRFortessa X-20. FlowJo (BD, v10.8) was used to analyze all cytometry data. Information on the antibodies used can be found in Table 2.2.2. Gating schemes used for analysis of flow cytometry data, including representative images, can be found in Figure 2.2.2.

Blood was collected within 5 min of euthanization using a 23 gauge needle and drawing directly from the heart. The needle was then removed from the syringe before expelling the blood into a 1.5 ml Eppendorf tube. Blood was kept on ice for 1hr, then centrifuged at 10,000g for 10 min. Serum was carefully drawn off the top without disturbing the coagulated blood cell pellet and transferred to a fresh 1.5 ml Eppendorf tube for storage at -20$^{o}$C.

### 2.2.4 ELISA

Serum and fecal samples collected from female mice at 5 weeks, 10 weeks and 15 weeks of age were assayed for immunoglobulin and Lcn-2 content using ELISA kits (Mabtech; R&D Systems). Protein was extracted from fecal samples by manual homogenization of 2-3 pellets in PBS + 0.05% Tween20 followed by 4 hr of agitation at 4°C, centrifugation (10,000g 10min @ 4°C), and collection of supernatant. Total protein concentration was determined using Nanodrop protein quantification (Fisher Scientific). Fecal samples were diluted $1/10^2$ (IgA), 1/10 (IgG & IgM), and 1/10 – $1/10^2$ (Lcn-2). Serum was diluted $1/10^3$ (IgA) and $1/10^5$ (IgG). Breast milk was diluted $1/10^3$ – $1/10^4$ (IgA), $1/10^3$ – $1/10^4$ (IgG), and $1/10^4$ – $1/10^5$ (IgM). All ELISA were run in duplicate or triplicate.

### 2.2.5 Gut Permeability Assays

At 7, 10 and 15 weeks of age, female mice were assessed for gut permeability via oral gavage with FITC-dextran beads (FD4; 0.4mg/g body weight; Cedarlane). Blood (approx. 80ul) was collected from the saphenous vein 4 hrs post-gavage, centrifuged at 10,000g for 10 min and the serum assayed for FD4 concentration against a standard curve.

### 2.2.6 Cytokine/receptor expression analysis (qPCR)

Ileum and colon sections were examined for expression of various mRNA. After euthanasia via $CO_2$ inhalation and removal of bowel contents, 2 cm section of small bowel tissue was excised approximately 1 cm from the cecum and frozen at -80°C in Trizol reagent (Invitrogen). Similarly, 2 cm section of colon was excised from an area approximately 2/3 from the cecum and frozen at -80°C in Trizol reagent. To extract RNA, samples were thawed on ice, homogenized manually, and topped up to 1 ml with Trizol reagent. 200 µl chloroform was added, samples were shaken vigorously, allowed to separate at room temperature for 5 minutes, then spun at 12,000g for 15 min at 4°C. The top aqueous layer (approx 500 µl) was carefully removed and transferred to a fresh collection tube containing equivalent volume of cold isopropanol. Samples were inverted to mix, incubated on ice for 10 min, then applied to an RNeasy spin column (Qiagen) for RNA purification following the Qiagen RNeasy kit protocol. To elute RNA, 40-75 µl of RNase/DNase-free $H_2O$ was applied to the column,

incubated at room temperature for 1 min, then spun for 1 min at 10,000g. RNA was quantified using OD 260 reading on a Nanodrop spectrophotometer (ThermoFisher) and purity assessed using the 260/280 and 260/230 ratios. RNA samples were stored at -80$^{o}$C.

cDNA was generated from purified RNA samples using the Superscript III Reverse Transcription kit (Invitrogen) and used as template for quantitative PCR reactions of various genes of interest. Primer sequences were either designed by myself or taken from published works, and the reactions were optimized with both Advance (Wisent) and PerfeCTa Supermix (Quantabio) SYBR green qPCR reaction mixes. qPCR reactions were performed on CFX96 TouchReal-Time PCR Detection System (BioRAD) and carried out in either duplicate or triplicate.

### 2.2.7 Histology & scoring of pancreata

Pancreata were excised from freshly euthanized 12-13 week female mice, placed into cassettes, immediately fixed in 10% formalin for >48 hr, then transferred to 70% ethanol for >24 hr. Samples were dehydrated and paraffin embedded by immersion in 50% ethanol (1 hr), 70% ethanol (1 hr), 80% ethanol (1 hr), 95% ethanol (1 hr), 100% ethanol (1.5 hr X3), toluene (1.5 hr X3), and paraffin wax at 60ºC (2 hr X2).

Tissue was then removed from cassettes, placed in hot wax molds and allowed to harden. 5 µm sections were placed on glass slides and allowed to dry overnight at 37$^{o}$C. Deparaffinization & rehydration was performed by immersion in toluene (5 min X2), 100% ethanol (2 min X2), 90% ethanol (2 min), 70% ethanol (2 min), 50% ethanol (2 min), and distilled $H_2O$ (2 min). Hematoxylin & eosin (H&E) staining was performed by immersion in hematoxylin (2 min) followed by rinsing in gently running $H_2O$ for 15 min, immersion in 70% ethanol (2 min), eosin (30 s), 100% ethanol (2 min X2), and toluene (2 min X2). Slides were coverslipped and sealed with DPX (distyrene + a plasticizer + xylene) mountant, then allowed to harden overnight at 37$^{o}$C. For each pancreas, 8X 5 µm sections were analyzed with a distance of ~60 µm between any two subsequent sections, allowing for analysis throughout the depth of the tissue. Islets were scored for degree of immune cell infiltration, where a score of 0 indicates no immune cells present, 1 indicates immune cells are visible on islet periphery, 2 indicates an infiltration <25% of islet area, 3 indicates an infiltration of 25% - 50% of islet

area, and 4 indicates an infiltration >50% of islet area. Islet scores from all 8 sections were summed, and the average islet infiltration score was calculated and plotted using GraphPad Prism 9 (https://www.graphpad.com).

### 2.2.8 Histology & scoring of bowel sections

Sections of large bowel approximately 3 cm in length were harvested from freshly euthanized female mice such that each section contained a complete fecal pellet. Whenever possible, a section from the middle of the large bowel was collected. The tissue was immediately placed in Carnoy's solution (60% ethanol, 30% chloroform, 10% glacial acetic acid) and fixed overnight at 4°C. The tissue was removed from the Carnoy's solution, cut transversely through the fecal pellet with a sharp blade, then transferred to 100% ethanol at 4°C. The 100% ethanol was changed twice over a span of 2-3 days, then the tissue was dehydrated and paraffin embedded as outlined in Section 2.2.7. The bowel sections were placed in the paraffin block such that sectioning of the tissue resulted in transverse sections. 7 μm sections were mounted on glass slides and dried overnight at 37°C.

Slide-mounted sections were deparaffinized and rehydrated as outlined in Section 2.2.7, then fluorescence in situ hybridization (FISH) was performed. Slides were incubated in wash buffer (0.9M NaCl, 20mM Tris-HCL, pH 7.2) at 50°C for 10 min, then incubated with a fluorescently labelled pan-bacterial 16S probe (Eub338, 5'GCTGCCTCCCGTAGGAGT3'; IDT) diluted to 100nM in wash buffer + 0.1% SDS at 50°C for overnight in a dark humidification chamber. Slides were washed in 50°C wash buffer for 10 min, then for 8 min in fresh wash buffer at room temperature. Lectin from *Ulex Europaeus* (agglutinin; Invitrogen) diluted to 20 μg/ml in PBS was added to the slides and incubated for 2 hr at room temperature in a dark humidification chamber. Slides were washed for 8 min in wash buffer at room temperature, then mounted with ProLong™ Gold Antifade Mountant with DNA Stain DAPI (Invitrogen). FISH slides were visualized and images collected on a Cytation 10 multimode plate reader (Agilent Biotek) using the 4X magnification lens. ImageJ software (NIH) was used to assess the thickness and integrity of the mucosal layer in a blinded fashion. For thickness assessment, 6 areas were chosen at regular intervals around the tissue section and the mucosal layer

measured at each. A minimum of 5 sections per sample were assessed, and an average thickness was generated and plotted using GraphPad Prism 9.

### 2.2.9 Microbiota analysis

Fecal pellets were collected as they were excreted into sterile 1.5 ml Eppendorf tubes and stored immediately at -80$^{o}$C. Frozen fecal pellets were weighted and DNA was extracted using the QIAamp Fast DNA Stool Mini Kit (Qiagen) following the protocol provided in the kit with inclusion of a 1 min bead-beating step with garnet beads (BioSpec Products) in a FastPrep-24 5G homogenizer (MP Biomedicals). Library prep was performed on purified DNA, targeting the V3-V4 region of the 16S rRNA gene according to the 16S metagenomic Sequencing Library Preparation protocol, and sequencing was performed on Illumina MiSeq v2 by McGill Genome Centre. Analysis of raw data and generation of analysis plots were performed by Dr. Tingting Ju in the Dept. of Agriculture, Food & Nutrition at the University of Alberta. Sequences were processed using the Quantitative Insights Into Microbial Ecology 2 (QIIME2, v2021.2) pipeline, and downstream analyses were performed in R (https://www.r-project.org/).

### 2.2.10 Metabolomic analysis

Fecal pellets were collected as they were excreted into sterile 1.5ml Eppendorf tubes. Samples were immediately stored at -80$^{o}$C. Frozen fecal material was delivered on dry ice to The Metabolomics Innovation Center (TMIC) at the University of Alberta for metabolomic profiling using High Performance Chemical Isotope Labeling Metabolomics. Analysis of raw data was carried out by TMIC personnel and entered into Microsoft Excel spreadsheets (.xlsx & .csv files). The .xlsx and .csv files were uploaded to MetaboAnalyst 5.0 (https://www.metaboanalyst.ca/home.xhtml) for identification of enriched or depleted metabolites, pathway analysis and generation of figures.

### 2.2.11 Breast milk collection & proteomic analysis

Milk was collected from breastfeeding dams 10-12 days postpartum. Dam and pups were physically separated for 4 hrs such that visual, olfactory and audible connections were maintained but pups could not nurse. The dam was then anesthetized with isoflurane and given

oxytocin (2 IU/kg) intraperitoneally. Milk was expressed by gently massaging inguinal nipples and collecting milk droplets with a sterile pipet. Upon collection of approx. 80-100 µl of milk, the dam was allowed to recover and then returned to her litter. Breast milk was stored at -20$^{o}$C.

Breast milk samples were thawed at 37$^{o}$C for 5 min, then mixed thoroughly. Milk was diluted 10 fold in PBS + 0.28% SDS and transferred to a 0.2 ml PCR tube nested inside a 1.5 ml Eppendorf tube. The samples were centrifuged at 14,000 rpm for 10 min to separate the fat and cellular components from the aqueous phase. The aqueous layer was gently collected and transferred to a fresh 0.2 ml tube and stored at -20$^{o}$C. Proteomic analysis was performed by Henry Wang in the laboratory of  Dr. Olivier Julien at the University of Alberta.

### 2.2.12 Breast milk antibody specificity assay

Breast milk samples were thawed at 37$^{o}$C for 5 min, then mixed thoroughly. Aliquots from samples were diluted 1/10 in FACS buffer containing PE conjugated antibody (either IgA, IgG or IgM). Samples were incubated on ice for 1.5 hrs.

Meanwhile, fecal pellets were collected from NOD.IgA HET pups (25 days of age) into sterile PBS+10% glycerol. In an anaerobic chamber, fecal matter was homogenized and passed through a 40 µm filter, then rinsed with sterile PBS. Flowthrough was spun in a centrifuge at 14,000g for 3 min, then resuspended in 1% paraformaldehyde (PFA) for 45 min on ice for fixation in an effort to keep obligate anaerobic bacteria from dying. Fecal pellets were then pelleted again at 14,000g for 3 min and resuspended in FACS buffer. Fecal pellets from 14 week NOD females and SCID NOD females were similarly collected and processed for use as controls.

An aliquot of fecal slurry + FITC conjugated SYTO16 (BioLegend) were added to each milk sample, mixed and incubated on ice for 45 min. Microbes were washed with FACS buffer, spun at 14,000g for 3 min, and resuspended in sorting buffer (PBS + 0.5%BSA + 2mM EDTA). PE-nanobeads (BioLegend) were added to each sample and incubated on ice for 15 min. Microbes were then washed with sorting buffer, pelleted as above, and resuspended in fresh sorting buffer. Samples were placed in magnets (Miltenyi) for 5 min, then supernatant

was poured off. This was repeated twice for a total of 3 positive selection steps. The positively selected microbes remaining in the tubes were washed with PBS, pelleted as above, and the microbial pellet stored at -80$^{o}$C to await 16S sequencing analysis. An aliquot of each sample was taken for flow cytometry analysis to ascertain degree of enrichment of each fraction.

### 2.2.13 FMT procedure

Fecal pellets were collected as they were excreted from appropriately aged and genotyped female mice directly into 1.5 ml Eppendorf tubes containing sterile 10% glycerol in PBS and placed in an anaerobic environment for 10 min. Samples were then immediately stored at -80$^{o}$C. Once enough fecal material was collected, all aliquots were thawed and transferred to an anaerobic chamber, where they were homogenized and passed through a 40 μm filter, rinsing with sterile 10% glycerol in PBS. Fecal material was aliquoted into fresh 1.5 ml Eppendorf tubes and returned to -80$^{o}$C. These constituted the donor fecal material.

7 week female NOD and NOD.IgA KO mice underwent daily gavage with 250 μl of antibiotic cocktail (2.5 mg/mL vancomycin, 5 mg/mL neomycin, 5 mg/mL ampicillin, 5 mg/mL metronidazole, amphotericin B) for 8 days. After a 2 day rest period, the mice received oral gavage of appropriate donor fecal material every second day for a total of 4 treatments. Specifically, one aliquot of donor fecal material per recipient was thawed at 37$^{o}$C for 5min, then pelleted at 14,000g for 3 min. The supernatant was reduced to approx. 200 μl, the fecal material resuspended by gentle pipetting, and the resulting fecal slurry administered to the recipient mouse. Male mice intended for breeding with FMT recipients underwent the same procedure.

2 days following the final FMT treatment, female mice were bred with an appropriately genotyped male FMT recipient such that the breeding produced NOD.IgA HET offspring. The offspring were weaned at 21-22 days of age and followed for disease incidence until 30 weeks of age.

### 2.2.14 Tables of antibodies, reagents & software

**Table 2.1 List of antibodies for flow cytometry**

| Antibody (anti-mouse) | Clone | Supplier | Catalog No. |
|---|---|---|---|
| CD45 BV711 | 30-F11 | BioLegend | 103147 |
| CD3 PE Cy7 | 17A2 | BioLegend | 100219 |
| CD19 APC Cy7 | 1D3/CD19 | BioLegend | 152411 |
| CD4 Alexa Fluor 488 | GK1.5 | BioLegend | 100425 |
| CD8 BV605 | 53-6.7 | BioLegend | 100743 |
| TCRγδ APC | GL3 | BioLegend | 118115 |
| FOXP3 PE | QA20A67 | BioLegend | 118903 |
| RORγt PE eFl 610 | AFKJS-9 | eBiosciences | 61-6981-82 |
| CD90.2 Alexa Fluor 700 | 30-H12 | BioLegend | 105320 |
| NKp46 BV650 | 29A1.4 | BioLegend | 137635 |
| Aqua Zombie live/dead stain | N/A | BioLegend | 423101 |
| CD138 BV650 | 281-2 | BioLegend | 142517 |
| BLIMP1 APC | 5E7 | BioLegend | 150007 |
| IgA PE | mA-6E1 | Fisher Scientific | 12-4204-82 |
| CD95 BV605 | SA367H8 | BioLegend | 152612 |
| GL7 Alexa Fluor 488 | GL7 | BioLegend | 144612 |
| CD86 PE Dazzle | GL-1 | BioLegend | 105041 |
| B220 Alexa Fluor 700 | RA3-6B2 | BioLegend | 103232 |
| CXCR5 BV711 | L138D7 | BioLegend | 145529 |
| PD1 BV605 | 29F.1A12 | BioLegend | 135219 |
| SIGLEC H PE | 551 | BioLegend | 129605 |
| CD44 APC | QA19A43 | BioLegend | 163603 |
| IgM PE | RMM-1 | BioLegend | 406508 |
| IgG PE | Poly4053 | BioLegend | 405307 |
| SYTO 16 | N/A | BioLegend | S7578 |
| TCRβ PE Cy5 | H57-597 | BioLegend | 109210 |

**Table 2.2 List of reagents**

| Item | Catalogue No. | Supplier |
|---|---|---|
| Diastix | 2804B | Ascensia Diabetes Care |
| Hank's Balanced Salt Solution (HBSS) | 311-513-CL | Wisent |
| EDTA | AC118445000 | Thermo Fisher Scientific |
| HEPES | ICN1688449 | MP Biomedicals Inc |
| RPMI 1640 medium | 350-002-CL | Wisent |
| Fetal bovine serum | F1051 | Sigma |
| Penn/Strep | P4333 | Sigma |
| L-glutamine | 25030081 | Gibco |
| NaPyruvate | 11-360-070 | Thermo Fisher Scientific |
| β-Mercaptoethanol | 60-24-2 | Sigma |
| MEM Non-essential amino acids | 11140-050 | Thermo Fisher Scientific |
| Collagenase IV | 17104019 | Gibco |
| DNase | D5025 | Sigma |
| Fc block | 422301 | BioLegend |
| Phosphate buffered saline (PBS) | BP399-20 | Thermo Fisher Scientific |
| Tween20 | MP1TWEEN201 | MP Biomedicals Inc |
| FITC-dextran beads | FD4-250MG | Cedarlane |
| isopropanol | A4641 | Thermo Fisher Scientific |
| Trizol | 10296010 | Invitrogen |
| Advance SYBR green qPCR reaction mix | 801-001-AR | Wisent |
| PerfeCTa SYBR green Supermix qPCR reaction mix | 95054-500 | Quantabio/VWR |
| 10% formalin | 22-050-104 | Thermo Fisher Scientific |
| toluene | T324-1 | Thermo Fisher Scientific |
| paraffin wax | 18614673 | Thermo Fisher Scientific |
| hematoxylin | H345-25 | Thermo Fisher Scientific |
| eosin | LC140258 | Thermo Fisher Scientific |
| DPX | 50980369 | Electron Microscopy Sciences |

| | | |
|---|---|---|
| agglutinin | L32476 | Invitrogen |
| ProLong™ Gold Antifade Mountant | P36931 | Invitrogen |
| garnet beads, 20mm | 11079120gar | BioSpec Products |
| SYTO16-FITC | S7578 | BioLegend |
| Bovine Serum Albumin | A8806 | Sigma |
| PE-nanobeads | 480080 | BioLegend |
| vancomycin | 111002498 | MilliporeSigma |
| neomycin | AAJ6149914 | Thermo Fisher Scientific |
| ampicillin | BP1760-5 | Thermo Fisher Scientific |
| metronidazole | AC210345000 | Thermo Fisher Scientific |
| amphotericin B | SV3007801 | Thermo Fisher Scientific |

**Table 2.3 List of commercial kits**

| Kit Name | Catalog No. | Supplier |
|---|---|---|
| FoxP3/Transcription Factor Staining Buffer Set | 00-5523-00 | eBioscience |
| ELISA Flex: Mouse IgA (ALP) | 3865-1AD-6 | Mabtech, Inc |
| Mouse IgM ELISA BASIC kit (HRP) | 3885-1H-6 | Mabtech, Inc |
| Mouse IgG ELISA BASIC kit (ALP) | 3825-1AD-6 | Mabtech, Inc |
| Mouse Lcn-2/NGAL DuoSet ELISA | DY1857-05 | R&D Systems |
| Superscript III Reverse Transcription kit | 4368814 | Invitrogen |
| QIAamp Fast DNA Stool Mini Kit | 51604 | Qiagen |
| RNeasy micro kit (50) | 74004 | Qiagen |

**Table 2.4 List of hardware & software**

| Hardware/Software | Supplier |
|---|---|
| FlowJo (BD, v10.8) | BD Biosciences |
| GraphPad Prism 9.0.1 | GraphPad Software, LLC |
| Cytation 10 multimode plate reader | Agilent Biotek |
| CFX96 Touch Real-Time PCR Detection System | BioRAD |
| NanoDrop 1000 | Thermo Fisher Scientific |
| ImageJ | National Institutes of Health (NIH) |
| FastPrep-24 5G homogenizer | MP Biomedicals |
| MetaboAnalyst 5.0 | https://www.metaboanalyst.ca/home.xhtml |
| Enrichr | https://maayanlab.cloud/Enrichr/ |
| BD LSRFortessa X-20 | BD Biosciences |
| QIIME2, v2021.2 | https://docs.qiime2.org/ |
| R | https://www.r-project.org/ |

# Chapter 3: Results

## 3.1 Introduction

The GI tract is an effective barrier between the host and the outside world. This is a site harboring a plethora of potential infectious microbes and immune-activating food antigen, posing a constant threat to host health and homeostasis. The ability to maintain a balanced microbiome and prevent infection, while at the same time suppressing overt inflammatory responses amidst a constant barrage of external stimuli, requires much diligence and continual immune surveillance. The recognition of microbial antigen and metabolites by a variety of cell types along the GI tract results in upregulation of mucosal defenses, including increased secretion of sIgA into the gut lumen. sIgA binding to lumenal targets inhibits microbial cellular activity, proliferation, and motility, while preventing their adherence to the epithelial barrier and neutralizing toxins and other microbial products. Thus, in conjunction with other mucosal barrier defenses, sIgA is a key maintainer of health and homeostasis along the GI tract. The apparent loss of this homeostasis in individuals affected by T1D particularly during the early pre-diabetic stages suggests a contribution of subpar mucosal defenses to T1D development. Furthermore, the observation that T1D patients exhibit abnormal IgA responses to gut bacteria[61,74] raises questions about the role of IgA in particular in promoting or preventing early diabetogenic events.

The increased incidence of selective IgA deficiency in individuals with T1D has been reported in a number of human studies in various ethnic populations in both children and adults[158–160]. This primary immunodeficiency has several causes, most often involving B lymphocyte defects, and affected individuals can present with a number of symptoms, or none at all[163]. Moreover, selective IgA deficiency and T1D share a common genetic risk allele, the HLA 8.1 haplotype[163]. Taken together, the data supports a connection between the two immune conditions, leading to the possibility that being deficient in IgA increases one's susceptibility to T1D. Based on this hypothesis, I followed disease incidence in the NOD.IgA colony to determine the effect of IgA deficiency on T1D in diabetes-prone mice.

## 3.2 Results

### 3.2.1 Effect of IgA deficiency on T1D incidence

Adult female mice in the NOD.IgA colony were tested weekly for the presence of glucosuria (>0.5 g/dL), an indicator of overt T1D. Mice were tested until 30 weeks of age according to our study design. We chose to focus our study on female mice for a couple of reasons. Firstly, disease incidence between male and female NOD mice is reportedly very different[15] and we found this to be true of our colony as well. Similarly, sex differences exist with respect to immune development and physiology. Thus, both incidence and experimental data would require analysis stratified by sex. In order to eliminate an effective doubling of workload and animal numbers, we made a decision early in the project to study the females. To date, 370 mice have been followed for disease and the data have revealed some unexpected results.

#### 3.2.1.1 T1D incidence is largely unaffected by IgA deficiency

Given the importance of IgA to gut immunity and homeostasis, I expected to find that IgA deficiency would alter the course of T1D such that the NOD.IgA KO cohort would have higher disease incidence. However, I found that the disease curves were similar between the NOD.IgA WT, HET and KO females. The modest differences that were apparent suggested that the NOD.IgA HET and KO cohorts fared better than the NOD.IgA WT cohort (**Fig 3.2.1.1**). At the end of 30 weeks, the disease incidence was 75.9% (22/29) for WT females, 66.3% for HET females (69/104), and 71.0% (44/62) for KO females (**Fig 3.2.1.1A**). When including and accounting for the animals that were used for experiments (and thus didn't reach the 30 week end of study mark), disease curve comparison using the log-rank (Mantel-Cox) test indicated there was no difference between the three curves (**Fig 3.2.1.1B**). When the Gehan-Breslow-Wilcoxon test, a statistical test that puts extra weight on incidence at early time points, was used to compare the curves, the result was a significant difference (p=0.014) between the WT and KO disease curves. This prompted me to compare the age of disease onset between the three genotype cohorts (**Fig 3.2.1.1C**). Using the Mann-Whitney statistical test, I found that the NOD.IgA KO females had a significantly later age of onset when compared to the NOD.IgA WT females (p=0.0053). Notably, the NOD.IgA HET females also had a trend toward later age of onset when compared to the NOD.IgA WT females (p=0.067).

This was an interesting observation, and an indication that we couldn't use the NOD.IgA HET animals as a suitable IgA-sufficient control for comparison with the NOD.IgA KO, as is frequently done in genetic studies.

Overall, IgA deficiency delayed T1D onset in female mice but didn't alter the incidence significantly over 30 weeks. This finding was unexpected, and disproved our initial hypothesis.

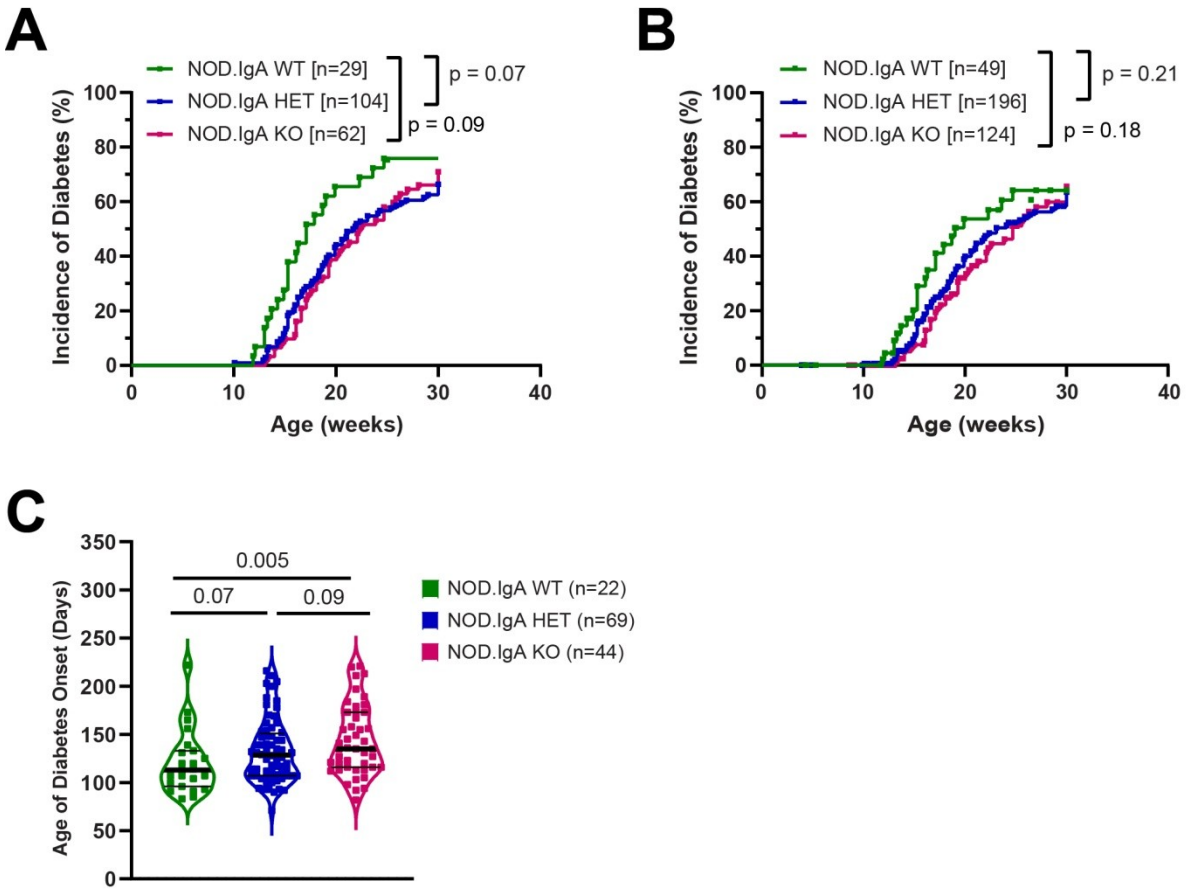


**Figure 3.2.1.1 Incidence of T1D in the novel NOD.IgA colony**

Incidence curve (**A**) shows T1D incidence in NOD.IgA WT (green), HET (blue) and KO (pink) female mice followed until 30 weeks of age or positive T1D diagnosis, where each data point represents one mouse. Incidence curve (**B**) shows T1D incidence in all NOD.IgA WT (green), HET (blue) and KO (pink) female mice born into the colony, including those sacrificed before 30 weeks of age. A violin plot (**C**) shows age of onset for T1D-positive NOD.IgA WT (green), HET (blue) and KO (pink) female mice, where mean +/- SEM is indicated for each cohort. p-values were determined using the Log-rank test for panels (A) & (B), and the Mann-Whitney U test for panel (C).

### 3.2.2 Exploring early and later life immunity in the novel IgA-deficient NOD strain

The NOD.IgA knockout is a novel strain of NOD mouse. Thus, we desired to characterize some of the immune differences between the full knockout (NOD.IgA KO) and the heterozygous (NOD.IgA HET) animals in comparison to the conventional NOD WT animals. Given that we had introduced the IgA knockout allele to the NOD strain via breeding with C57BL/6 IgA KO mice, we chose to use the WT offspring of our NOD x C57BL/6 IgA KO crosses (NOD.IgA WT) as our WT comparison. In this way, we would account for any residual C57BL/6 genetic contributions, minimal as they might be after >12 generations of backcrossing to the NOD strain.

#### 3.2.2.1 NOD.IgA HET and KO animals exhibit heightened GI immunity

The loss of IgA immunity would be most impactful at the mucosal surfaces, primarily in the gut, due to these tissues being the largest reservoir of $IgA^+$ B lymphocytes and PC. Thus I began characterization by assessing humoral responses in the gut. I collected fecal material from female NOD.IgA WT, HET & KO mice at 5, 10, 15, 20, >25 weeks of age as well as at disease onset, and used enzyme linked immunosorbent assay (ELISA) to determine the IgA, IgG and IgM content. The choice of these three immunoglobulin isotypes was intentional. First, I wanted to verify that the NOD.IgA KO were indeed deficient for IgA production. Secondly, the NOD.IgA HET genotype is different from the conventional heterozygous genotype typically generated in genetic experiments of this sort. Because successful rearrangement of one immunoglobulin heavy chain gene results in allelic exclusion, some B lymphocytes will be able to produce IgA upon class switching and others will not, depending on which heavy chain gene was successfully rearranged. If the choice of heavy chain gene undergoing rearrangement is random and unaffected by the loss of the α switch region, and the class switch process is also unaffected by the genetic manipulation, then roughly half of the B cells/PC in the NOD.IgA HET will be capable of producing IgA. However, these are broad assumptions that are difficult to ascertain. Indeed, I found that there was a considerable difference in fecal IgA content between the NOD.IgA HET and WT females, with the NOD.IgA HET animals producing significantly more IgA at 10 weeks (1.8X more) and 15 weeks (2.3X more) (**Fig 3.2.2.1A**). As anticipated, the NOD.IgA KO animals exhibited no fecal IgA. By 20 weeks of age, gut IgA production declined in the NOD.IgA HET mice,

whereas an increase was noted in the NOD.IgA WT animals. These differences in IgA production are more likely a result of gut physiological or environmental differences (for instance, differences in the microbiota) rather than genetically determined by the loss of one α switch region. To determine whether disease progression had any effect on gut IgA production, I looked at fecal IgA concentration in the weeks prior to disease diagnosis and found no obvious pattern (**Fig 3.2.2.1B**).

IgM is also produced in the gut, albeit at lower levels, and can be transported into the gut lumen via the same pIgR that mediates IgA transport[66]. Although IgM usually doesn't play a major role in mucosal humoral immunity, I wondered if a loss of IgA might be compensated for with increased IgM production and lumenal transport in the NOD.IgA KO mice. I found that fecal IgM levels were considerably elevated in the NOD.IgA KO mice at all ages, even at 5 weeks when overall fecal Ig levels were otherwise low across the genotypes (**Fig 3.2.2.1C**). This supports the hypothesis that a deficiency in IgA can induce increased expression of IgM, albeit at levels significantly lower than those achieved by IgA. Furthermore, the elevated IgM level at 5 weeks suggests the presence of early mucosal tissue activation possibly for the purpose of combating threatened homeostasis, an indication that IgM does not effectively correct for IgA deficiency.

In contrast to IgA and IgM, which are produced during homeostasis in an effort to maintain healthy microbial balance, intestinal IgG production is often a response to a specific pathogenic challenge[115,116]. IgG molecules secreted in the murine lamina propria are transported across the gut epithelium via the FcRn[115]. I assessed the levels of IgG in the NOD.IgA cohorts via ELISA and found that at 10-15 weeks both NOD.IgA HET and KO cohorts had moderately elevated fecal concentration of IgG compared to the NOD.IgA WT animals (**Fig 3.2.2.1E**). To ascertain whether this was indeed indicative of gut inflammation, I measured the concentration of fecal Lipocalin-2 (Lcn-2) in each sample. Lcn-2 is an anti-microbial pro-inflammatory molecule produced primarily by neutrophils and IEC in response to pro-inflammatory stimuli, and is frequently used as a biomarker for tissue inflammation[173]. I found that compared to the NOD.IgA WT, by as early as 10 weeks fecal Lcn-2 levels were becoming significantly elevated in the NOD.IgA HET cohort and by 15 weeks, the same was true in the NOD.IgA KO cohort. In contrast, the NOD.IgA WT cohort showed a marginal

increase in fecal Lcn-2 levels around the 10 week period with levels dropping back to baseline by 15 weeks (**Fig 3.2.2.1E**).

T1D has been well associated with gut inflammation in both animal and human studies, so I looked at the fecal Lcn-2 levels in relation to their proximity to disease diagnosis. I found that the fecal Lcn-2 level peaked in the 3-5 weeks prior to diagnosis and was at its lowest level once glucosuria was present (**Fig 3.2.2.1F**). This observation explains the later timing of increased inflammation in the NOD.IgA KO cohort, given their delayed disease onset compared to the NOD.IgA WT cohort. However, the heightened degree of inflammation in both NOD.IgA HET & KO cohorts is interesting, since neither cohort showed an elevated incidence of disease.

I was interested in knowing if IgA deficiency and the resulting elevated GI humoral response affected lymphocyte populations in a long-term manner. To answer this, I assessed B and T lymphocyte populations in various tissues of 12 week old NOD.IgA WT, HET and KO mice (**Fig 3.2.2.1G-J**). I included the large and small bowel tissues, as well as the MLN, since these were the tissues most directly affected by the chronically elevated pro-inflammatory environment. I also assessed lymphocyte populations in the PLN to determine immune activity within proximity of the pancreas, and I included the spleen to ascertain if there were any overt systemic differences in lymphocyte populations. In the large bowel tissue, I observed a subtle increase in B lymphocytes in both the NOD.IgA HET and KO cohorts when compared to the NOD.IgA WT animals, but no changes in PC, $CD4^+$ or $CD8^+$ lymphocyte proportions. The small bowel tissue showed no differences in any of these populations between the three cohorts. The MLN exhibited an increased proportion of B lymphocytes, along with decreased proportions of both $CD4^+$ and $CD8^+$ lymphocytes in the NOD.IgA KO animals. The same trend was observed in the PLN of these mice. The spleen harbored similar B and T lymphocyte proportions in all three cohorts. Importantly, this data indicated that the introduction of the IgA KO allele did not affect B cell/PC populations beyond the ability to class switch to IgA.

Taken together, the NOD.IgA HET and KO cohorts showed a heightened degree of GI immune activity in the weeks preceding T1D diagnosis. This mucosal immune activity may have contributed to the disease process or perhaps was a response to mucosal events occurring

during disease onset and progression. Either way, given the lack of increased T1D incidence in these two cohorts, it did not appear to further drive autoimmunity. Indeed, it seemed to have somewhat dampened T cell-mediated immune activity in the MLN and PLN, while boosting B lymphocyte populations there and in the colon. Moreover, a lack of IgA in the NOD.IgA KO animals promoted the production of IgM likely as a compensatory mechanism. In Chapter 4, I will discuss how maternal IgA status further dictates GI phenotypes in NOD.IgA HET and KO animals.

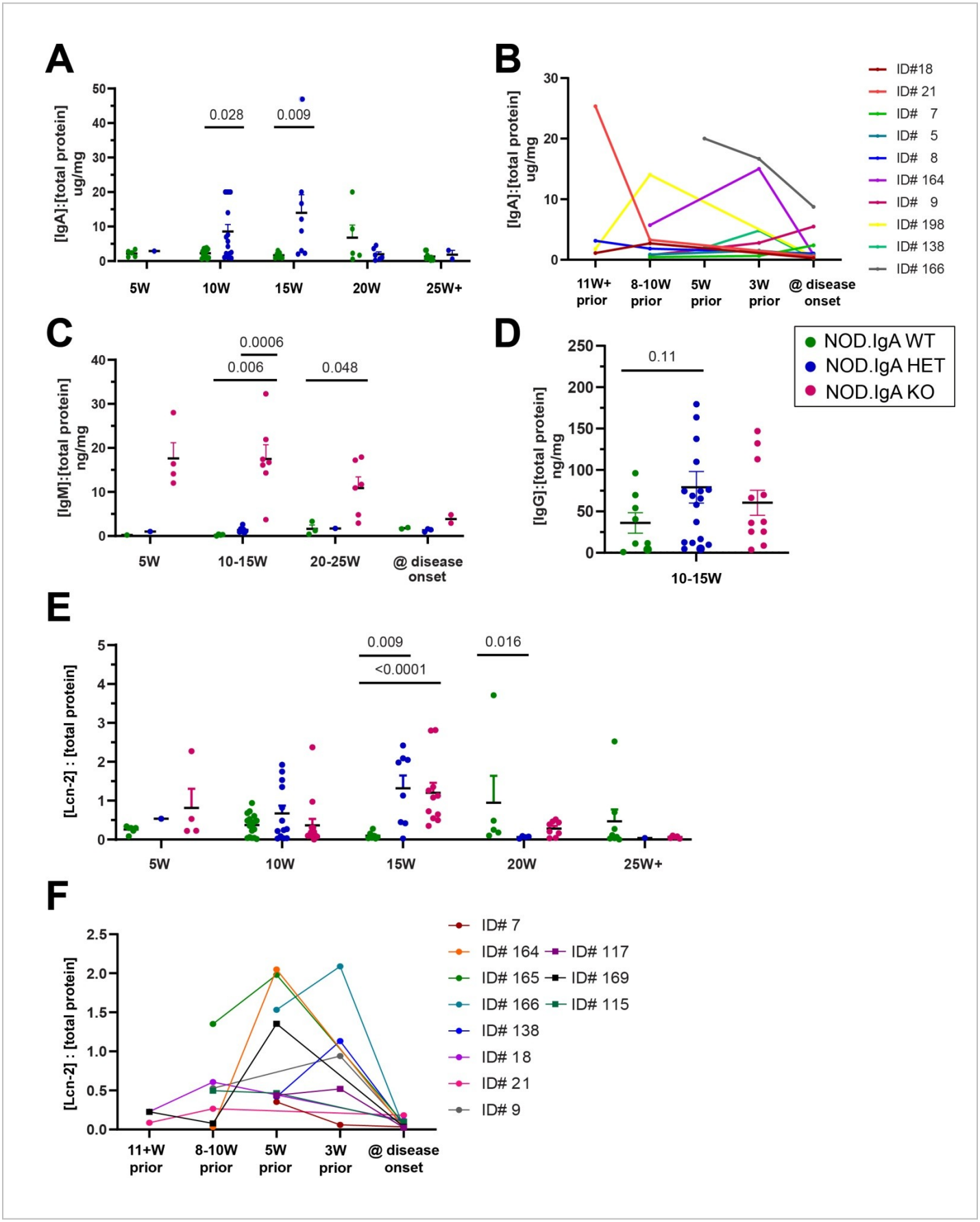
A
[IgA]:[total protein] ug/mg
0.028
0.009
5W
10W
15W
20W
25W+
B
[IgA]:[total protein] ug/mg
11W+ prior
8-10W prior
5W prior
3W prior
@ disease onset
ID#18
ID# 21
ID# 7
ID# 5
ID# 8
ID# 164
ID# 9
ID# 198
ID# 138
ID# 166
C
[IgM]:[total protein] ng/mg
0.0006
0.006
0.048
5W
10-15W
20-25W
@ disease onset
D
[IgG]:[total protein] ng/mg
0.11
10-15W
NOD.IgA WT
NOD.IgA HET
NOD.IgA KO
E
[Lcn-2] : [total protein]
0.009
<0.0001
0.016
5W
10W
15W
20W
25W+
F
[Lcn-2] : [total protein]
11+W prior
8-10W prior
5W prior
3W prior
@ disease onset
ID# 7
ID# 164
ID# 117
ID# 165
ID# 169
ID# 166
ID# 115
ID# 138
ID# 18
ID# 21
ID# 9

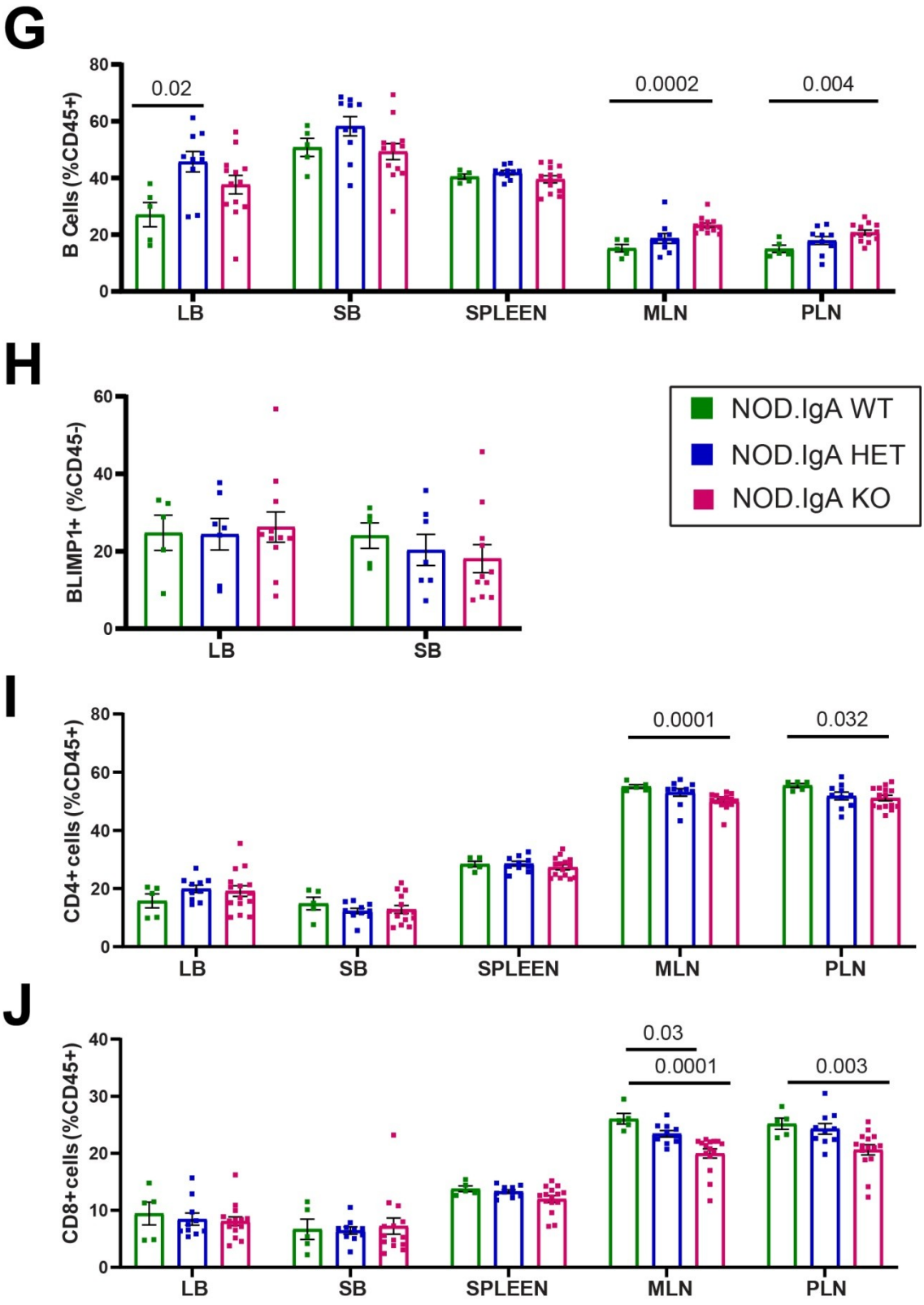
G
B Cells (%CD45+)
0.02
0.0002
0.004
LB
SB
SPLEEN
MLN
PLN
H
BLIMP1+ (%CD45-)
NOD.IgA WT
NOD.IgA HET
NOD.IgA KO
I
CD4+ cells (%CD45+)
0.0001
0.032
J
CD8+ cells (%CD45+)
0.03
0.0001
0.003

**Figure 3.2.2.1 GI immune responses in the NOD.IgA colony**

Fecal IgA levels (**A**) in NOD.IgA WT (green) and HET (blue) female mice at various ages (weeks). Fecal IgA levels (**B**) in the weeks preceding T1D diagnosis in individual animals. Fecal IgM levels (**C**) in NOD.IgA WT (green), HET (blue) and KO (pink) female mice at various ages (weeks). Fecal IgG levels (**D**) in NOD.IgA WT (green), HET (blue) and KO (pink) female mice @ 10-15 weeks of age. Fecal Lcn-2 levels (**E**) in NOD.IgA WT (green), HET (blue) and KO (pink) female mice at various ages (weeks). Fecal Lcn-2 levels (**F**) in the weeks preceding T1D diagnosis in individual animals. All fecal protein levels are expressed as a ratio of total protein present. B cell (**G**), plasma cell (**H**), $CD4^+$ T cell (**I**) and $CD8^+$ T cell (**J**) populations present in large bowel (LB), small bowel (SB), spleen, mesenteric lymph nodes (MLN) and pancreatic lymph node (PLN) at 12 weeks of age. Mean +/- SEM are indicated for all data, and p-values were determined using the Mann-Whitney U test.

### 3.2.2.2 Gut permeability is delayed in NOD.IgA HET and KO cohorts

Gut permeability is frequently detected in individuals during the early stages of T1D and is a possible mechanism contributing to the generation of autoimmunity[65]. As such, I assessed the three genotypes for degree of gut permeability in the early stages of disease onset (7 and 10 weeks of age), then again at 15 weeks of age in those that had yet to develop overt disease. I used a method involving oral gavage of fluorochrome-labeled dextran beads followed by detection of these beads in saphenous blood collected 4 hours later. This method assays gut permeability throughout the GI tract without differentiating between small and large intestinal permeability.

NOD.IgA WT females showed greatest gut permeability at 7 weeks, with gradually declining permeability at 10 & 15 weeks. The NOD.IgA KO cohort showed the opposite trend, with low permeability at 7 weeks that gradually increased through 10 weeks to peak at 15 weeks . As a group, permeability in the NOD.IgA HET cohort didn't change substantially with age but showed a fair bit more variability between animals than did the other two cohorts, particularly at 7 & 10 weeks of age. With respect to the NOD.IgA WT and KO cohorts, NOD.IgA HET permeability at 7 weeks was lower than WT and higher than KO, and at 15 weeks was higher than WT and lower than KO (**Fig 3.2.2.2A**).

Because the trends modestly mimicked the timing of disease incidence, particularly with respect to the NOD.IgA WT and KO cohorts, I sought to determine a pattern of gut permeability as a function of proximity to disease onset, similar to the peak in inflammation (ie Lcn-2 levels) observed in the weeks prior to diagnosis. However, I could not discern a pattern; the last measurements taken prior to diagnosis were located throughout the spread of data points, showing no consistency with being either the highest or lowest values at a given age (**Fig 3.2.2.2B-D, data points bordered in red**). When I compared gut permeability over time in each animal, noting the proximity of each measurement to the age at diagnosis, still no pattern emerged, due in part to not having enough longitudinal data points. Indeed I could find no pattern at all within each genotype. Some animals had low permeability at 7 weeks, which increased substantially by 10 weeks and remained the same at 15 weeks. Other animals showed progressive increase in permeability over the three time points, while others exhibited permeability which started low, peaked at 10 weeks, then decreased again by 15 weeks (**Fig**

**3.2.2.2B-D**). I next attempted to find a correlation between age at disease onset and gut permeability measurements at 7, 10 & 15 weeks but simple linear regression analyses showed very weak correlation at all three ages (**Fig 3.2.2.2E-G**).

In summary, gut permeability changes showed strong differences between the three genotype cohorts. Permeability in the NOD.IgA WT cohort was high at an early age and dropped considerably by 15 weeks, while the NOD.IgA KO cohort showed the opposite trend. However, the relevance of this gut permeability and its contribution to disease progression is difficult to determine as no patterns were apparent with respect to timing of T1D onset. I speculate that this variability is in large part due to the asynchronous dynamics and heterogeneous nature of T1D development in the NOD model.

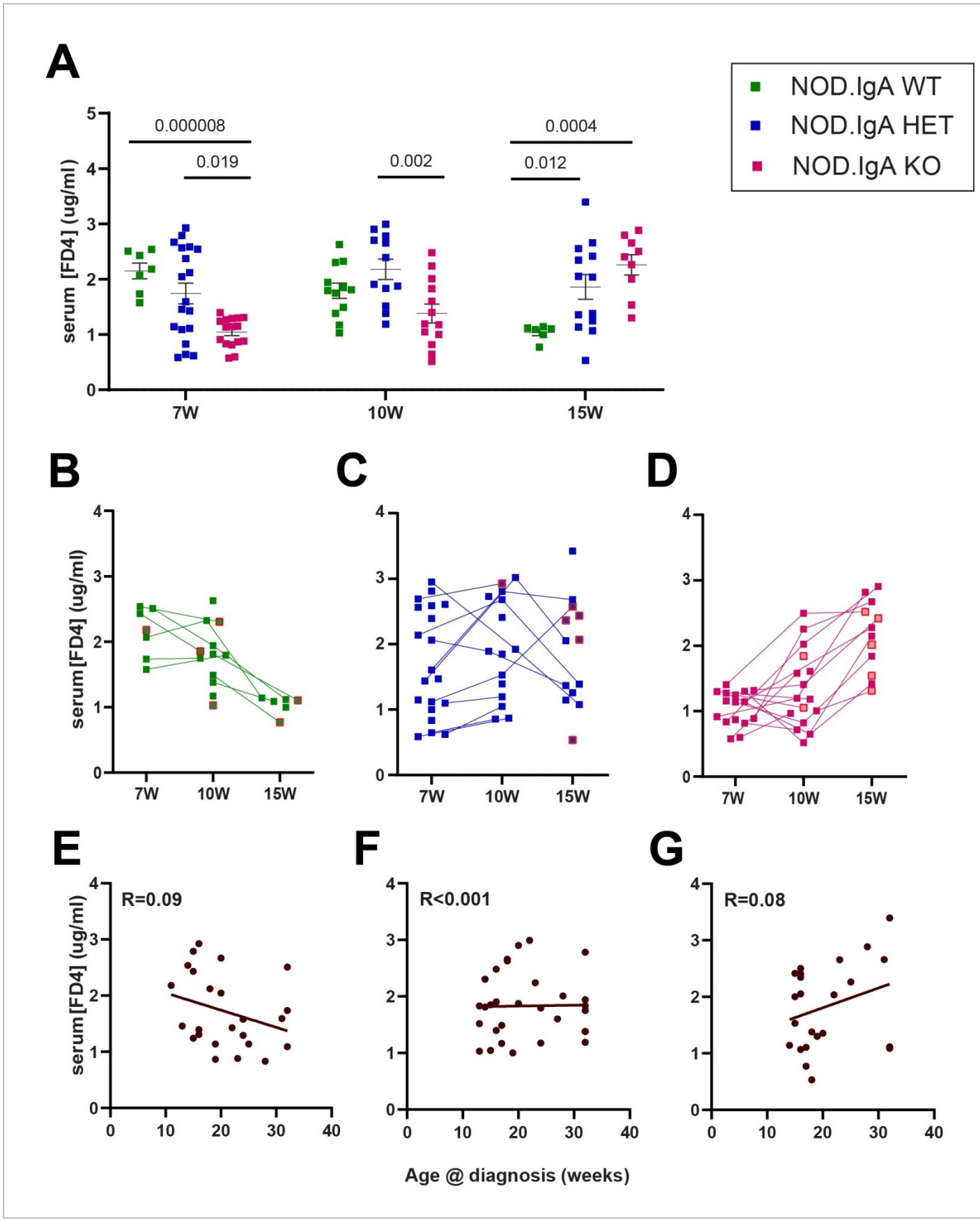
A
NOD.IgA WT
NOD.IgA HET
NOD.IgA KO
serum [FD4] (ug/ml)
0.000008
0.019
0.002
0.0004
0.012
7W
10W
15W
B
C
D
serum [FD4] (ug/ml)
7W
10W
15W
E
F
G
serum [FD4] (ug/ml)
R=0.09
R<0.001
R=0.08
Age @ diagnosis (weeks)

**Figure 3.2.2.2 Gut permeability in the NOD.IgA colony**

Gut permeability (**A**) in NOD.IgA WT (green), HET (blue) and KO (pink) mice at 7, 10 and 15 weeks of age, as measured by FD4 concentration in serum 4 hours after oral gavage. Gut permeability in NOD.IgA WT (**B**), HET (**C**) and KO (**D**) mice, where connecting lines between time points indicate measurements on the same mouse. Red-bordered data points indicate the last permeability measurement taken prior to T1D diagnosis. Correlations between age at T1D diagnosis and gut permeability at 7 (**E**), 10 (**F**) and 15 (**G**) weeks of age. For panel (**A**), mean +/- SEM are indicated and p-values were determined using the Mann-Whitney U test.

### 3.2.2.3 Serum immunoglobulin levels indicate both disease- and genotype-dependent systemic humoral responses

Without IgA to help maintain homeostasis in the gut mucosa, changes in microbial communities can lead to the colonization or overgrowth of invasive or pathogenic microorganisms and increased microbial translocation across the gut epithelial barrier, promoting a state of heightened mucosal tissue inflammation and a resultant systemic immune response. Additionally, a deficiency of serum IgA may result in compensatory heightened IgM or IgG production. Thus, we were interested in exploring how the loss of IgA might affect systemic humoral immunity in our colony. I performed ELISA on serum samples taken from adult female mice either during the pre-diabetic stage or at diagnosis and compared the IgA, IgG and IgM concentrations between the three genotypes. I found that serum IgA was similar between the NOD.IgA WT and HET animals in the pre-diabetic stage, and also similar between the two cohorts upon diabetes diagnosis. Indeed, the serum IgA concentrations appeared to be dependent on disease state rather than genotype; both cohorts showed a (near) significant increase in serum IgA levels after presenting with disease (**Fig 3.2.2.3A**). Furthermore, animals from both cohorts that became diabetic after 20 weeks of age showed greater levels of serum IgA compared to those presenting with diabetes prior to 20 weeks of age (**Fig 3.2.2.3B).** In comparison, serum samples from non-diabetic animals showed only modest increase in IgA levels with increasing age (**Fig 3.2.2.3B**). This sort of disparity in disease characteristics as a function of age at diagnosis has been noted in human T1D populations. Those diagnosed at earlier ages tend to exhibit higher levels of circulating AA, along with a greater degree of B lymphocyte and $CD8^+$ T lymphocyte islet infiltration and more pro-inflammatory $CD4^+$ T lymphocytes[3]. In this study, serum IgA concentration showed a fairly strong positive correlation with age at diagnosis in the diabetic NOD.IgA WT cohort ($R^2$=0.73) (**Fig 3.2.2.3C**).

Serum IgG concentrations, unlike IgA, were largely unaffected by disease status. Within each of the three genotype cohorts, the difference between the pre-diabetic and diabetic serum IgG levels were insignificant (**Fig 3.2.2.3D**). Rather, genotype appeared to be the major determinant of serum IgG, with the NOD.IgA KO cohort showing significantly higher levels in both the pre-diabetic and diabetic groups compared to the NOD.IgA WT and HET cohorts. Although it's tempting to speculate that the increased serum IgG observed in NOD.IgA KO

animals was a compensation for a lack of serum IgA, it doesn't show the same response to disease as the IgA serum levels did. In this respect, IgM is a much more likely candidate for IgA-deficiency compensation in the NOD.IgA KO. Their serum IgM levels were comparable to those of the NOD.IgA WT and HET animals in the pre-diabetes stage, but increased substantially after disease diagnosis (**Fig 3.2.2.3E**). Unlike IgA, however, age at disease diagnosis didn't appear to have an effect on IgM concentrations.

In summary, serum IgA level was associated with disease status in IgA-sufficient animals. Moreover, those that presented with less aggressive disease exhibited a stronger systemic IgA response. In IgA-deficient animals, systemic IgG responses were elevated in steady state whereas a systemic IgM response followed T1D diagnosis, mimicking the disease-dependent IgA response in the IgA-sufficient cohorts.

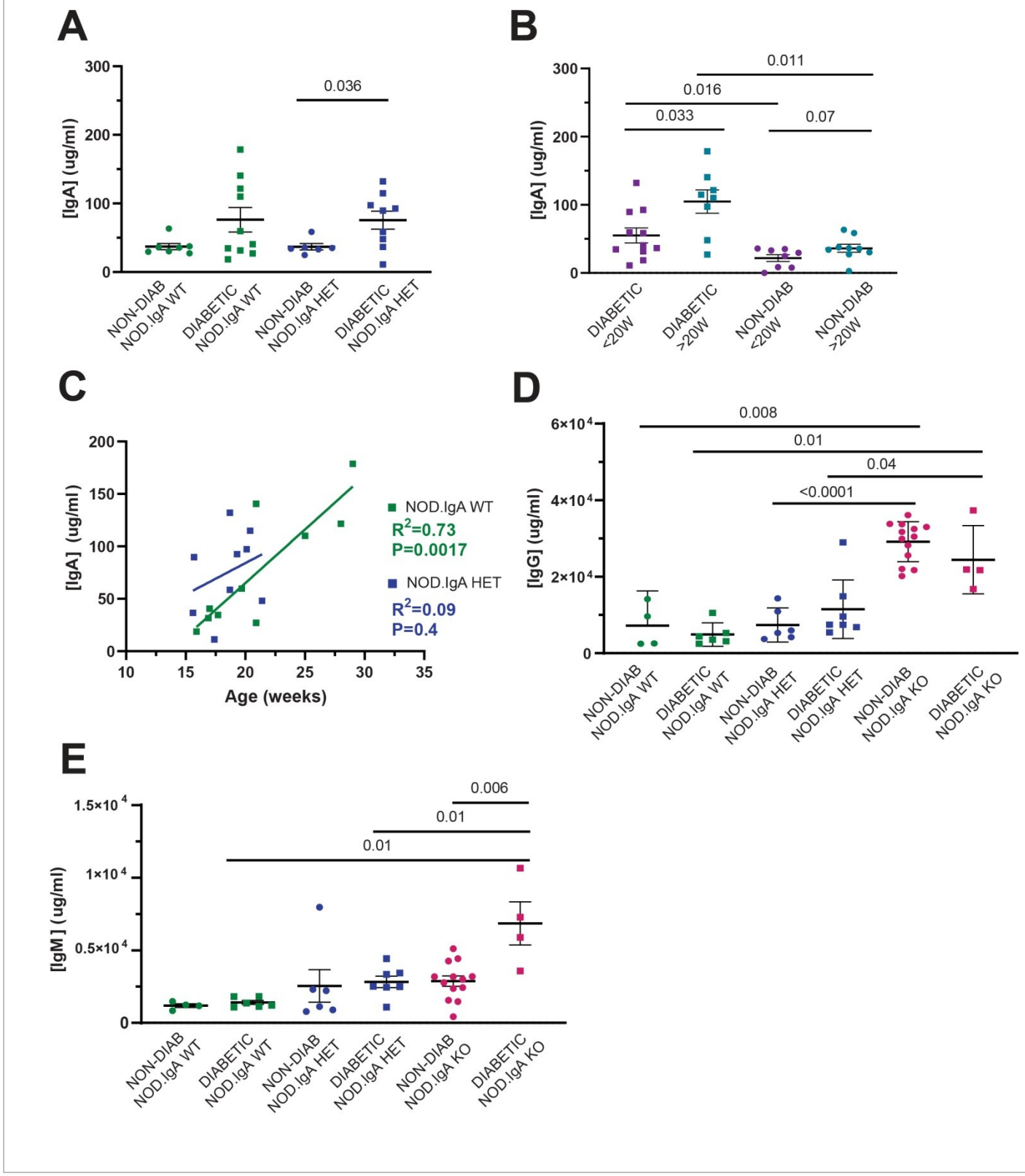
A
[IgA] (ug/ml)
300
200
100
0
0.036
NON-DIAB NOD.IgA WT
DIABETIC NOD.IgA WT
NON-DIAB NOD.IgA HET
DIABETIC NOD.IgA HET
B
[IgA] (ug/ml)
0.011
0.016
0.033
0.07
DIABETIC <20W
DIABETIC >20W
NON-DIAB <20W
NON-DIAB >20W
C
[IgA] (ug/ml)
200
150
100
50
0
10
15
20
25
30
35
Age (weeks)
NOD.IgA WT
R2=0.73
P=0.0017
NOD.IgA HET
R2=0.09
P=0.4
D
[IgG] (ug/ml)
6×10⁴
4×10⁴
2×10⁴
0
0.008
0.01
0.04
<0.0001
NON-DIAB NOD.IgA WT
DIABETIC NOD.IgA WT
NON-DIAB NOD.IgA HET
DIABETIC NOD.IgA HET
NON-DIAB NOD.IgA KO
DIABETIC NOD.IgA KO
E
[IgM] (ug/ml)
1.5×10⁴
1×10⁴
0.5×10⁴
0
0.006
0.01
0.01
NON-DIAB NOD.IgA WT
DIABETIC NOD.IgA WT
NON-DIAB NOD.IgA HET
DIABETIC NOD.IgA HET
NON-DIAB NOD.IgA KO
DIABETIC NOD.IgA KO

**Figure 3.2.2.3 Serum antibody levels in pre-diabetic and diabetic animals in the NOD.IgA colony**

Serum IgA concentration in pre-diabetic and diabetic NOD.IgA WT (green) and HET (blue) mice according to disease status (**A**) and age at diagnosis (**B**, **C**). Serum IgG (**D**) and IgM (**E**) concentration in pre-diabetic and diabetic NOD.IgA WT (green), HET (blue) and KO (pink) mice according to disease status. Mean +/- SEM are indicated for all data, and p-values were determined using the Mann-Whitney U test.

### 3.2.3 Exploring the effect of IgA deficiency on the microbiome of NOD mice

IgA production in the GI mucosa is upregulated in response to both host-derived and microbiota-provided stimuli. High affinity IgA is produced when host defenses encounter pathogenic or more invasive species in an effort to neutralize toxins, prevent infection and restore homeostasis. Commensal-reactive IgA, generally of lower affinity, tend to recognize cell surface antigen common to a broad range of species. Whether of high or low affinity, IgA binding to microbial cells results in inhibition of colony growth and nutrient acquisition, and prevents encroachment on the host epithelial barrier. IgA-bound glycans can also bind to various molecules on microbial cells and secure them in the mucus layer. Together, the various modes of action employed by IgA result in modulation of the host microbiota and maintenance of homeostasis. In light of this, a complete deficiency of IgA would most certainly result in shifts in the microbiome composition and we sought to ascertain what this would look like in our novel NOD.IgA colony.

#### 3.2.3.1 IgA deficiency affects the presence of specific members of the early microbiome

To ascertain how complete IgA deficiency affects microbiome colonization during early life, I collected fecal material from NOD.IgA WT, HET and KO mice at 5 weeks of age (n=6, 3, 6, respectively). 16S rRNA sequencing was performed and the bacterial composition was compared between the three cohorts. Interestingly, the results from principal component analyses (PCA) clearly showed that IgA sufficiency was not the strongest determinant of microbiome composition. Indeed, microbiota composition of the NOD.IgA HET and KO cohorts were remarkably similar to one another (p=1.0) and differed significantly from those of the NOD.IgA WT cohort (**Fig 3.2.3.1A)**. Furthermore, NOD.IgA HET and KO animals showed similar alpha diversity, which was considerably lower than that of the NOD.IgA WT animals (**Fig 3.2.3.1B**).

Having already determined that the NOD.IgA HET cohort was not an adequate IgA-sufficient control for comparison with NOD.IgA KO animals, I focused on comparing the microbiome composition between NOD.IgA WT and KO cohorts. I found that there were a number of notable differences. NOD.IgA WT mice showed enrichment for Lachnospiraceae (9 species)

and Muribaculaceae (10 species) families, as well as two *Alistipes* species and two *Eubacterium* species (**Fig 3.2.3.1C**). NOD.IgA KO mice were enriched for *Akkermansia muciniphila* and one *Parabacteroides* species (**Fig 3.2.3.1C).**

When I explored the metadata to elucidate an explanation for the similarities seen between the NOD.IgA HET & KO cohorts, I found that while all samples from the NOD.IgA WT cohort were collected from animals born into litters of a single genotype, samples from the NOD.IgA HET and KO cohorts were collected from animals born into litters of mixed genotype. Although this was unintentional, I chose these particular animals in an attempt to limit extra variables. Given the strong influence of maternal factors in offspring microbiome modulation, my intention had been to ensure that all dams were IgA-sufficient so any differences perceived in offspring microbiota would be due to their genotype. However, in order to obtain NOD.IgA KO offspring from IgA-sufficient dams, a breeding scheme which resulted in mixed NOD.IgA HET & KO litters was required (**Fig 2.1.2E**). Thus, it appears from this data that sharing a womb and early life experiences with siblings results in very similar microbiota regardless of IgA sufficiency status. Moreover, it is more complicated than this - 4 different litters are represented by the 3 HET & 6 KO animals. The only variable that unifies these two cohorts, while setting them apart from the NOD.IgA WT animals, is that the HET & KO pups were born to NOD.IgA HET dams whereas the NOD.IgA WT animals were born to NOD dams (see breeding schemes in **Fig 2.1.2**). Having already established that NOD.IgA HET and WT females differ significantly, it is very possible that this accounts for the microbiome differences between their IgA-sufficient offspring. Paternal factors may also be playing a part despite the prompt removal of the sire from the cage, since 7 of the 9 NOD.IgA HET and KO progeny were sired by NOD.IgA KO males (one litter was sired by a NOD.IgA HET male), in contrast to the NOD.IgA WT animals that were all sired by NOD males. Alternatively, it is possible that the sharing of microorganisms between littermates resulted in a microbiome composition that was unique from those of NOD.IgA HET and KO pups born into single genotype litters. If this was the case, where IgA deficiency-induced modifications in some pups have the ability to significantly alter the microbiome of the entire litter, this speaks to the degree of influence that IgA has on the microbiota. Thus, in hindsight, including samples from single genotype litters of NOD.IgA HET animals would have been very informative.

Thus, the most certain conclusions I can draw from this data set are that (1) microbiota between littermates are very similar in composition, regardless of whether or not a pup is IgA-sufficient, and (2) microbiome colonization is a complex process, subject to influences by many variables even within carefully-controlled animal studies. This data set suggests that, in the absence of microorganism sharing between genotypes, IgA deficiency results in a decline of several Lachnospiraceae and Muribaculaceae family members, concomitant with an increase of *Akkermansia muciniphila* and one *Parabacteroides* species in the early microbiome.

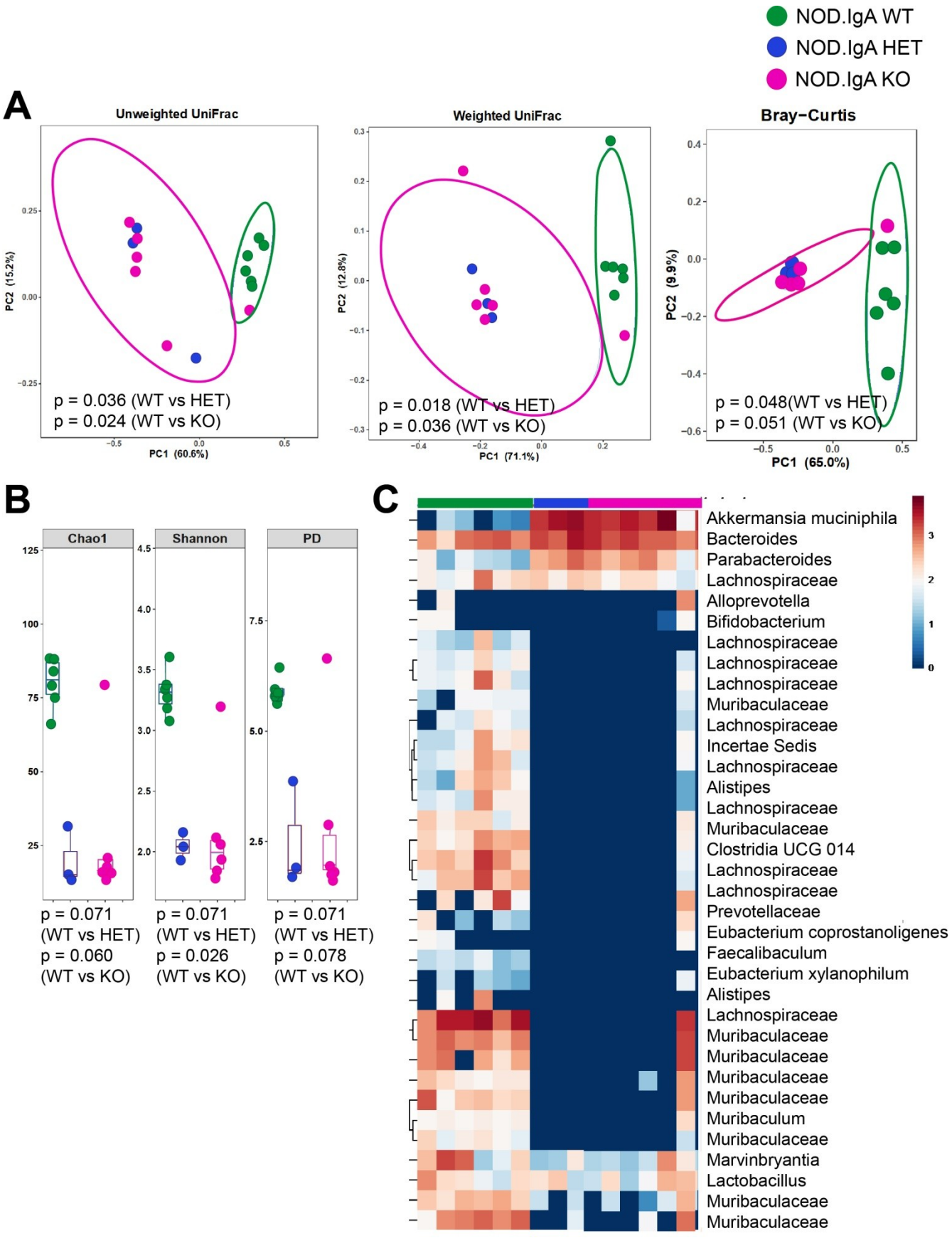
NOD.IgA WT
NOD.IgA HET
NOD.IgA KO
A
Unweighted UniFrac
PC2 (15.2%)
PC1 (60.6%)
p = 0.036 (WT vs HET)
p = 0.024 (WT vs KO)
Weighted UniFrac
PC2 (12.8%)
PC1 (71.1%)
p = 0.018 (WT vs HET)
p = 0.036 (WT vs KO)
Bray−Curtis
PC2 (9.9%)
PC1 (65.0%)
p = 0.048(WT vs HET)
p = 0.051 (WT vs KO)
B
Chao1
Shannon
PD
p = 0.071
(WT vs HET)
p = 0.060
(WT vs KO)
p = 0.071
(WT vs HET)
p = 0.026
(WT vs KO)
p = 0.071
(WT vs HET)
p = 0.078
(WT vs KO)
C
Akkermansia muciniphila
Bacteroides
Parabacteroides
Lachnospiraceae
Alloprevotella
Bifidobacterium
Lachnospiraceae
Lachnospiraceae
Lachnospiraceae
Muribaculaceae
Lachnospiraceae
Incertae Sedis
Lachnospiraceae
Alistipes
Lachnospiraceae
Muribaculaceae
Clostridia UCG 014
Lachnospiraceae
Lachnospiraceae
Prevotellaceae
Eubacterium coprostanoligenes
Faecalibaculum
Eubacterium xylanophilum
Alistipes
Lachnospiraceae
Muribaculaceae
Muribaculaceae
Muribaculaceae
Muribaculaceae
Muribaculum
Muribaculaceae
Marvinbryantia
Lactobacillus
Muribaculaceae
Muribaculaceae

**Figure 3.2.3.1 Analysis of the early microbiota in NOD.IgA WT, HET & KO mice**

Analysis of NOD.IgA WT (green), HET (blue) and KO (pink) microbiome composition in fecal samples taken at 5 weeks of age, showing (**A**) principal component analysis plots, (**B**) alpha diversity measures, and (**C**) heatmap of taxa enrichment between the three cohorts. Each dot represents one animal. P values were determined using Wilcoxon rank sum exact test. Raw data analysis and image production was performed by Dr. Tingting Ju (laboratory of Dr. Ben Willing) in the Faculty of Agricultural, Life and Environmental Sciences at the University of Alberta.

## 3.3 Discussion

The importance of sIgA to mucosal immunity, coupled with plentiful reports of aberrant IgA responses in T1D-affected individuals, led us to hypothesize that the complete absence of IgA from the immune repertoire would result in mal-adaptations in the gut microbiota, creating prime conditions for triggering of autoimmune responses and leading to earlier onset and/or increased incidence of T1D in our novel NOD.IgA colony. The most striking discovery was that IgA deficiency did not alter T1D incidence, and in fact delayed its onset significantly. This delay in onset was accompanied by a similar delay in gut permeability, but heightened gut humoral responses starting as early as 5 weeks of age and persisting into adulthood. IgA-deficient animals compensated for this deficiency with increased production of luminal and serum IgM. Serum IgG was also elevated in adulthood, possibly a response to changes in the microbiota, as has been demonstrated by others[119]. Moreover, when early microbial sharing between IgA-sufficient and -deficient pups was present, IgA sufficiency on its own wasn't a strong contributor to microbiome composition. In these situations, dispersion of microorganisms between animals of differing genotypes masked any influence from IgA modulation. However, the microbiota differences between the NOD.IgA WT and KO animals was significant, suggesting that IgA deficiency in the absence of microbial sharing may drive considerable microbiome modulation.

The connection between selective IgA deficiencies and T1D in humans is unclear, particularly when taking into account studies that show increased GI sIgA levels in T1D patients[61]. Moreover, our finding that IgA deficiency delays T1D in NOD mice further confounds the subject. An explanation for this apparent contradiction may involve an understanding that differences exist between systemic and mucosal IgA class switch induction and IgA production[67]. Selective IgA deficiency is diagnosed by measuring serum IgA alone, with no assessment of mucosal IgA production. Moreover, selective IgA deficiencies are frequently not a result of mutations in the α switch or constant regions, but involve mutations affecting B lymphocyte maturation and/or differentiation. For example, selective IgA deficiency has been linked with mutations in BAFF and APRIL as well as mutations in their receptors[163]. Since signalling through these receptors influences a number of downstream processes, such as B lymphocyte maturation and differentiation to PC and memory B cell phenotypes, it is very

possible that the link between selective IgA deficiency and T1D is related to the function of B cells/PC rather than the loss of systemic IgA. Indeed, B lymphocytes and PC play important roles in immunity beyond antibody production, and $IgA^+$ PC have been shown to be indispensable in the amelioration of autoimmune-mediated destruction in animal models of multiple sclerosis[174]. Since I did not observe a decline in systemic or mucosal B lymphocytes or PC in our IgA-deficient NOD model, we anticipate that these additional immune functions were unaffected by the introduction of the IgA deletion allele.

The effects of complete IgA deficiency on immune function in the GI mucosa, and the subsequent modulation of the microbiota, are undeniably complex and multifaceted. sIgA can target specific, more invasive or pathogenic species, so its absence would leave the host prone to infection. Even in the absence of overt infection, such as our controlled experiments in SPF housing conditions, overgrowth of invasive species could heighten inflammation along the GI tract. Indeed, I observed signs of increased GI inflammation in the NOD.IgA KO cohort from as early as 5 weeks of age. These effects would trigger changes in the microbial community, as well as contribute to risk factors associated with T1D onset. Furthermore, lacking sIgA with commensal species cross-reactivity would be expected to contribute to dynamic changes in the microbiota. Thus, it was somewhat surprising to find that significant microbiome differences did not exist between the IgA-sufficient and -deficient mice when the maternal variable was controlled. Furthermore, we did not observe increased T1D incidence in the IgA-deficient cohort, possibly because GI-associated risk factors are already amplified in NOD mice[162]. Moreover, IgA deficiency in this study, as well as in others[164,169], is compensated to some degree by increased IgM and IgG production. The pIgR is capable of trans-epithelial transport of polymeric IgM, perhaps allowing for a degree of microbiome manipulation in the absence of sIgA. Furthermore, our data provides compelling evidence of increased IgG presence in the gut lumen of IgA-deficient animals, likely via FcRn-mediated transport[115], which can provide a means of controlling invasive or pathogenic species. Perhaps this compensation is one reason why selective IgA deficiencies do not often lead to life-threatening health outcomes[75,163].

One difficulty that plagued my study was that of trying to ensure appropriate timing of comparison between the three genotypes. Most studies either age-match their experimental

animals, or in a disease model, ensure that experimental animals are at the same stage of disease development. In our model of spontaneous T1D, this proved very difficult to do. Since T1D onset is spontaneous, and age at diagnosis varies between 12 - 30 weeks of age, age-matching animals seemed largely irrelevant and determining stage of disease was not possible for terminal procedures, where mice could no longer be followed for overt T1D. As a solution to this problem, albeit an imperfect one, I chose 12 weeks of age as the 'adult' stage for any experimental comparisons requiring a lethal procedure; since no animal in my study became diabetic before this age, it constituted a dependably pre-diabetic adult age.

An extension of this difficulty arose with breeding dams. Undeniably, disease processes at work during pregnancy and breastfeeding affected various developmental aspects of the offspring, and I found this very difficult to control for. Any dam that tested positive for glucosuria while pregnant or breastfeeding was euthanized along with her litter. However, this didn't control for variables introduced to offspring when dams developed glucosuria within days of weaning, since disease-related physiological effects would undoubtedly have been present for weeks prior to diagnosis. On the other hand, the practical and financial consequences of discarding all offspring from dams diagnosed within 2 weeks of weaning made this an impractical option. Thus, unaccounted variables certainly exist within the data discussed in this thesis and are in part a reason for some of the variability seen throughout.

# Chapter 4: Results – Maternal Dysbiosis as an Influencer of Disease in Offspring

## 4.1 Introduction

The mammalian microbiome functions as a complex organic input/output device. Numerous outputs are attributed to the microbiota and have been the subjects of much research for the last few decades. Broadly, they can be categorized into topics such as 'host health', 'immune development & regulation', and 'gut homeostasis'. T1D development is one such output and its pathogenesis is attributable to the synergistic effects of numerous input factors. These factors are complex, showing much variation between individuals, and include things like diet, infection history, use of antibiotics, geographical location, rural vs. urban living, genetic predispositions, etc[108]. Although we are just beginning to understand how these factors may be contributing to outcomes such as T1D, there is overwhelming evidence to support that they do strongly contribute.

Maternal factors and their influence as input to microbiome development is a subject that has received considerable attention. The effects of birth mode and breastfeeding have been widely studied, with the majority of studies confirming their influence on offspring microbiome composition and long-term health[108]. Similarly, most studies support that the maternal microbiome is a major contributor to a child's microbiome composition[108]. Microbes from the maternal microbiome seed the neonatal GI tract, establishing early colonization and influencing the colonization of species that follow. The infant microbiome is also key to neonatal immune development, influencing the expanding lymphocyte populations and dictating the repertoire of tolerated antigens[94]. With all this in mind, the observation that mothers can transmit disease-associated dysbiosis to their offspring[166,167] leads to the erroneous assumption that T1D susceptibility is increased for children from affected mothers. Indeed, the finding that affected mothers appear to provide their offspring with protection from T1D[33–43] is of particular interest to us. In this chapter, I discuss my data comparing maternal IgA-sufficient vs -deficient NOD.IgA HET cohorts, to dissect the impact of IgA deficiency-induced maternal dysbiosis on offspring gut microbe-immune interactions and T1D development.

## 4.2 Results

### 4.2.1 Effect of maternal IgA deficiency on T1D incidence in offspring

The unexpected observations that IgA deficiency did not alter T1D incidence in our mouse model but contributed to heightened immune responses and an altered GI environment, led me to question whether maternal IgA deficiency may have an effect on subsequent generations. I have shown that a lack of IgA resulted in changes in the microbiota community in T1D-prone females (Section 3.2.3), a situation similar to what is observed in human mothers affected by T1D. Moreover, vertical transmission of disease-associated dysbiosis has been reported in studies on gestational and type II diabetes[165–168]. Here, I hypothesized that IgA deficiency-induced maternal dysbiosis would be reflected in offspring, contributing to an inflammatory GI environment, improper immune regulation and elevated T1D incidence. To explore this, I analyzed the incidence of T1D in the NOD.IgA colony from the perspective of maternal origin to determine how maternal IgA deficiency affected disease incidence in offspring.

#### 4.2.1.1 Maternal IgA deficiency alters disease susceptibility in the next generation

The various breeding schemes allowed me to investigate T1D incidence in our colony based on maternal origin; that is, whether an animal was born to IgA-sufficient or -deficient dam. Using the same incidence data reported in Section 3.2.1.1, I compared the incidence of disease in the NOD.IgA HET and KO cohorts when taking into account the maternal genotype. This was not a possible comparison for the NOD.IgA WT animals, as they are all offspring of IgA-sufficient dams. When comparing the NOD.IgA KO offspring from WT dams (mIgA+ KO) to those from KO dams (mIgA- KO), the disease curves looked very similar and there was no difference in age at disease onset (**Fig 4.2.1.1A,C**). When comparing the HET offspring from NOD.IgA WT vs KO dams (mIgA+ HET and mIgA- HET, respectively) I observed a significant difference in disease incidence such that mIgA- HET offspring had a decreased incidence over 30 weeks, although age at onset was unaltered (**Fig 4.2.1.1B,C**). These observations suggest that maternal factors from an IgA-deficient dam reduce offspring susceptibility to disease during the neonatal period, and this protection is maintained in IgA-sufficient offspring. However, without endogenous IgA production, as is the case for NOD.IgA KO offspring, the early protective phenotype is lost and disease incidence returns to

elevated levels. Upon further contemplation, I wondered whether this protective maternal effect was being mediated by the dysbiotic microbiome present in the NOD.IgA KO dams and influencing both microbiome establishment and immune system development in the offspring during the neonatal period. To investigate this, I endeavored to characterize the early microbiome as well as both mucosal and systemic immune development in the two HET cohorts.

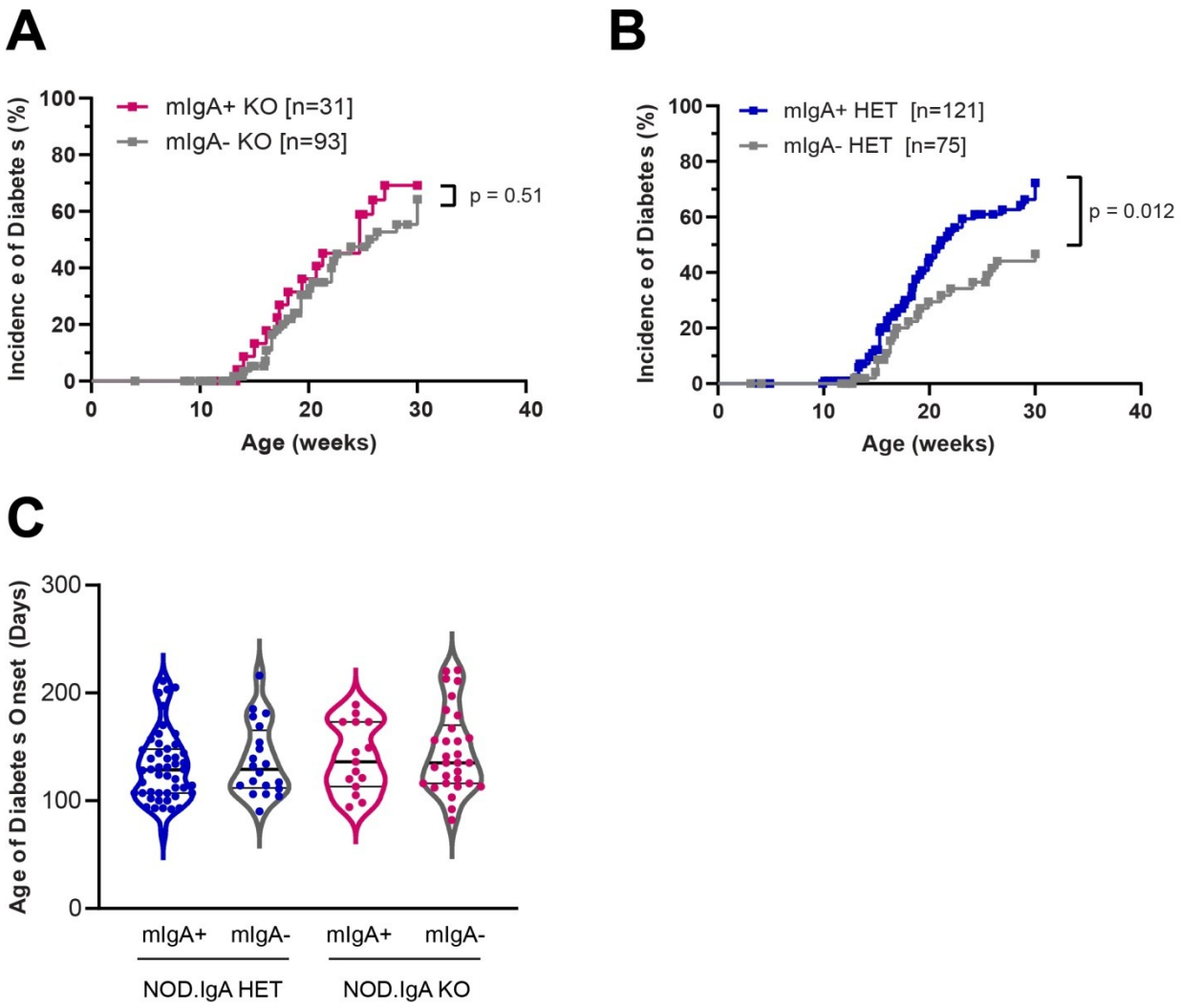


**Figure 4.2.1.1 Incidence of T1D in offspring from IgA-sufficient vs -deficient dams**

Incidence curve (**A**) shows T1D incidence in NOD.IgA KO offspring born to IgA-sufficient (pink) and -deficient (grey) dams. Incidence curve (**B**) shows T1D incidence in NOD.IgA HET offspring born to IgA-sufficient (blue) and -deficient (grey) dams. Violin plot (**C**) shows age of onset of T1D in each of the four cohorts, where mean +/- SEM is indicated for each cohort. p-values were determined using the Log-rank test for panels (A) and (B), and the Mann-Whitney U test for panel (C).

### 4.2.2 Maternal IgA deficiency-induced microbiome changes in IgA-sufficient offspring

The discovery that maternal IgA deficiency lowered T1D incidence in the following generation prompted me to re-examine my initial hypothesis. Indeed, the observation of a protective effect in the mIgA- HET cohort concurs with what is reported amongst human T1D populations - that disease prevalence is lowered when children are born to affected mothers vs. affected fathers[33–43]. Thus, I revised my theory, hypothesizing that maternal dysbiosis arising from complete IgA deficiency results in bolstered immune development in offspring, enhancing immune regulation and lowering T1D incidence in later life. In the following sections, I explore the effects of IgA deficiency on the maternal microbiome, and how these changes modulate microbiome development in offspring.

#### 4.2.2.1 Multi-generational IgA deficiency promotes a highly diverse microbiome in NOD.IgA KO dams

As described in Section 2.1.2, I designed breeding schemes with much attention to detail. mIgA+ HET offspring were derived from mating NOD females with NOD.IgA KO males (**Figure 2.1.2C**). These NOD dams were all from the NOD strain, thus were of a long line of IgA-sufficient dams. Conversely, mIgA- HET offspring were generated from NOD.IgA KO females mated with NOD males (**Figure 2.1.2D**). These NOD.IgA KO dams were all progeny of NOD.IgA KO dams (**Figure 2.1.2B**), thus from >3 generations of maternal IgA-deficiency. After so many generations lacking both endogenous and maternally-provided IgA, I sought to investigate the effects on the NOD.IgA KO microbiome in an effort to determine whether these dams harbored a microbiome substantially different than that of the NOD dams.

Fecal material from 10-15 week NOD (n=6) and NOD.IgA KO (n=10) females were analyzed for bacterial content using 16S rRNA sequencing. Comparison of the bacterial communities using principal component analyses yielded differing results depending on the type of analysis used – unweighted UniFrac showed a significant overall difference between the two dam groups (p=0.004) (**Figure 4.2.2.1A**), while weighted UniFrac and Bray-Curtis analyses determined the differences were not significant (p=0.25 & 0.11, respectively). Using various measures of alpha diversity, each showed a significantly more diverse microbiome community in the NOD.IgA KO females (**Figure 4.2.2.1B**). Significantly enriched taxa included

Lachnospiraceae (5 species), Rikenellaceae (2 species), and Oscillospiraceae (3 species). One species from the genus *Lactobacillus* and one from the family Butyricicoccaceae were noted to be enriched but did not reach significance (**Figure 4.2.2.1C**). Conversely, several taxa present in the NOD females were depleted in the NOD.IgA KO females, and included species from the families Lachnospiraceae (1), Muribaculaceae (4), and Atopobiaceae (1) (**Figure 4.2.2.1C**). Notably, the avid mucin degrader *Akkermansia muciniphila* was found enriched in the NOD females, particularly at 10 weeks of age, but depleted in the NOD.IgA KO females, and one *Parabacteroides* species was modestly over-representation in some of the NOD females (**Figure 4.2.2.1C**). Overall, multi-generational IgA deficiency boosted the diversity of bacterial species comprising the microbiota, while at the same time facilitating the depletion of other species, including *Akkermansia muciniphila.*

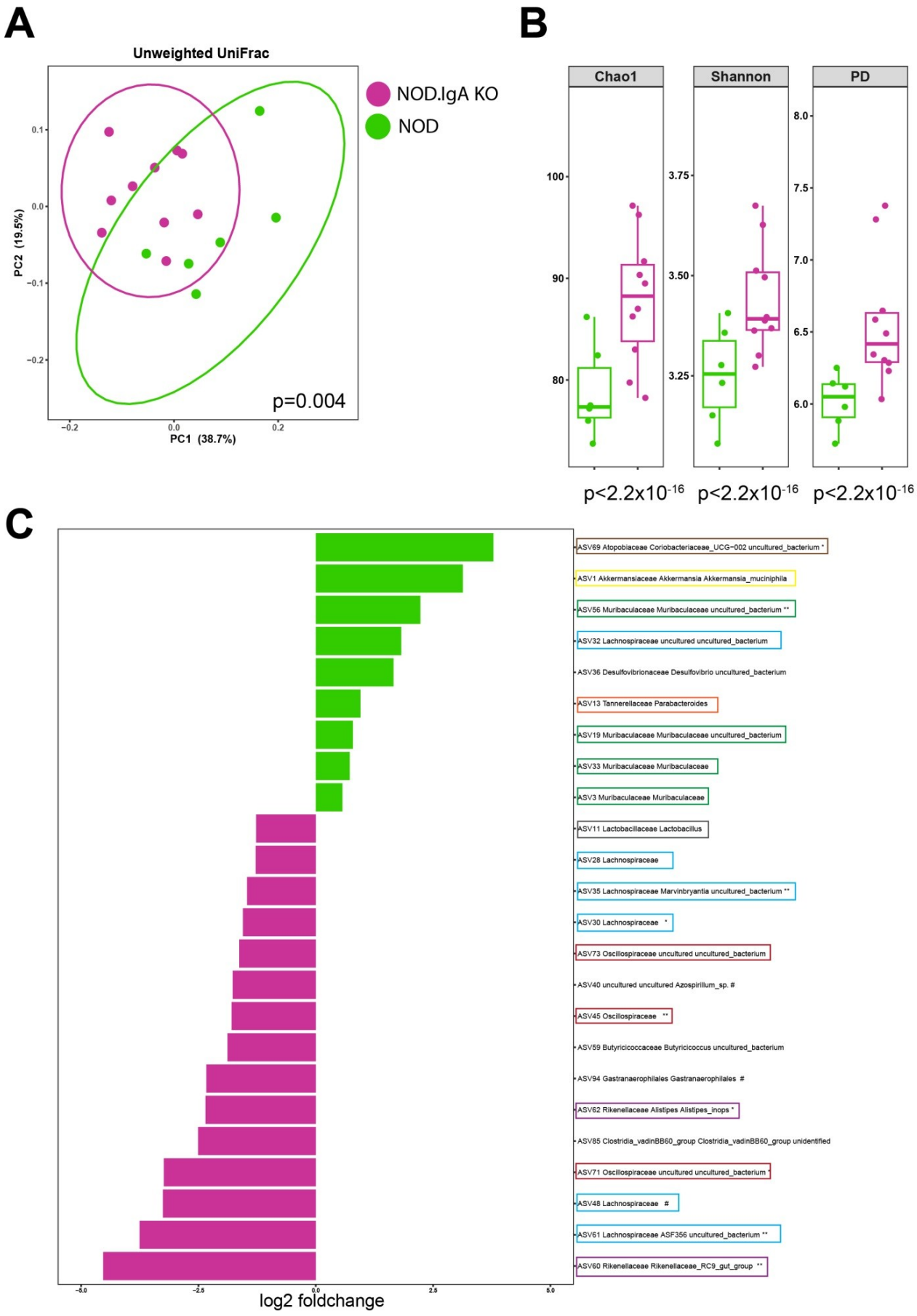
A
Unweighted UniFrac
NOD.IgA KO
NOD
p=0.004
PC1 (38.7%)
PC2 (19.5%)
B
Chao1
Shannon
PD
p<2.2x10-16
p<2.2x10-16
p<2.2x10-16
C
ASV69 Atopobiaceae Coriobacteriaceae_UCG−002 uncultured_bacterium *
ASV1 Akkermansiaceae Akkermansia Akkermansia_muciniphila
ASV56 Muribaculaceae Muribaculaceae uncultured_bacterium **
ASV32 Lachnospiraceae uncultured uncultured_bacterium
ASV36 Desulfovibrionaceae Desulfovibrio uncultured_bacterium
ASV13 Tannerellaceae Parabacteroides
ASV19 Muribaculaceae Muribaculaceae uncultured_bacterium
ASV33 Muribaculaceae Muribaculaceae
ASV3 Muribaculaceae Muribaculaceae
ASV11 Lactobacillaceae Lactobacillus
ASV28 Lachnospiraceae
ASV35 Lachnospiraceae Marvinbryantia uncultured_bacterium **
ASV30 Lachnospiraceae *
ASV73 Oscillospiraceae uncultured uncultured_bacterium
ASV40 uncultured uncultured Azospirillum_sp. #
ASV45 Oscillospiraceae **
ASV59 Butyricicoccaceae Butyricicoccus uncultured_bacterium
ASV94 Gastranaerophilales Gastranaerophilales #
ASV62 Rikenellaceae Alistipes Alistipes_inops *
ASV85 Clostridia_vadinBB60_group Clostridia_vadinBB60_group unidentified
ASV71 Oscillospiraceae uncultured uncultured_bacterium *
ASV48 Lachnospiraceae #
ASV61 Lachnospiraceae ASF356 uncultured_bacterium **
ASV60 Rikenellaceae Rikenellaceae_RC9_gut_group **
log2 foldchange

**Figure 4.2.2.1 Microbiome analysis of NOD and NOD.IgA KO adult females**

Principal component analysis (PCA) plot (**A**) of NOD (green) and NOD.IgA (pink) microbiota from 16S rRNA sequencing data. Alpha diversity (**B**) of the two female cohorts using three different diversity measures. Barplot (**C**) showing taxa enriched in NOD (green) and NOD.IgA KO (pink) females. Lachnospiraceae members are boxed in turquoise, Muribaculaceae in green, Oscillospiraceae in red, Rikenellaceae in purple, *Parabacteroides* in orange, Atopobiaceae in brown, *Lactobacillus* in grey and *Akkermansia muciniphila* in gold. Raw data analysis and image production was performed by Dr. Tingting Ju (laboratory of Dr. Ben Willing) in the Faculty of Agricultural, Life and Environmental Sciences at the University of Alberta.

#### 4.2.2.2 Early microbiome composition is heavily influenced by maternal IgA status

My data provided evidence of considerable differences in the microbiota composition of the two groups of dams used to generate the mIgA+ and mIgA- HET cohorts. This scenario, where two genetically-identical offspring cohorts were birthed by genetically- and phenotypically-distinct dams, provided an excellent opportunity to explore the influence of maternal factors, particularly the maternal microbiome, on offspring microbiome development.

Fecal material from 5 week old mIgA+ and mIgA- HET females were collected and their bacterial composition determined via 16S rRNA sequencing. As a group, the two cohorts showed significant differences in composition ($p=0.025$) and clustered based on maternal heritage (**Figure 4.2.2.2A**). Furthermore, the alpha diversity present in each group strongly reflected that of their respective dam, with the mIgA- HET cohort showing significantly more diversity ($p<0.005$) than the mIgA+ cohort (**Figure 4.2.2.2B**). Not surprisingly, some of the species found enriched in NOD dams showed increased prevalence in the mIgA+ HET cohort. These included both *Akkermansia muciniphila* and *Parabacteroides* species. Likewise, some species present at increased proportions in the NOD.IgA KO dams, including several Lachnospiraceae species, *Alistipes inops*, and one *Lactobacillus* species, were enriched in the mIgA- HET offspring (**Figure 4.2.2.2C**).

Some of the increased diversity apparent in the mIgA- HET cohort, along with a number of enriched species, could not be accounted for strictly by maternal transmission. Although these species were very likely present in the dams, they were not enriched in NOD.IgA KO dams. Hence, this is evidence of additional factors influencing the growth of these species in NOD.IgA HET offspring, factors independent of IgA status and initial maternal seeding. These species included those belonging to Lachnospiraceae, Muribaculaceae, Prevotellaceae, *Enterorhabdus*, *Alistipes, Bifidobacterium*, *Rikenella*, and *Lactobacillus* (**Figure 4.2.2.2C, yellow star**). These elusive influences were also apparent in the observation that some bacterial species enriched in NOD dams were found in increased prevalence in mIgA- HET

offspring (**Figure 4.2.2.2C, red star**). Possible explanations for these observations will be discussed in Section 4.3.

By 10-15 weeks of age, microbiome composition differences between the two NOD.IgA HET cohorts had largely vanished. Principal component analyses no longer showed significance (**Figure 4.2.2.2D**) and alpha diversity appeared comparable in most of the samples (**Figure 4.2.2.2E**). The one distinction that persisted was the enrichment of *Akkermansia muciniphila* in the mIgA+ HET cohort (**Figure 4.2.2.2F**). This finding is in line with other studies on the early microbiome, where sub-optimal GI events during the weaning period led to dysregulated autoimmunity in adulthood, but did not leave a detectable mark on the microbiota[79,81].

In summary, the early microbiota of each NOD.IgA HET cohort showed considerable similarities to the maternal microbiota, both with respect to the alpha diversity present as well as the presence or absence of specific community members. Furthermore, there was evidence of species enrichment in the mIgA- HET cohort that appeared independent of the maternal microbiome. The differences in microbiome composition between the two HET cohorts seen at 5 weeks were largely lost in adulthood, underscoring the importance of early microbiome influences on long-term health despite a lack of compositional differences in adulthood.

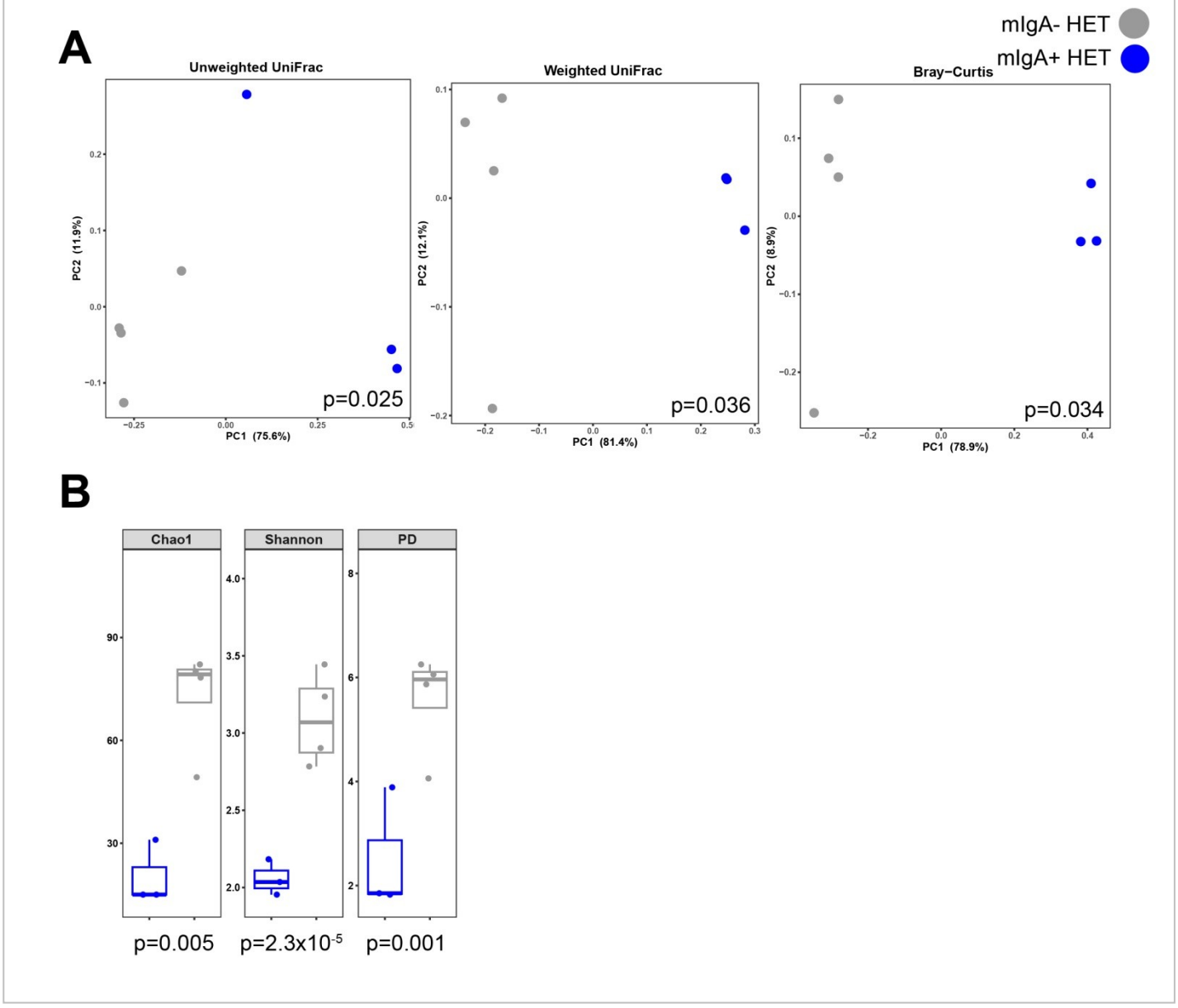
A
mIgA- HET
mIgA+ HET
Unweighted UniFrac
Weighted UniFrac
Bray−Curtis
PC2 (11.9%)
PC1 (75.6%)
p=0.025
PC2 (12.1%)
PC1 (81.4%)
p=0.036
PC2 (8.9%)
PC1 (78.9%)
p=0.034
B
Chao1
Shannon
PD
p=0.005
p=2.3x10-5
p=0.001

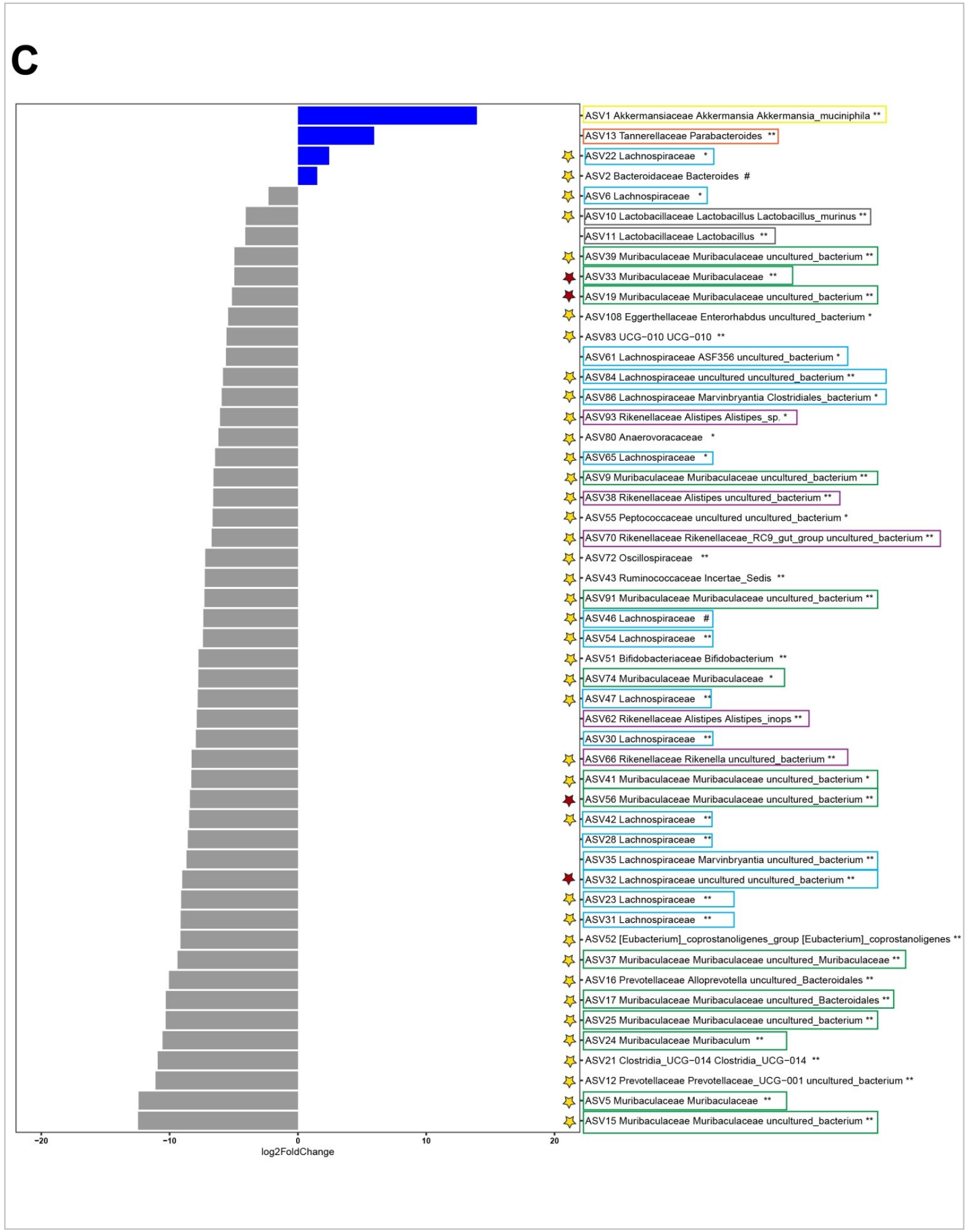
C
ASV1 Akkermansiaceae Akkermansia Akkermansia_muciniphila **
ASV13 Tannerellaceae Parabacteroides **
ASV22 Lachnospiraceae *
ASV2 Bacteroidaceae Bacteroides #
ASV6 Lachnospiraceae *
ASV10 Lactobacillaceae Lactobacillus Lactobacillus_murinus **
ASV11 Lactobacillaceae Lactobacillus **
ASV39 Muribaculaceae Muribaculaceae uncultured_bacterium **
ASV33 Muribaculaceae Muribaculaceae **
ASV19 Muribaculaceae Muribaculaceae uncultured_bacterium **
ASV108 Eggerthellaceae Enterorhabdus uncultured_bacterium *
ASV83 UCG-010 UCG-010 **
ASV61 Lachnospiraceae ASF356 uncultured_bacterium *
ASV84 Lachnospiraceae uncultured uncultured_bacterium **
ASV86 Lachnospiraceae Marvinbryantia Clostridiales_bacterium *
ASV93 Rikenellaceae Alistipes Alistipes_sp. *
ASV80 Anaerovoracaceae *
ASV65 Lachnospiraceae *
ASV9 Muribaculaceae Muribaculaceae uncultured_bacterium **
ASV38 Rikenellaceae Alistipes uncultured_bacterium **
ASV55 Peptococcaceae uncultured uncultured_bacterium *
ASV70 Rikenellaceae Rikenellaceae_RC9_gut_group uncultured_bacterium **
ASV72 Oscillospiraceae **
ASV43 Ruminococcaceae Incertae_Sedis **
ASV91 Muribaculaceae Muribaculaceae uncultured_bacterium **
ASV46 Lachnospiraceae #
ASV54 Lachnospiraceae **
ASV51 Bifidobacteriaceae Bifidobacterium **
ASV74 Muribaculaceae Muribaculaceae *
ASV47 Lachnospiraceae **
ASV62 Rikenellaceae Alistipes Alistipes_inops **
ASV30 Lachnospiraceae **
ASV66 Rikenellaceae Rikenella uncultured_bacterium **
ASV41 Muribaculaceae Muribaculaceae uncultured_bacterium *
ASV56 Muribaculaceae Muribaculaceae uncultured_bacterium **
ASV42 Lachnospiraceae **
ASV28 Lachnospiraceae **
ASV35 Lachnospiraceae Marvinbryantia uncultured_bacterium **
ASV32 Lachnospiraceae uncultured uncultured_bacterium **
ASV23 Lachnospiraceae **
ASV31 Lachnospiraceae **
ASV52 [Eubacterium]_coprostanoligenes_group [Eubacterium]_coprostanoligenes **
ASV37 Muribaculaceae Muribaculaceae uncultured_Muribaculaceae **
ASV16 Prevotellaceae Alloprevotella uncultured_Bacteroidales **
ASV17 Muribaculaceae Muribaculaceae uncultured_Bacteroidales **
ASV25 Muribaculaceae Muribaculaceae uncultured_bacterium **
ASV24 Muribaculaceae Muribaculum **
ASV21 Clostridia_UCG-014 Clostridia_UCG-014 **
ASV12 Prevotellaceae Prevotellaceae_UCG-001 uncultured_bacterium **
ASV5 Muribaculaceae Muribaculaceae **
ASV15 Muribaculaceae Muribaculaceae uncultured_bacterium **
−20
−10
0
10
20
log2FoldChange

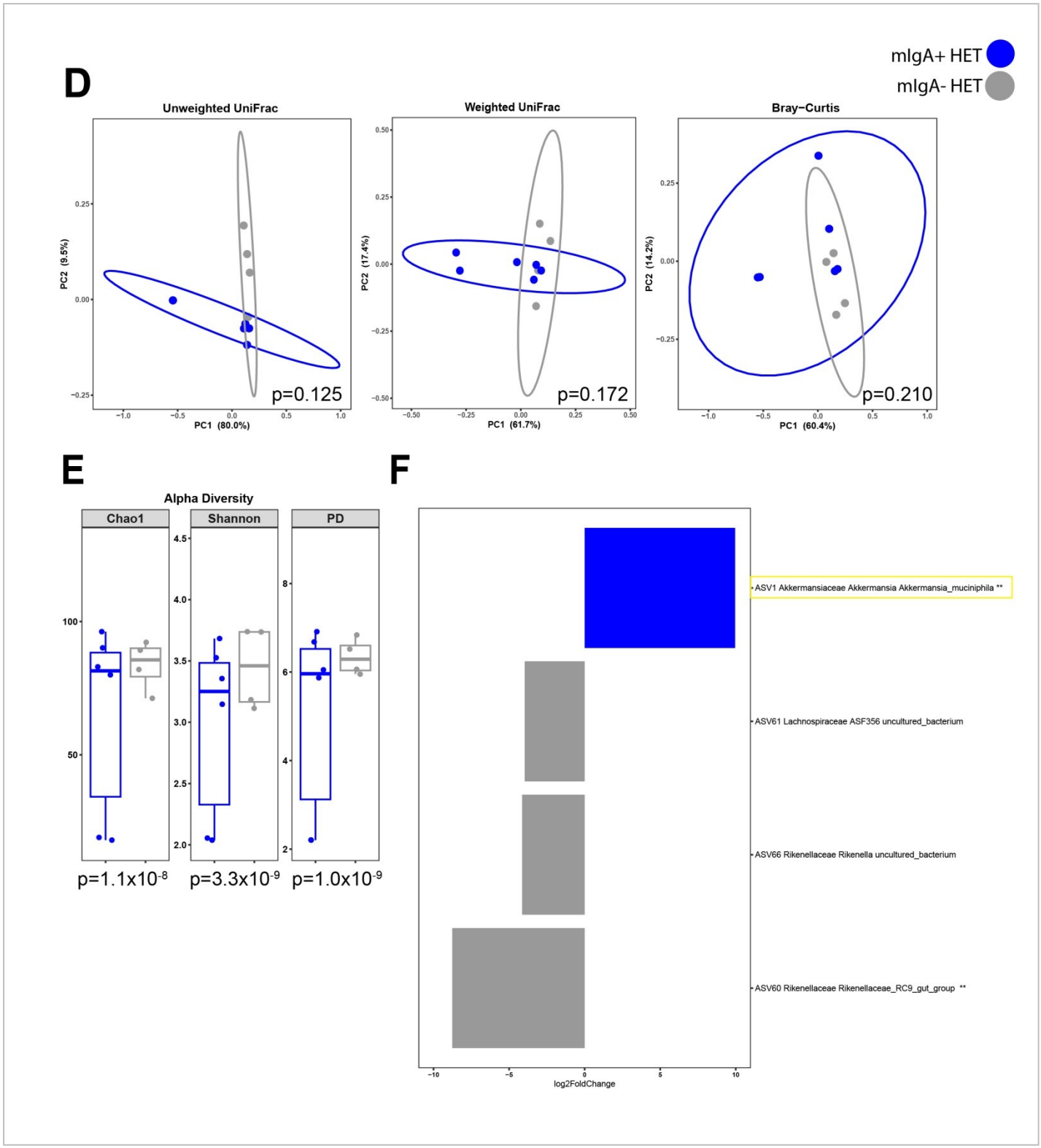
mIgA+ HET
mIgA- HET
D
Unweighted UniFrac
Weighted UniFrac
Bray−Curtis
PC2 (9.5%)
PC1 (80.0%)
p=0.125
PC2 (17.4%)
PC1 (61.7%)
p=0.172
PC2 (14.2%)
PC1 (60.4%)
p=0.210
E
Alpha Diversity
Chao1
Shannon
PD
p=1.1x10-8
p=3.3x10-9
p=1.0x10-9
F
ASV1 Akkermansiaceae Akkermansia Akkermansia_muciniphila **
ASV61 Lachnospiraceae ASF356 uncultured_bacterium
ASV66 Rikenellaceae Rikenella uncultured_bacterium
ASV60 Rikenellaceae Rikenellaceae_RC9_gut_group **
log2FoldChange

**Figure 4.2.2.2 Microbiome analysis of NOD.IgA HET cohorts**

Principal component analysis (PCA) plots (**A**) of mIgA+ HET (blue) and mIgA- HET (grey) microbiota at 5 weeks of age. Alpha diversity (**B**) of the two NOD.IgA HET cohorts at 5 weeks using three different diversity measures. Barplot (**C**) showing taxa enriched in each NOD.IgA HET cohort at 5 weeks. Lachnospiraceae members are boxed in turquoise, Muribaculaceae in green, Rikenellaceae in purple, *Parabacteroides* in orange, *Lactobacillus* in grey and *Akkermansia muciniphila* in gold. Red stars identify taxa that show enrichment in both adult NOD and mIgA- HET offspring. Yellow stars identify taxa enriched in offspring cohorts that were not associated with either dam cohort.
Analysis of adult (10-15 weeks) mIgA+ HET (blue) and mIgA- HET (grey) microbiota, including principal component analysis (PCA) plots (**D**), alpha diversity plots (**E**), and barplot (**F**) showing taxa enrichment. Raw data analysis and image production was performed by Dr. Tingting Ju (laboratory of Dr. Ben Willing) in the Faculty of Agricultural, Life and Environmental Sciences at the University of Alberta.

#### 4.2.2.3 Maternal IgA deficiency contributes to an altered metabolome in offspring

The metabolome is a term referring to the complete collection of small molecule chemicals present within an environment, tissue or sample. In the context of the mammalian gut, the metabolome consists of all metabolic substrates, end products, and intermediates involved in biochemical pathways performed by the host and the microorganisms residing in the gut. Besides being important for innumerable metabolic processes carried out by host and microbes, these small molecules are key mediators of communication between the host and microbiome. Amongst the most thoroughly studied metabolites are the SCFA acetate, propionate and butyrate. In addition to their metabolic effects, these molecules are important ligands involved in a number of host signalling pathways, including immune signalling both locally and systemically[154,175]. Overwhelmingly, SCFA are anti-inflammatory in nature, driving a tolerogenic immune response and boosting gut barrier integrity and defenses[154]. Similarly, the indole class of molecules, derived from tryptophan metabolism, help sustain barrier defenses and maintain homeostasis via signalling through the aryl hydrocarbon receptor (AhR) expressed by various immune and barrier cells[175]. Conversely, some metabolites arising from protein fermentation, such as p-cresol, ammonia, phenol and hydrogen sulfide, have been postulated to have negative impacts on gut integrity, immune regulation and overall host health[175,176].

The metabolome of an individual is driven largely by the composition of the microbiome and is strongly influenced by the presence or absence of key genera[175]. Because of the differences in microbiome composition observed between the mIgA+ and mIgA- HET cohorts, we performed metabolomic analysis of fecal samples from each cohort at 5 weeks of age. Fecal samples were sent to The Metabolomics Innovation Center (TMIC) in the University of Alberta Chemistry Department, where they were analyzed via high performance chemical isotope labeling liquid chromatography-mass spectrometry (HP-CIL LC-MS). An average of 4422 metabolites were detected per sample, 1466 (33%) of which were identified with confidence.

Using MetaboAnalyst 5.0 (https://www.metaboanalyst.ca) to visualize the results, the relative levels of each identified metabolite was compared between the two HET cohorts. Using principal component analysis, I found that the metabolome of each cohort clustered based on

maternal origin (**Fig 4.2.2.3A**). Furthermore, I found a number of metabolites that were significantly altered between the two cohorts, 453 (33%) of which were identified (**Fig 4.2.2.3B**). 359 metabolites were increased >2-fold in the mIgA- HET cohort, while 290 were decreased >2-fold. I began by comparing metabolites known to have anti-inflammatory effects. Somewhat surprisingly, acetate, propionate and butyrate were all significantly decreased in the mIgA- HET cohort (**Fig 4.2.2.3C**). Similarly, all identified indole derivatives were decreased in this cohort, as were the three identified phenolic compounds. Several pro-inflammatory lipid mediators, including prostaglandins B2, C2, H2, I2 and leukotrienes B4 & E4, were detected at lower concentrations in the mIgA- HET cohort (**Fig 4.2.2.3D**). Of the metabolites that were increased in the mIgA- HET samples, many were molecules involved in amino acid metabolism. Indeed, when pathway analysis was performed, several amino acid metabolism pathways were found to be significantly altered between the two HET cohorts (**Fig 4.2.2.3E**). Additionally, folate biosynthesis and a pathway referred to as 'one carbon pool by folate' were identified as being substantially altered. The 'one carbon pool by folate' pathway, also referred to as 'one carbon metabolism', is involved in the production of 1C units for use in biochemical processes such as epigenetic modifications, amino acid biosynthesis and homeostasis[177]. Exploring the ways in which altered amino acid metabolism and one carbon metabolism potentially contribute to the disease protection seen in the mIgA- HET cohort is an intriguing future direction.

Communication via microbial metabolites is only effective insofar as the host has the ability to sense and respond to those metabolites. Thus, I assessed the expression of various genes associated with the recognition of and response to metabolites via quantitative PCR (qPCR). I found that mIgA- HET mice exhibited higher ileal expression of AhR and the SCFA receptors GPR41 & GPR43, suggesting these mice had an enhanced ability to sense and respond to the microbiota (**Fig 4.2.2.3F**).

Another mode of communication involves the activation of pattern recognition receptors on gut epithelial and immune cells. This frequently results in upregulation of genes involved in barrier impermeability. One such gene is Cldn1, which codes for the tight junction protein claudin-1 and serves to enhance the impermeability of the gut epithelial barrier[178]. I found that

claudin-1 was upregulated in some members of the mIgA- HET cohort, though the overall result was not significant (**Fig 4.2.2.3G**).

In summary, maternal IgA deficiency contributed to significant changes in the early metabolome of the offspring and to amplified expression of metabolite receptors, enhancing the ability of the offspring to sense the microbiome. Many of the metabolomic differences were supportive of our findings of an increased inflammatory environment along the GI tract in the mIgA- HET cohort in the early post-weaning period. Future efforts will focus on deciphering whether these metabolite alterations persist in the islet and PLN environment, and whether specific altered metabolites modify autoimmune disease development.

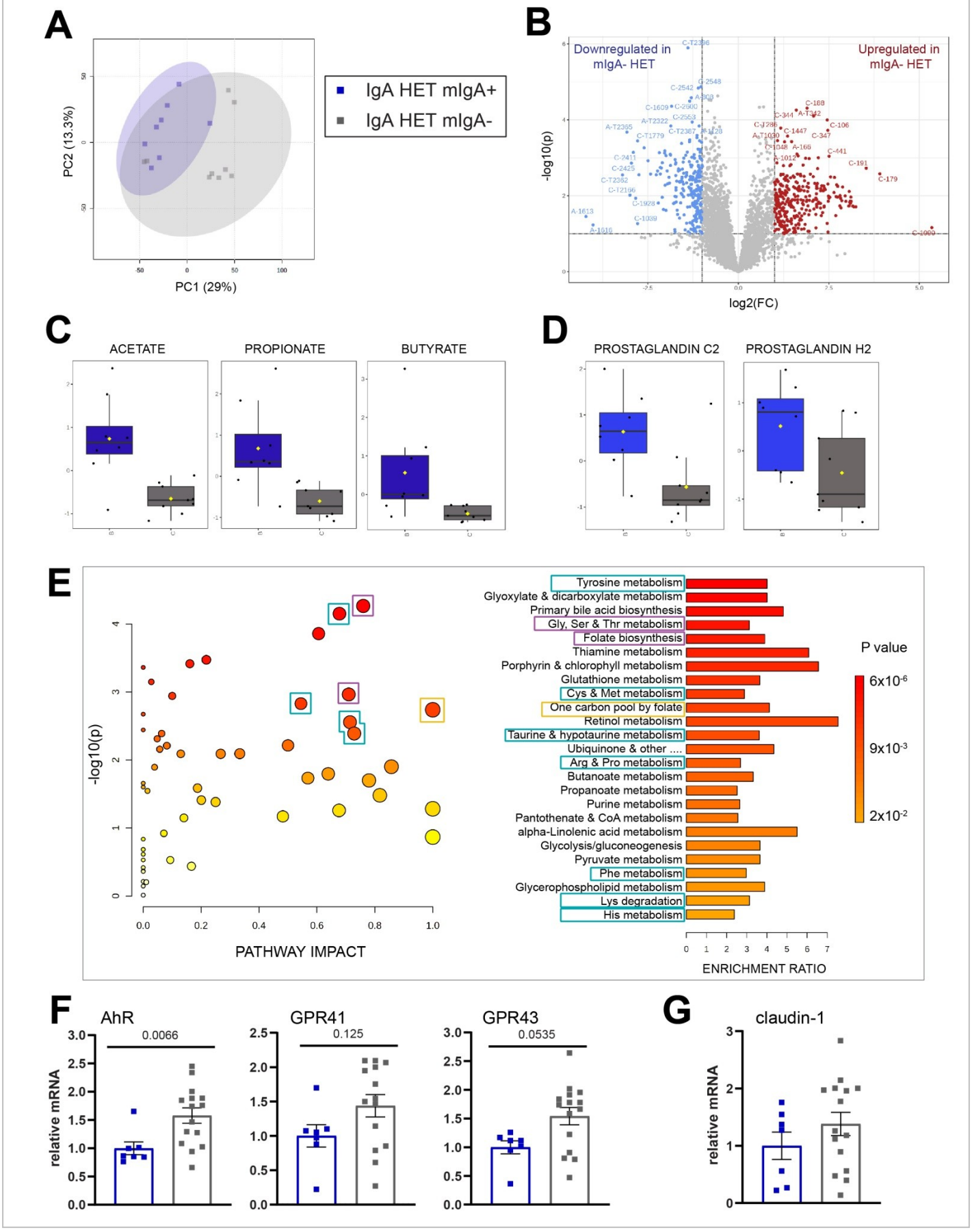
A
IgA HET mIgA+
IgA HET mIgA-
PC2 (13.3%)
PC1 (29%)
B
Downregulated in mIgA- HET
Upregulated in mIgA- HET
-log10(p)
log2(FC)
C
ACETATE
PROPIONATE
BUTYRATE
D
PROSTAGLANDIN C2
PROSTAGLANDIN H2
E
-log10(p)
PATHWAY IMPACT
Tyrosine metabolism
Glyoxylate & dicarboxylate metabolism
Primary bile acid biosynthesis
Gly, Ser & Thr metabolism
Folate biosynthesis
Thiamine metabolism
Porphyrin & chlorophyll metabolism
Glutathione metabolism
Cys & Met metabolism
One carbon pool by folate
Retinol metabolism
Taurine & hypotaurine metabolism
Ubiquinone & other ....
Arg & Pro metabolism
Butanoate metabolism
Propanoate metabolism
Purine metabolism
Pantothenate & CoA metabolism
alpha-Linolenic acid metabolism
Glycolysis/gluconeogenesis
Pyruvate metabolism
Phe metabolism
Glycerophospholipid metabolism
Lys degradation
His metabolism
P value
6x10-6
9x10-3
2x10-2
ENRICHMENT RATIO
F
AhR
0.0066
GPR41
0.125
GPR43
0.0535
relative mRNA
G
claudin-1
relative mRNA

**Figure 4.2.2.3 Metabolomic profile comparison between NOD.IgA HET cohorts**

Principal component analysis (**A**) of metabolome of 5 week old mIgA+ (blue) and mIgA- (grey) HET mice. Volcano plot (**B**) showing metabolites that are up-regulated (red) and down-regulated (blue) in the mIgA- HET cohort. Comparison of fecal short chain fatty acids (**C**) and prostaglandin (**D**) levels between mIgA+ (blue) and mIgA- (grey) HET mice. Analysis showing the impact of metabolite concentration differences on metabolic pathways (**E**). Pathways involving amino acid (aa) metabolism are boxed in turquoise, those involving aa pathways affecting folate production in purple, and 'one carbon pool by folate' pathway in gold. Relative comparison of *Ahr*, *FFAR3* (GPR41), *FFAR2* (GPR43) (**F**) and *cldn-1* (**G**) mRNA levels in 4-5 week old mIgA+ (blue) and mIgA- (grey) HET mice. For panels (**F**) & (**G**), mean +/- SEM are indicated, and p-values were determined using the Mann-Whitney U test.

### 4.2.3 Early life immunity in NOD.IgA HET offspring from IgA-sufficient and -deficient dams

The striking difference in disease incidence between the NOD.IgA HET offspring from IgA-insufficient vs -deficient dams led me to hypothesize that there were maternal factors at work during the neonatal period that either promoted or dampened efficient immune regulation. In order to understand the nature of this aberrant immune development, I sought to characterize and contrast these two offspring cohorts with respect to many of the same elements explored in Section 3.2.2. In doing so, I hoped to elucidate some of the mechanisms by which maternal IgA deficiency-induced dysbiosis might contribute to lowered disease susceptibility.

#### 4.2.3.1 Maternal IgA deficiency yields offspring with signs of increased gut inflammation early in life

Proper neonatal immune development involves the induction of GI immune responses that would generally be considered pro-inflammatory. These include the induction of humoral responses as naive B lymphocytes encounter antigen from the colonizing microbiota. Hence, I sought to characterize the humoral responses along the GI tract to determine if differences existed between the mIgA+ and mIgA- HET cohorts at 5 weeks of age. I found that fecal IgA was highly variable in both groups and thus showed no differences between the cohorts (**Fig 4.2.3.1A**). Fecal IgM was low in both groups, while IgG levels were slightly elevated in some members of the HET mIgA- cohort (**Fig 4.2.3.1B,C**). To assess the extent of inflammation in the gut, I again looked at fecal Lcn-2 levels. Reflective of the trend seen with IgG and IgM, fecal Lcn-2 levels were slightly elevated in the HET mIgA- cohort (**Fig 4.2.3.1D**). Indeed, I found a slight but significant positive correlation between fecal IgG and Lcn-2 levels (**Fig 4.2.3.1E**) indicating that a proportion of the mIgA- HET cohort experienced heightened intestinal pro-inflammatory immune responses that involved the induction of IgG.

Another measure of GI inflammation commonly used for inflammatory bowel diseases is increased colonic weight:length ratio. I found that the mIgA- HET cohort showed an elevated colonic weight:length ratio, further evidence of increased inflammation along the colon. However, the ratio was affected not by colonic shortening, as is the case in colitis, but by increased weight of the colon (**Fig 4.2.3.1F-H**). An explanation for this is unclear, but

suggests that the immune processes at work in this cohort are different than those that contribute to inflammatory diseases in adulthood.

Overall, mIgA- HET offspring exhibited signs of an elevated pro-inflammatory environment in the colon at 5 weeks of age. This finding is in accordance with decreased SCFA levels present at the same time point, and in light of the disease resistance present in this cohort, raises questions regarding the current dogma that views GI inflammation at steady state as detrimental to health.

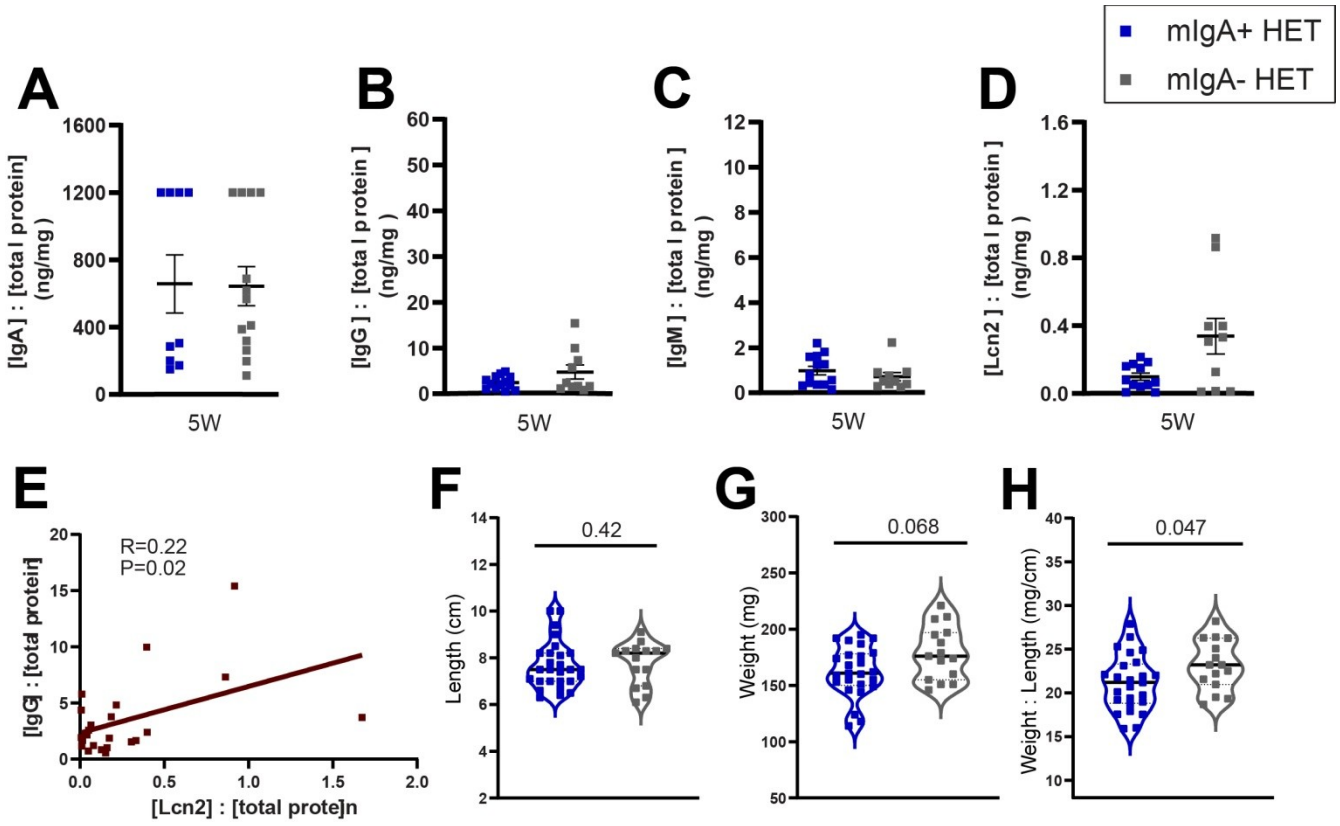


**Figure 4.2.3.1 GI immune responses in NOD.IgA HET cohorts at 5 weeks of age**

Fecal IgA (**A**), IgG (**B**), IgM (**C**) and Lcn-2 (**D**) levels, expressed as ratios of total protein, in mIgA+ (blue) and mIgA- (grey) HET mice at 5 weeks of age. Correlation (**E**) of fecal IgG and Lcn-2 levels in 5 week NOD.IgA HET mice. Colonic length (**F**), weight (**G**) and weight:length ratio (**H**) for mIgA+ (blue) and mIgA- (grey) HET mice at 5 weeks of age. Mean +/- SEM are indicated for all data, and p-values were determined using the Mann-Whitney U test.

### 4.2.3.2 Offspring of IgA-deficient dams show evidence of a stronger weaning reaction

Hallmarks of an appropriately robust response to the microbiota during the pre-weaning period are the proliferation of immune cell populations and the induction of immune-related gene expression along the GI tract[79,81,94]. Since these events occur from approximately 2-4 weeks of age, I chose to assess immune cell populations in the large bowel, small bowel and MLN at 3 weeks and 4 weeks of age in an effort to find differences that set the mIgA- HET cohort apart (**Table 4.2.3.2**). The first thing I noted was that immune cell population comparisons were litter-dependent within the mIgA+ and mIgA- HET cohorts, and even within litters, the data varied a fair bit. This wasn't surprising, since disease susceptibility varied by litter as well, and there were a proportion of mice in both cohorts that resisted developing T1D despite having the same maternal origin and genetics. Indeed, this is a conundrum in animal studies such as this project; there are variables at work that we have yet to understand.

Within the large and small bowels, I found a modest decrease in the B lymphocyte compartment in the mIgA- HET cohort (**Fig 4.2.3.2A**). The proportion of $CD86^{hi}$ B lymphocytes was comparable between cohorts, but CD86 mean fluorescence intensity (MFI) at 3 weeks was modestly but significantly increased in the mIgA- HET cohort, suggesting an enhanced ability to participate in T lymphocyte activation (**Fig 4.2.3.2B**). Additionally, the proportion of $IgA^{+}$ B lymphocytes was greater in the mIgA- HET cohort. Within the PC population, the mIgA- HET cohort showed a higher proportion of IgA-producing $BLIMP1^{+}$ cells with a greater overall IgA MFI, indicating more IgA production per cell on average (**Fig 4.2.3.2C**). When assessing the T lymphocyte compartment in the mIgA- HET cohort, I noted a modest increase in $CD3^{+}$ proportions in both large and small bowels. The $CD4^{+}$ and $CD8^{+}$ populations were marginally increased in the large and small bowels, respectively (**Fig 4.2.3.2D&E**). Within both tissues, $CD8^{+}$ and $CD4^{+}$ populations appeared less antigen experienced at 4 weeks as assessed by $CD44^{hi}$ expression (**Fig 4.2.3.2F**). Interestingly, at 3 weeks both T lymphocyte populations showed more antigen experience (greater $CD44^{hi}$ proportion) in small bowel tissue from the mIgA- HET cohort, suggesting an environment of T lymphocyte maturation suppression, or perhaps an influx of naive T lymphocytes, during this period. A similar pattern was noted in the large bowel, where $CD44^{hi}$ proportions were equal between cohorts at 3 weeks, but showed a decline by 4 weeks in the mIgA- HET cohort.

$CD4^+$ $FOXP3^+$ Tregs and $CD4^+FOXP3^+RORgt^+$ iTregs are important regulatory T lymphocyte populations in the GI tract that promote immune tolerance to both dietary and luminal microbial antigens. Their induction during early life and persistence into later life has been shown to be important for resistance to immuno-regulatory diseases such as T1D. Surprisingly, with the exception of a minor trend toward higher proportion in mIgA- HET cohort 3 week large bowel tissue, I did not observe a reproducible difference in Treg or iTreg proportions between the HET cohorts. However, I did note differences in the γδT lymphocyte proportions in the small bowel tissue at 3 weeks and 4 weeks (**Fig 4.2.3.2G**). This population was increased in the mIgA- HET cohort.

The MLN is an important site for induction of immune activation or tolerance in response to microbial and dietary antigen. Interestingly, I found trends in MLN immune populations that were in direct contrast to what I observed in the bowel tissue itself (**Table 4.2.3.2**). At 3 weeks, mIgA- HET mice showed more B lymphocytes but fewer T lymphocytes than their counterparts. They showed fewer γδT cells, fewer Treg and iTreg proportions, but a greater proportion of $CD44^{hi}$ $CD4^+$ T lymphocytes. Interestingly, a greater proportion of $CD4^+$ T lymphocytes expressed the inhibitory receptor PD1. Also of interest were the follicular helper T lymphocytes ($T_{fh}$) and the germinal center (GC) B lymphocytes in the MLN. Published studies[119] have shown the ability of maternal antibodies, particularly IgG and IgA, to reduce $T_{fh}$ numbers and suppress the development of GC in the MLN. Given that the mIgA- HET offspring received no maternal IgA, I was curious how this would affect GC development in the MLN. I found that at 3 weeks, mIgA- HET offspring exhibited increased proportions of both $T_{fh}$ ($CD4^+PD1^+CXCR5^+$) and GC B lymphocyte ($CD95^+GL7^+$) populations (**Fig 4.2.3.2H,I**), indicating a weakening of this maternal suppressive function.

The differences I observed in the neonatal GI immune cell populations prompted me to assess the degree of induction of immune-related genes in the two NOD.IgA HET cohorts. Since pups are weaned at 21 days of age and others have reported the weaning reaction occurring within the days following weaning[79,80], I assayed ileal tissues between 25 days and 30 days of age. Using qPCR, I looked at expression of a number of pro-inflammatory factors (IL-1β, IL-6, IFNγ, Lcn-2) as well as some anti-inflammatory factors (IL-10, TGFβ). I found that, similar to immune cell populations, there was a fair bit of variability within each group that appeared

litter-dependent. Despite this, there were definite trends towards greater pro- and anti-inflammatory responses in the mIgA- HET cohort. I found greater expression of IL-10 ($p=0.064$), IFNγ ($p=0.066$) and Lcn-2 ($p=0.047$), with a trend towards more TFGβ and IL-6 in mIgA- HET mice (**Fig 4.2.3.2J**). I also assessed expression of IL-1β and IL-23, both pro-inflammatory cytokines, and found no difference between the two HET cohorts.

Taken together, this data provides compelling evidence that maternal IgA deficiency fosters changes in the neonatal GI environment that results in stronger induction of immune responses from a variety of intestinal cell populations, contributing to a more robust weaning reaction.

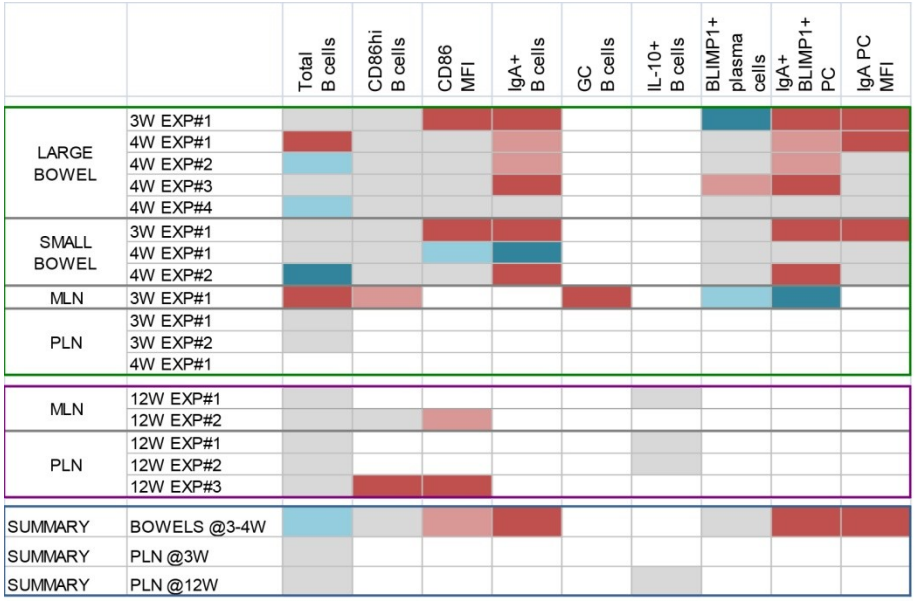
Total B cells
CD86hi B cells
CD86 MFI
IgA+ B cells
GC B cells
IL-10+ B cells
BLIMP1+ plasma cells
IgA+ BLIMP1+ PC
IgA PC MFI
LARGE BOWEL
3W EXP#1
4W EXP#1
4W EXP#2
4W EXP#3
4W EXP#4
SMALL BOWEL
3W EXP#1
4W EXP#1
4W EXP#2
MLN
3W EXP#1
PLN
3W EXP#1
3W EXP#2
4W EXP#1
MLN
12W EXP#1
12W EXP#2
PLN
12W EXP#1
12W EXP#2
12W EXP#3
SUMMARY
BOWELS @3-4W
SUMMARY
PLN @3W
SUMMARY
PLN @12W

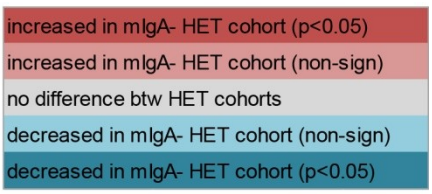
increased in mIgA- HET cohort (p<0.05)
increased in mIgA- HET cohort (non-sign)
no difference btw HET cohorts
decreased in mIgA- HET cohort (non-sign)
decreased in mIgA- HET cohort (p<0.05)

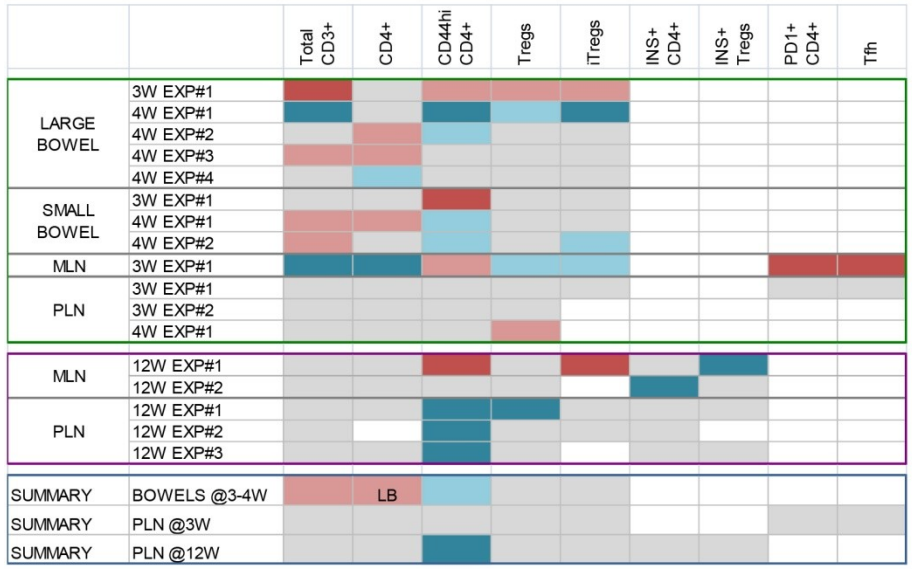
Total CD3+
CD4+
CD44hi CD4+
Tregs
iTregs
INS+ CD4+
INS+ Tregs
PD1+ CD4+
Tfh
LARGE BOWEL
3W EXP#1
4W EXP#1
4W EXP#2
4W EXP#3
4W EXP#4
SMALL BOWEL
3W EXP#1
4W EXP#1
4W EXP#2
MLN
3W EXP#1
PLN
3W EXP#1
3W EXP#2
4W EXP#1
MLN
12W EXP#1
12W EXP#2
PLN
12W EXP#1
12W EXP#2
12W EXP#3
SUMMARY
BOWELS @3-4W
LB
SUMMARY
PLN @3W
SUMMARY
PLN @12W

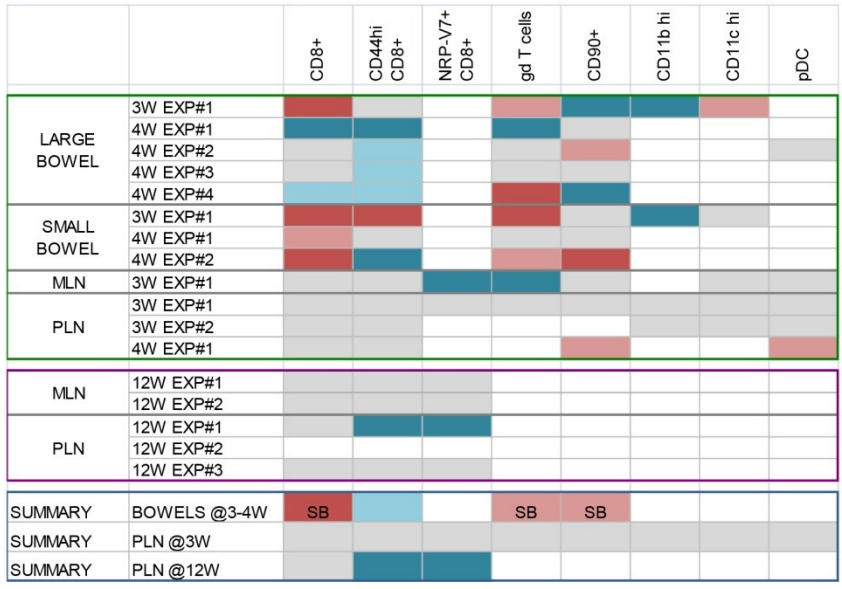
CD8+
CD44hi CD8+
NRP-V7+ CD8+
gd T cells
CD90+
CD11b hi
CD11c hi
pDC
LARGE BOWEL
3W EXP#1
4W EXP#1
4W EXP#2
4W EXP#3
4W EXP#4
SMALL BOWEL
3W EXP#1
4W EXP#1
4W EXP#2
MLN
3W EXP#1
PLN
3W EXP#1
3W EXP#2
4W EXP#1
MLN
12W EXP#1
12W EXP#2
PLN
12W EXP#1
12W EXP#2
12W EXP#3
SUMMARY
BOWELS @3-4W
SB
SB
SB
SUMMARY
PLN @3W
SUMMARY
PLN @12W

**Table 4.2.3.2 Immune cell population comparisons in NOD.IgA HET cohorts**

Summary of flow cytometry analysis of various immune cell populations in large bowel (LB), small bowel (SB), mesenteric lymph nodes (MLN), and pancreatic lymph node (PLN) at 3 weeks, 4 weeks and 12 weeks of age. Comparisons are made such that results indicate differences in mIgA- HET cohort with respect to the mIgA+ HET cohort. For each comparison, significance was determined using the Mann-Whitney U test.

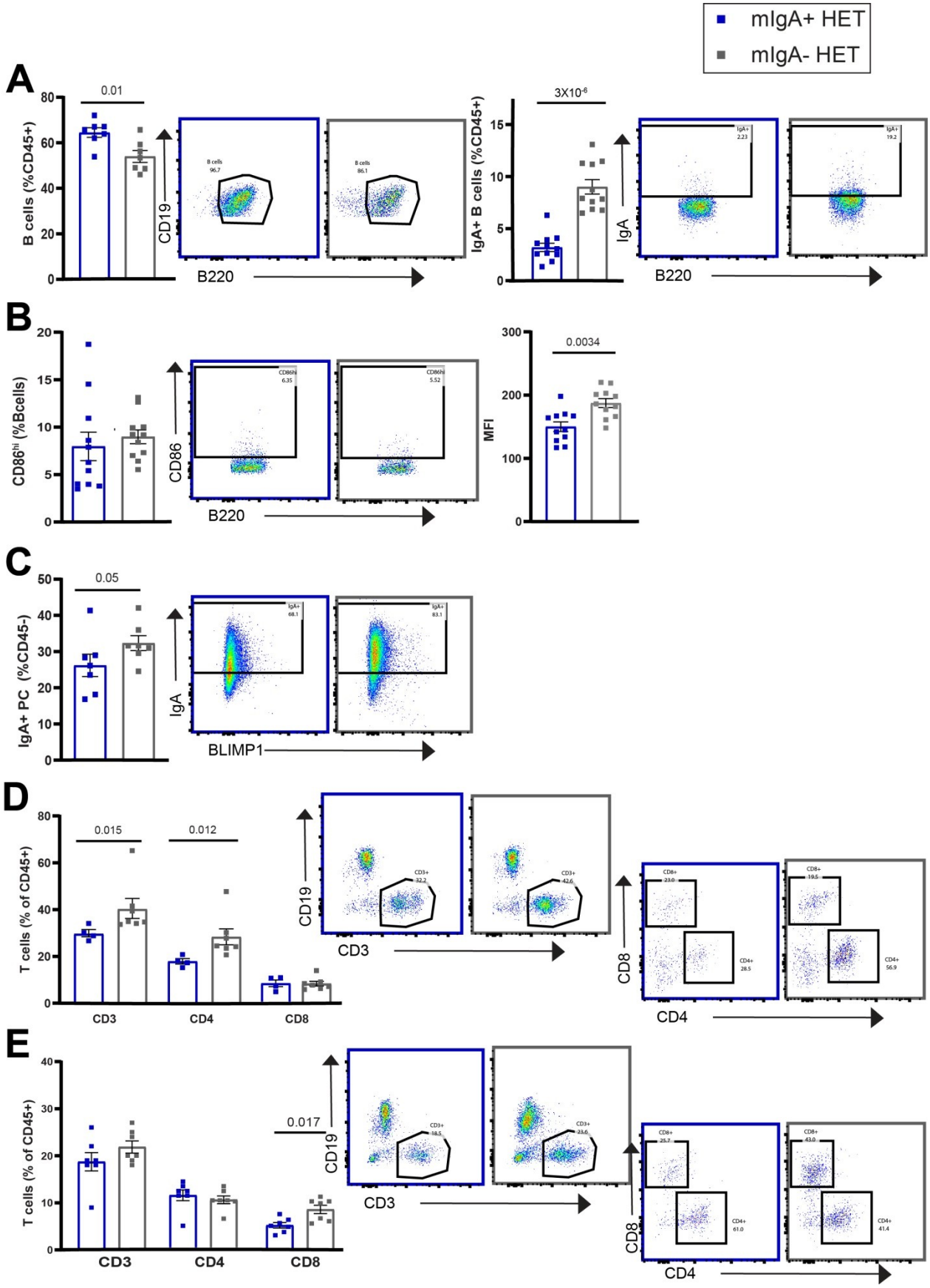
mIgA+ HET
mIgA- HET
A
B cells (%CD45+)
0.01
CD19
B220
IgA+ B cells (%CD45+)
3X10-6
IgA
B220
B
CD86hi (%Bcells)
CD86
B220
MFI
0.0034
C
IgA+ PC (%CD45-)
0.05
IgA
BLIMP1
D
T cells (% of CD45+)
0.015
0.012
CD3
CD4
CD8
CD19
CD3
CD8
CD4
E
T cells (% of CD45+)
0.017
CD3
CD4
CD8
CD19
CD3
CD8
CD4

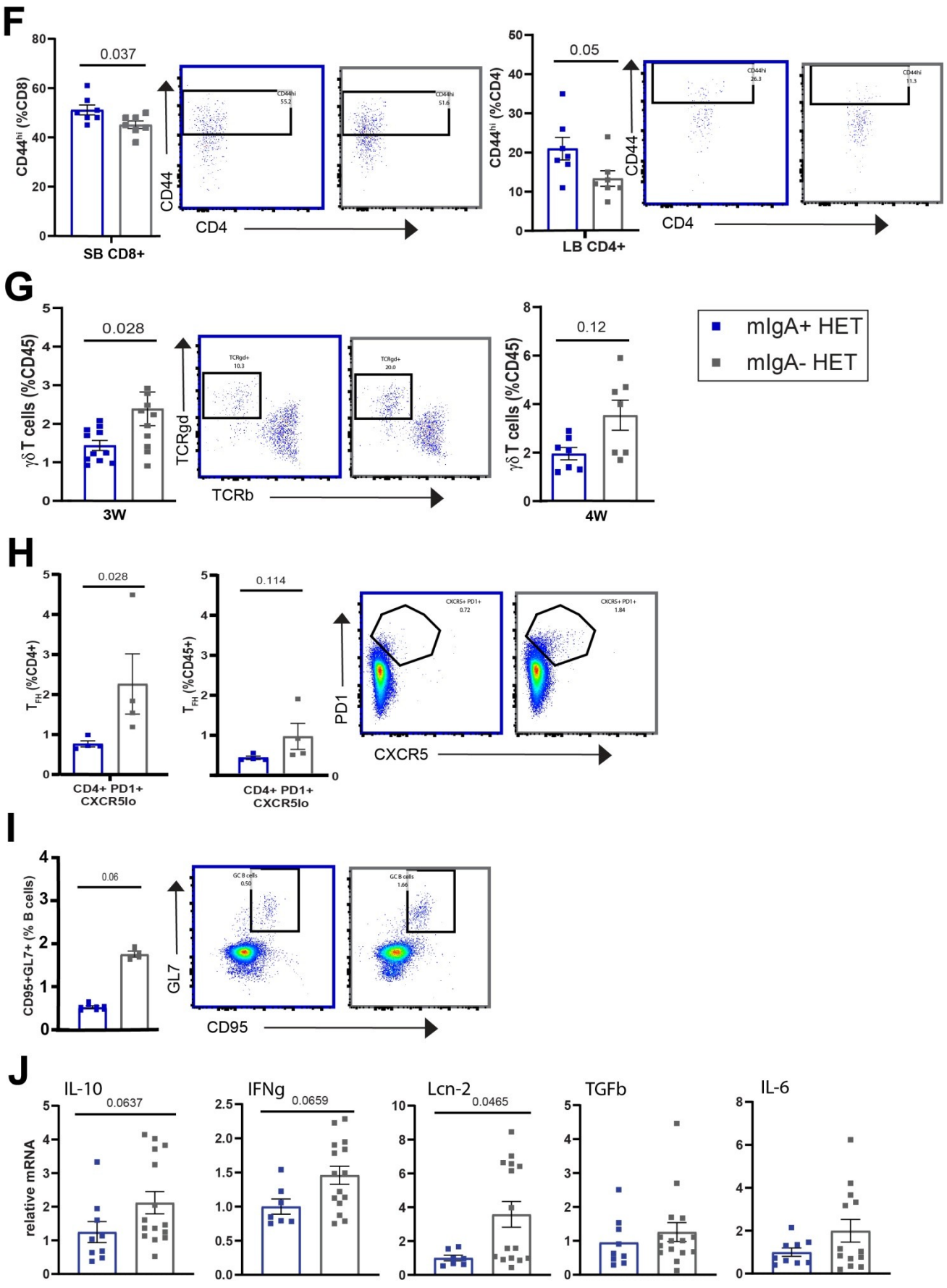
F
0.037
CD44hi (%CD8)
SB CD8+
CD44
CD4
0.05
CD44hi (%CD4)
LB CD4+
CD44
CD4
G
0.028
γδ T cells (%CD45)
3W
TCRgd
TCRb
0.12
γδ T cells (%CD45)
4W
mIgA+ HET
mIgA- HET
H
0.028
TFH (%CD4+)
CD4+ PD1+ CXCR5lo
0.114
TFH (%CD45+)
CD4+ PD1+ CXCR5lo
PD1
CXCR5
I
0.06
CD95+GL7+ (% B cells)
GL7
CD95
J
IL-10
0.0637
relative mRNA
IFNg
0.0659
Lcn-2
0.0465
TGFb
IL-6

**Figure 4.2.3.2 GI immune cell populations in NOD.IgA HET cohorts at 3-4 weeks**

Flow cytometry analysis of GI immune cell populations at 3 & 4 weeks, with bar plots and representative FACS plots, where mIgA+ HET data is indicated in blue and mIgA- HET data is indicated in grey. (**A**) total B cells (left) & $IgA^+$ B cells (right) in the small bowel; (**B**) $CD86^{hi}$ B cells in the small bowel, with CD86 mean fluorescence intensity; (**C**) $IgA^+$ plasma cells in small bowel; (**D**) total T cells, $CD4^+$, & $CD8^+$ T cell populations in the large bowel; (**E**) total T cells, $CD4^+$, & $CD8^+$ T cell populations in the small bowel; (**F**); CD44 expression by small bowel $CD8^+$ T cells (left) and large bowel $CD4^+$ T cells (right); (**G**) γδT cell populations in the small bowel at 3 weeks (left) and 4 weeks (right); (**H**) follicular helper T cells and (**I**) germinal center B cells in mesenteric lymph nodes of 3 week mice. (J) Expression of various cytokines and immune factors in ileal tissue of 5 week NOD.IgA HET mice. Each data point represents one mouse, and mean +/- SEM is indicated for each data set. p-values were determined using the Mann-Whitney U test.

#### 4.2.3.3 Maternal IgA deficiency promotes a heightened systemic immune response at weaning with no evidence of islet autoimmunity

Just as immune cell populations within the GI environment undergo expansion during the pre- and early post-weaning period, so too do immune populations throughout other lymphoid tissues. I sought to explore how maternal IgA deficiency and dysbiosis contribute to differences in systemic immune responses during this time period. I used ELISA to assay for serum IgA and IgG in mIgA+ and mIgA- HET mice at 3 weeks and 5 weeks of age and found some interesting differences. At both these time points, serum Ig was relatively low in both cohorts. Even so, differences between the cohorts were evident. At 3 weeks, the mIgA- HET cohort showed significantly higher serum IgA and IgG than the mIgA+ HET group (**Fig 4.2.3.3A,B**). This is an important observation, as previous studies have shown that the introduction of the microbiota is sufficient to initiate a systemic humoral response[87] and the composition of the microbiome can dictate the strength of a humoral response, at least in the mucosal tissue[143]. From 3 weeks to 5 weeks, both serum IgA and IgG levels remained relatively static in the mIgA- HET cohort, whereas both increased in the mIgA+ HET cohort. Indeed, it appeared as if both cohorts had a similar systemic humoral response, but this response occurred earlier in the mIgA- HET cohort.

T1D involves the infiltration of autoreactive lymphocytes and myeloid cells into the islets, where beta cell destruction is carried out primarily by $CD8^+$ T lymphocytes that recognize various islet-specific antigens. In NOD mice, several studies have identified autoreactive $CD8^+$ T lymphocytes that recognize the peptide NRP-V7 (a mimic of the T1D associated autoantigen IGRP) within the context of MHCI allele H-2D(b), as well as insulin-reactive $CD4^+$ T lymphocytes that bind a peptide fragment of the insulin B chain presented by MHCII allele I-A(g7). One method of detecting these autoreactive lymphocytes via flow cytometry utilizes a fluorescently-labeled tetramer, a molecule comprising 4 [MHC+peptide+biotin] units bonded together with streptavidin. We were generously gifted tetramers that would allow us to identify both NRP-V7-specific $CD8^+$ T lymphocytes and INSB-specific $CD4^+$ T lymphocytes.

In order to identify the characteristics of immune cells within proximity of the pancreas, I analyzed the immune cell populations present in the PLN via flow cytometry. I hoped to

identify early differences in the PLN that would provide a rationale for the decreased incidence of disease seen in the mIgA- HET cohort. I determined that analysis at 3- 4 weeks would identify differences occurring as a response to maternal influences and/or the weaning reaction. However, I saw no differences in PLN B or T lymphocyte proportions. Moreover, $CD4^+$ and $CD8^+$ T lymphocytes showed similar levels of CD44 expression, and Treg populations were present in low but equivalent proportions (**Fig 4.2.3.3C-E**). Importantly, no NRP-$V7^+$ $CD8^+$ T lymphocytes were detected in either cohort. This result is in line with other studies, supporting the notion that in the early post-weaning period, the disease process has yet to initiate any pancreatic involvement.

Overall, the mIgA- HET cohort appeared to have an earlier, more sustained systemic humoral response, though neither cohort showed any evidence of autoimmune activity in the PLN. Whether this early systemic response was a result of microbiota colonization differences, perhaps because of certain taxa being present or absent, is a topic for future studies. Alternatively, the possibility that the serum IgG at 3 weeks was, at least in part, of maternal origin raises interesting questions about how maternal IgA deficiency may affect maternal antibody transfer during the breastfeeding period.

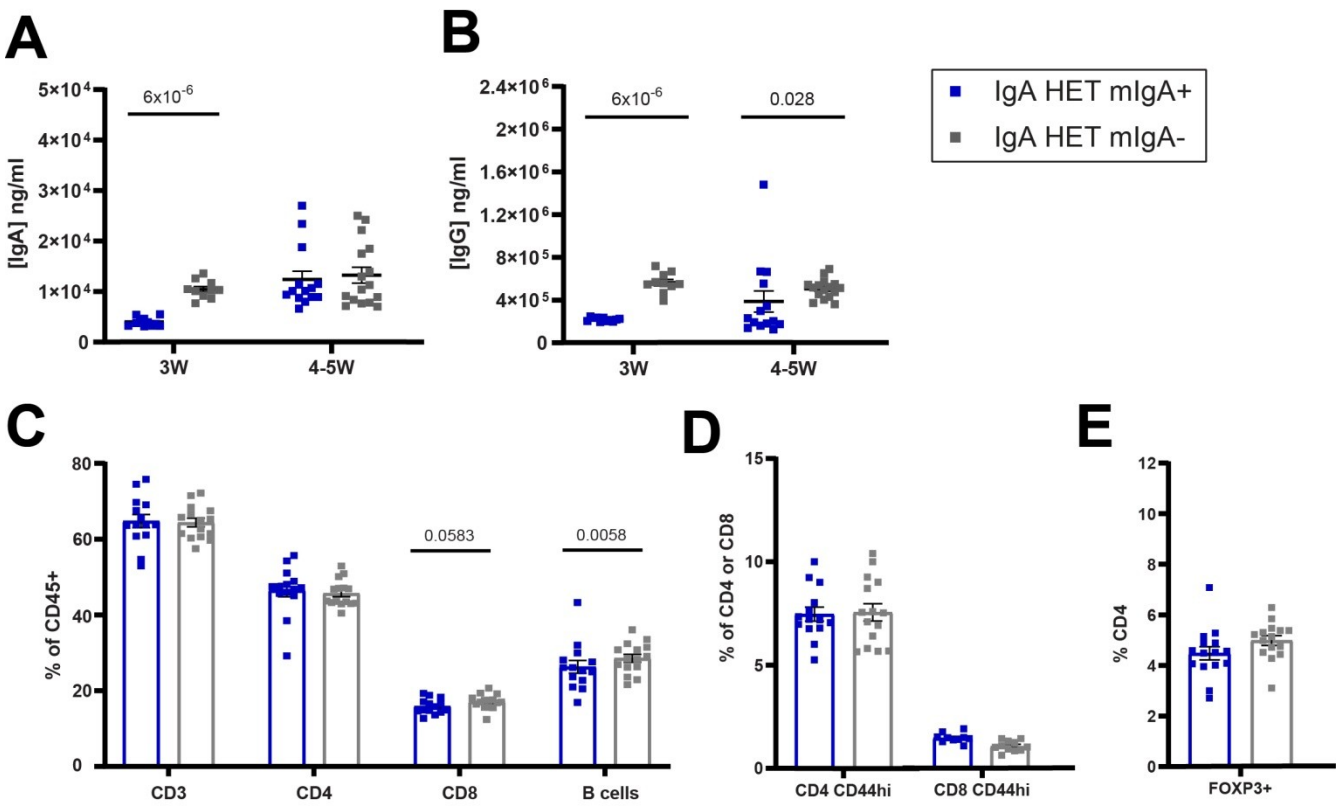


**Figure 4.2.3.3 Non-GI immunity in NOD.IgA HET cohorts in early life**

Serum IgA (**A**) and IgG (**B**) in mIgA+ (blue) and mIgA- (grey) HET cohorts at 3 weeks and 4-5 weeks of age. Immune cell populations in the pancreatic lymph nodes (PLN) at 3 weeks of age, comparing B cell and T cell populations (**C**), T cell CD44$^{hi}$ populations (**D**) and regulatory T cell populations (**E**). Mean +/- SEM are indicated for all data, and p-values were determined using the Mann-Whitney U test.

### 4.2.4 Effects of maternal IgA deficiency on adult NOD.IgA HET immunity & disease pathogenesis

The effects of maternal IgA deficiency on various aspects of neonatal immune development and the early GI environment led me to question whether some of these effects persisted into adulthood. Additionally, I was interested in exploring how increased GI inflammation during the post-weaning period contributed to barrier integrity in adulthood and how this may affect islet immunity. In mice, 'adulthood' is generally >6 weeks of age, although I found that female NOD.IgA mice were small and still appeared juvenile even at 8-9 weeks. Instead, I chose to evaluate immunity and gut barrier physiology in >10 week NOD.IgA HET mice, an age at which the majority of mice are still several weeks from overt T1D.

#### 4.2.4.1 Maternal IgA deficiency leads to elevated systemic and GI antibody responses in adulthood

During the weaning period, mIgA- HET mice exhibited higher serum IgA and IgG levels than their counterparts and showed signs of increased immune activity in the GI tract. In order to determine whether these differences were sustained into adulthood, I assayed fecal material from mIgA+ and mIgA- HET mice at 10 weeks and 15 weeks of age, and serum at 12-14 weeks of age.

Similar to the 5 week time point, I found that fecal IgA was highly variable in both cohorts. Within both groups, a proportion of mice had fecal IgA levels below 400ng/mg of total protein, while others boasted more than 3 times that amount (**Fig 4.2.4.1A**). In contrast to this, fecal IgG and IgM showed a clear pattern of increased abundance in mIgA- HET mice at both 10 weeks and 15 weeks of age (**Fig 4.2.4.1B,C**). So too did fecal Lcn-2 abundance, particularly at 10 weeks of age. By 15 weeks, Lcn-2 levels had risen in the mIgA+ HET mice such that the difference between the groups was non-significant, again suggesting a delay of immune response in this higher T1D risk cohort (**Fig 4.2.4.1D**).

Serum antibody levels rose considerably in both NOD.IgA HET cohorts from the weaning period to adulthood, with IgG showing a 3-fold to 4-fold increase and IgA increasing more than 6-fold. Despite this, the mIgA- HET cohort exhibited moderately higher levels for both antibody isotypes at 12-14 weeks of age (**Fig 4.2.4.1E,F**).

Recalling the relationship between serum IgA levels and disease status (Section 3.2.2.3), it is important to note that none of the mice had glucosuria at the time of serum collection. Furthermore, since there is no difference in disease onset age between the two NOD.IgA HET cohorts, it is likely that any mice that would eventually have presented with T1D were at approximately the same stage of disease progression. This is important - though fecal Lcn-2 levels peak in the 3-5 weeks prior to T1D diagnosis, the increased Lcn-2 levels in mIgA- HET animals likely weren't attributable to being closer to diagnosis. Interestingly, the highest fecal Lcn-2 levels were found in the mIgA- HET cohort, the same cohort that shows the lowest T1D incidence, suggesting that this flare in pro-inflammatory activity may in fact discourage disease-related processes at this time point.

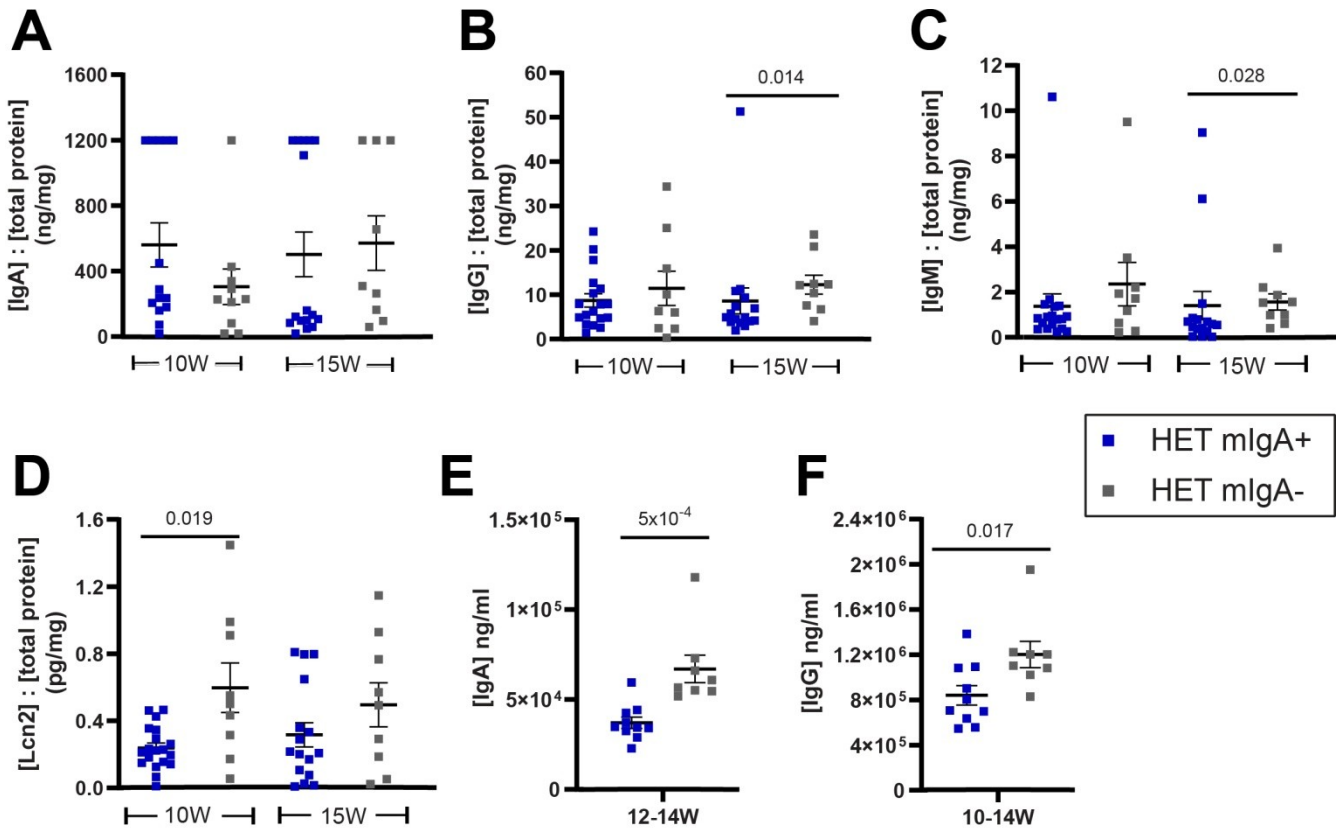


**Figure 4.2.4.1 Serum and fecal antibody levels in adult NOD.IgA HET mice**

Fecal levels of IgA (**A**), IgG (**B**), IgM (**C**) and Lcn-2 (**D**) in 12-14 week mIgA+ (blue) and mIgA- (grey) HET mice. Serum levels of IgA (**E**) and IgG (**F**) in 12-14 week mIgA+ (blue) and mIgA- (grey) HET mice. Mean +/- SEM are indicated for all data, and p-values were determined using the Mann-Whitney U test.

### 4.2.4.2 Maternal IgA deficiency regulates gut barrier function later in life

An important function of both small and large bowel physiology is the ability to keep the lumenal contents of the GI tract in the lumen. The mucus layer plays a vital role in this respect, ensuring that the community of microorganisms that reside along the GI tract don't come into direct contact with the epithelial barrier. In the large bowel, where the microbiota is most dense, the mucus layer is a two-fold blockade. The inner mucus layer, which lays directly over the epithelial cells, is very dense and virtually sterile, while the outer mucus layer is looser and harbors both bacteria and their products. Both mucus layers contain the various antimicrobial factors secreted by the underlying epithelial and mucosal immune tissues, working to trap encroaching microbial cells[179]. At the same time, the epithelial layer itself must maintain a selectively-impermeable barrier. Particularly in the small bowel, where active absorption and diffusion of dietary components across the epithelium is necessary, the IEC must dynamically respond to numerous queues governing the degree of permeability across the barrier.

Various causes of bowel inflammation, including infections[180,181] and non-communicable diseases[182], have been associated with altered thickness and function of the mucus layer, and both human[161] and animal studies[162] have shown evidence of a defective mucus layer in T1D. Histologically, I assessed the colonic mucus layer in the two NOD.IgA HET cohorts to determine if there were differences in mucus layer thickness, integrity or bacterial localization. At 12 weeks of age, I observed an enhanced colonic mucus layer in the mIgA- HET cohort, both with respect to thickness of the layer and the overall integrity (**Fig 4.2.4.2A**). Although I found no evidence of bacterial encroachment directly on the epithelial barrier in either cohort, the reduced thickness of the mucus layer in the mIgA+ HET specimens allowed the bulk of the microbiota to be in closer proximity to the barrier (**Fig 4.2.4.2B**).

T1D is associated with increased gut permeability both prior to diagnosis and in new-onset patients[65]. When I had initially tested gut permeability in the NOD.IgA HET group and compared them to the NOD.IgA WT cohort (Section 3.2.2.2), I found much variability in the results. I speculated that this may be due to the maternal variable, but after comparing results from mIgA+ HET to mIgA- HET cohort, the data points remained fairly spread out at both 7 and 10 weeks of age (**Fig 4.2.4.2C**). At 15 weeks, however, permeability declined in the

mIgA+ cohort and increased in the mIgA- cohort, making the two cohorts significantly different from one another.

In an attempt to understand the physiological relevance of gut permeability and how it might contribute to disease susceptibility, I assessed gut permeability in C57BL/6 female mice at the same three time points (**Fig 4.2.4.2C**). Since C57BL/6 mice are not genetically susceptible to T1D and do not develop the disease without experimental manipulation, I deduced that any evidence of gut permeability would be unrelated to T1D either as a trigger event or as a result of disease processes. Surprisingly, C57BL/6 mice had the highest gut permeability of any NOD.IgA cohort at all three age points assessed, and at 15 weeks of age had permeability equivalent to that of the mIgA- HET cohort. There are three possible ways to interpret these findings. One, that the observed degree of gut permeability is physiologically normal and largely unrelated to T1D processes. Two, that gut permeability is physiologically normal and an important part of immune regulation even into adulthood, thus its decline in the various NOD.IgA cohorts may be associated with disease etiology. This conclusion is consistent with the finding that the most disease-resistant offspring, the mIgA- HET cohort, has heightened gut permeability at 15 weeks. The third possibility is that the range of permeability detected in our NOD.IgA cohorts is within a physiologically normal range and thus far below what would be considered a truly permeable gut, such as is seen in other conditions of bowel inflammation. Regardless of the correct interpretation, the data clearly demonstrate that maternal IgA deficiency plays a role in regulating gut physiology and barrier function in a lifelong manner.

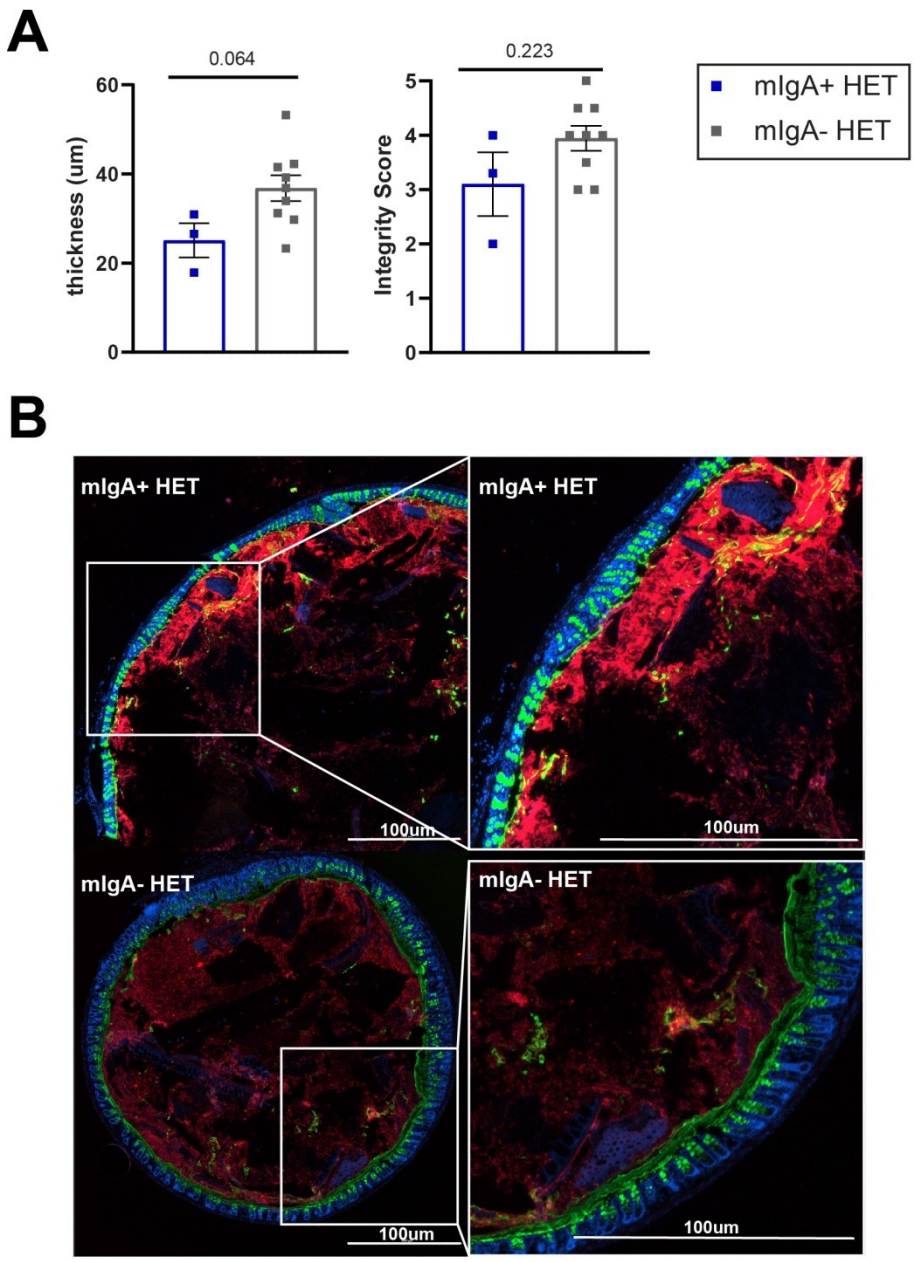
A
0.064
0.223
thickness (um)
Integrity Score
mIgA+ HET
mIgA- HET
B
mIgA+ HET
mIgA+ HET
mIgA- HET
mIgA- HET
100um
C
serum [FD4] (ug/ml)
0.001
7W
10W
15W
mIgA+ HET
mIgA- HET
C57BL/6

**Figure 4.2.4.2 Gut barrier properties in adult NOD.IgA HET mice**

Mucus layer thickness and overall integrity (**A**) in mIgA+ (blue) and mIgA- (grey) HET mice at 12-13 weeks of age. Representative cross-sectional images of the large bowel (**B**) showing bacteria (red), mucus (green) and intestinal epithelial layer (blue). Gut permeability (**C**) in C57BL/6 mice (black), mIgA+ (blue) and mIgA- (grey) HET mice at 7, 10 & 15 weeks of age. Error bars represent mean +/- SEM, and p-values were determined using the Mann-Whitney U test.

#### 4.2.4.3 Offspring of IgA-deficient dams exhibit signs of reduced autoimmunity at 12 weeks

The numerous theories put forward to explain the priming and activation of autoreactive lymphocytes all have one thing in common – these primed lymphocytes eventually encounter self-antigen, prompting their full activation, differentiation and proliferation. In T1D, this very likely occurs in the PLN, or possibly in the pancreas itself, where beta cell-specific antigen is abundant. The newly generated autoreactive T lymphocyte army begins to mediate antigen-specific killing of the beta cells, contributing to a pro-inflammatory environment that further draws immune cells, resulting in a condition called insulitis.

Since these events occur long before glucosuria is detected, I wanted to assess the PLN immune cell populations as well as the degree of insulitis in the NOD.IgA HET cohorts at 12-13 weeks of age. This would indicate whether or not disease processes were occurring at similar rates in the two cohorts despite the later difference in incidence. This is important to consider, as there are a few possibilities that could account for the difference in disease incidence. One scenario is that early events in the initiation of the disease, possibly those occurring in the GI tract, were repressed in the mIgA- HET mice, in which case I expected to see decreased insulitis and fewer PLN activated T lymphocytes in these mice when compared to mIgA+ HET mice of similar age. Alternatively, initial autoimmune activation may have occurred in a similar manner and rate, but the immune-mediated beta cell damage was mitigated to some extent by inhibitory mechanisms of peripheral tolerance. Indeed, H&E staining of pancreata cannot identify the phenotype or function of the infiltrated lymphocytes, leaving the possibility that some may be regulatory T or B lymphocytes. In this scenario, a similar degree of insulitis might be observed in the two NOD.IgA HET cohorts despite yielding quite different physiological outcomes.

When assessing pancreata of 12-13 week female mice, for each specimen I looked at 8 tissue sections taken 60 μm apart so that I could visualize islets located throughout the pancreas. I used a scoring scale from 0-4, where 0 indicated no immune cells present and 4 indicated an islet that was >50% infiltrated with lymphocytes (**Fig 4.2.4.3A**). I then analyzed and plotted the results in a few different ways. In the first method, I calculated the average islet infiltration for each specimen and plotted this in a bar graph (**Fig 4.2.4.3B**). In a second method, I

calculated the proportion of islets contributing to each score 0 through 4 in each NOD.IgA HET cohort and plotted these in a stacked bar graph (**Fig 4.2.4.3C**). Lastly, I calculated the proportion of mice with average islet infiltration scores of [<1], [1-1.99], [2-2.99], & [3-4] and plotted these using a stacked bar graph (**Fig 4.2.4.3D**). Regardless of how the data was analyzed, the results clearly indicated that the mIgA- HET cohort had reduced insulitis at 12-13 weeks of age, suggesting that the disease process was inhibited, and that autoreactive lymphocytes were either not reaching the pancreas to the same extent or were not proliferating comparably within the islets.

Furthermore, in the PLN I observed some immunological differences that could explain the disparity in disease incidence between the mIgA+ and mIgA- HET cohorts. I observed decreased populations with $CD44^{hi}$ expression within the $CD4^{+}$ and $CD8^{+}$ T lymphocyte compartments in the mIgA- HET cohort (**Fig 4.2.4.3E,F**) indicating that there was reduced immune activation within proximity of the pancreas in these mice. Furthermore, although I was able to detect autoreactive $CD8^{+}$ T lymphocytes within the PLN of both cohorts, they were present in lower numbers in the mIgA- HET mice (**Fig 4.2.4.3G**). Notably, insulin-reactive $CD4^{+}$ T lymphocyte were present at very low proportions (<1%) in both cohorts, but the majority (>85%) of these were $FOXP3^{+}$, indicating they played a regulatory role within the PLN (**Fig 4.2.4.3H,I**) and fewer of them were antigen experienced ($CD44^{hi}$) in the mIgA-HET cohort (**Fig 4.2.4.3J**).

In summary, I observed a lesser degree of insulitis, accompanied by less immune activation and fewer autoreactive $CD8^{+}$ T lymphocytes in the PLN of adult pre-diabetic mIgA- HET mice in comparison to their counterpart cohort. Taken together with the incidence data, and noting that a delay of disease processes is ruled out since I observed no difference in age at diagnosis, this data suggests that maternal IgA deficiency results in the inhibition of autoimmune initiation in the early stages of T1D.

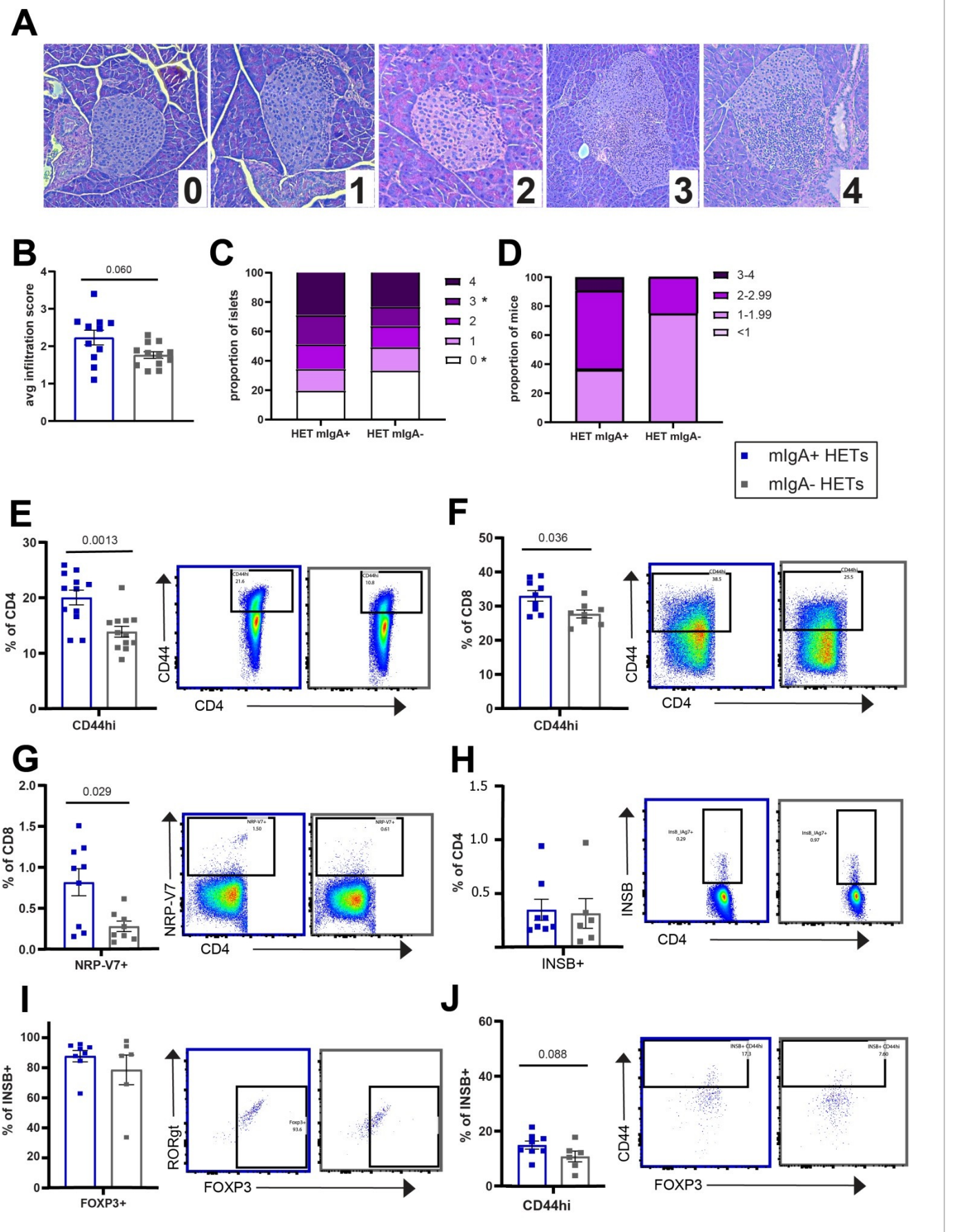
A
0
1
2
3
4
B
avg infiltration score
0.060
C
proportion of islets
HET mIgA+
HET mIgA-
4
3 *
2
1
0 *
D
proportion of mice
3-4
2-2.99
1-1.99
<1
mIgA+ HETs
mIgA- HETs
E
0.0013
% of CD4
CD44hi
CD44
CD4
F
0.036
% of CD8
CD44hi
CD44
CD4
G
0.029
% of CD8
NRP-V7+
NRP-V7
CD4
H
% of CD4
INSB+
INSB
CD4
I
% of INSB+
FOXP3+
RORgt
FOXP3
J
0.088
% of INSB+
CD44hi
CD44
FOXP3

**Figure 4.2.4.3 Insulitis and PLN T cell populations in 12 week NOD.IgA HET cohorts**

Insulitis scoring scale, with representative images of each score (**A**). Insulitis scores of mIgA+ (blue) and mIgA- (grey) HET mice, displayed as average score per mouse (**B**), proportion of islets receiving each score (**C**), and proportion of mice with average scores within each indicated category (**D**). Proportion of antigen-experienced $CD4^+$ (**E**) and $CD8^+$ (**F**) T cells in the PLN, as measured by $CD44^{hi}$ expression, with representative FACS plots. Assessment of NPR-V7-reactive $CD8^+$ T cells in the PLN, expressed as percentage of total $CD8^+$ population (**G**) with representative FACS plots. Assessment of insulin-reactive $CD4^+$ T cells in the PLN, showing proportion of $INS^+$ $CD4^+$ cells within total $CD4^+$ population (**H**), proportion of $FOXP3^+$ Treg cells within total $INS^+$ $CD4^+$ population (**I**), and proportion of $CD44^{hi}$ within total $INS^+$ $CD4^+$ population (**J**) with representative FACS plots for each. Error bars represent mean +/- SEM, and p-values were determined using the Mann-Whitney U test.

### 4.2.5 Postnatal Maternal Influences

Maternal influences are abundant and continually active during the pre-, peri- and post-natal periods. During gestation, maternal antibodies, immune cells, and antibody-antigen complexes (Ab-Ag) have been shown to gain access to the preborn baby and influence the development of the early immune system[94]. During birth, vaginal microorganisms act as early colonizers of the largely sterile neonatal GI tract, impacting the establishment of the early microbiome. After birth, post-natal factors delivered primarily through the breast milk influence both the neonatal immune system and the expansion of the microbiome. I wanted to explore the source and mechanism of the protection afforded the mIgA- HET cohort by the NOD.IgA KO dams and started by separating pre- & peri-natal influences from post-natal factors. I did this using cross-fostering experiments, where NOD.IgA HET pups born to NOD dams were fostered to NOD.IgA KO dams within 24 hours of birth, and vice-versa. Importantly, because breast milk composition is temporally dynamic, I ensured that a dam receiving a foster litter had just delivered her own litter in order to avoid any variables associated with parturitional age. I reasoned that if the maternal protection was arising from pre- or peri-natal factors, fostering would have no effect on disease incidence in the offspring. However, if fostering of mIgA+ HET offspring to NOD.IgA KO dams resulted in reduced disease incidence, and the reverse scenario yielded offspring with escalated disease incidence, this would be evidence that post-natal factors are the major influencers of disease susceptibility.

#### 4.2.5.1 Heightened disease susceptibility in offspring of IgA-sufficient dams is attenuated by fostering to IgA-deficient dams

Starting from 12 weeks of age, fostered NOD.IgA HET offspring were tested weekly for glucosuria in a blinded manner identical to non-fostered offspring. T1D incidence was recorded and plotted in a disease incidence curve until mice had reached 30 weeks of age. The fostering of NOD dam-born NOD.IgA HET pups to NOD.IgA KO dams (hitherto called $F^{KO}$ mIgA+ HET) resulted in significantly reduced T1D incidence when compared to mIgA+ HET who were not fostered ($p=0.006$) or were fostered to another NOD dam ($p=0.04$) (**Fig 4.2.5.1A**). This strongly suggests that post-natal factors from NOD.IgA KO dams protect against T1D development in these mice. Interestingly, results from the reverse scenario (IgA KO dam-born NOD.IgA HET pups fostered to NOD dams, hitherto called $F^{WT}$ mIgA- HET)

have indicated that the situation may be more complex than this. Although the number of $F^{WT}$ mIgA- HET mice (n=10) may be too low to make an accurate assessment, and none have reached 30 weeks yet, only five have developed T1D in this cohort, making their disease incidence curve equivalent to the non-fostered mIgA- HET cohort (**Fig 4.2.5.1B**). This could indicate that in addition to post-natal factors, there are pre- or peri-natal factors influencing disease. In order to fully explore these complexities, one would need to employ embryo transplant experiments and/or Cesarean section deliveries, which are both beyond the scope of this thesis but are excellent possibilities for future direction of this work.

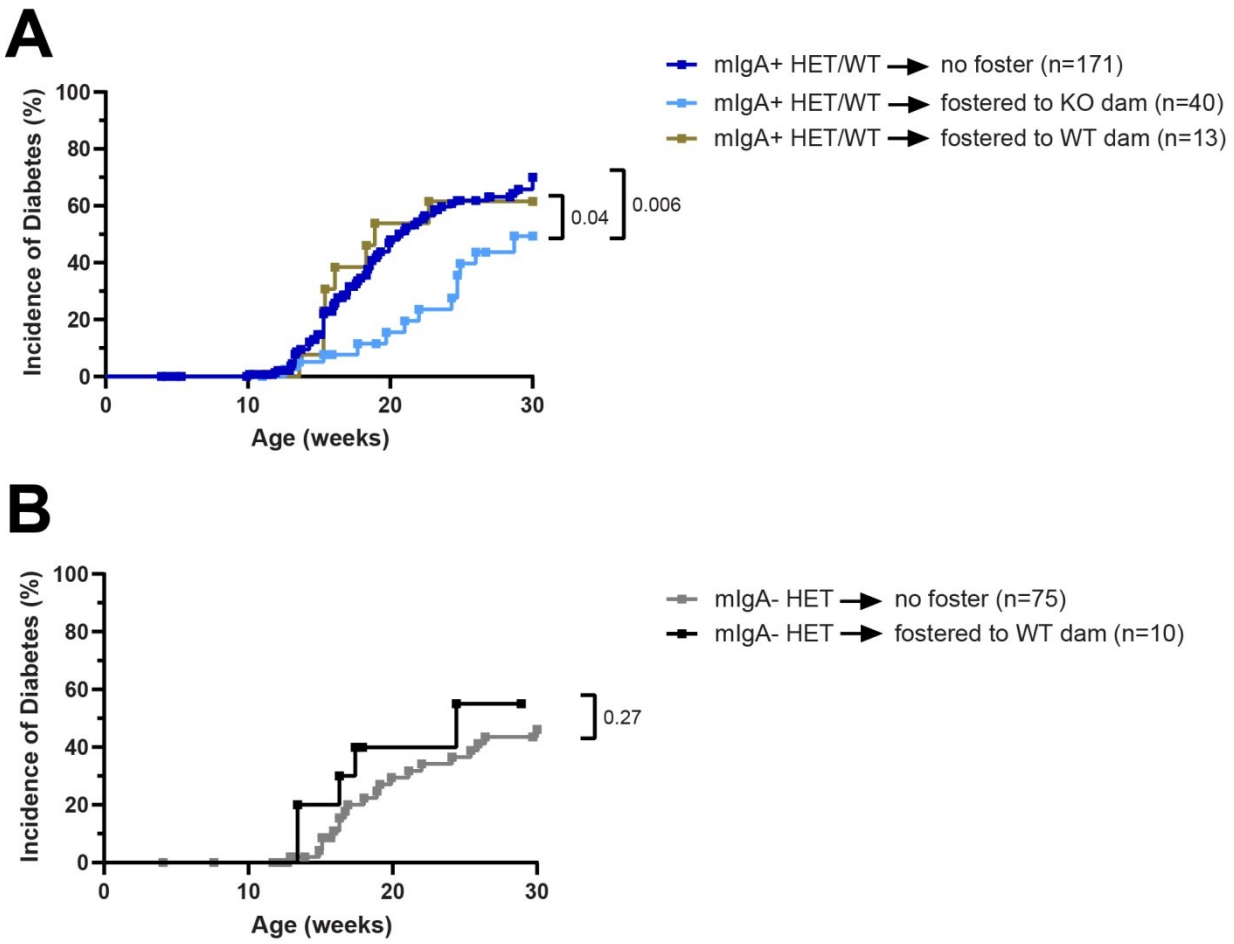


**Figure 4.2.5.1 T1D incidence in IgA-sufficient offspring fostered at birth**

Disease incidence curves for fostered offspring, showing T1D incidence of (**A**) NOD dam-born IgA-sufficient offspring fostered to NOD.IgA KO dams (light blue), in comparison to those not fostered (dark blue) or fostered to another NOD dam (brown). T1D incidence (**B**) of NOD.IgA KO-dam born IgA-sufficient offspring fostered to NOD dams (black) in comparison to those not fostered (grey). p-values were determined using the Log-rank test.

#### 4.2.5.2 IgA-deficient dams compensate for loss of breast milk IgA with increased levels of IgG and IgM

IgA is the most abundant antibody in breast milk, followed by IgG, then IgM[83]. Breast milk antibodies contribute to neonatal development in various ways. They act as a passive form of immunity in the early postnatal period, providing protection against enteric and systemic infections[115,116]. They help modulate neonatal microbiome colonization by coating microorganisms, thereby keeping their growth in check. Breast milk antibodies have been implicated in the maintenance of a tolerogenic environment unique to the neonatal intestine, helping to suppress $CD4^+$ T lymphocyte maturation[118] and GC development[119]. Furthermore, studies have demonstrated that breast milk IgG has isotype-specific functions, owing to its capacity to be transported across the gut epithelium and trafficked to various lymphoid tissues via FcRn-expressing immune cells[140–142]. In situations where IgG Ab-Ag complexes are trafficked in this manner, the result is induction of antigen-specific Treg populations and generation of long-lasting tolerogenic responses[140–142].

In comparison to NOD.IgA WT milk, the most obvious difference of breast milk from NOD.IgA KO dams is a lack of IgA. Considering the propensity I had seen of NOD.IgA KO animals to compensate for IgA deficiency, I quantified IgG and IgM concentrations in breast milk samples collected from NOD.IgA WT and KO dams, anticipating differences. Most notably, there was no difference in overall antibody concentration between the two groups of dams ($p=0.5$) despite the deficiency of IgA in one cohort. Furthermore, the IgA concentrations in the breast milk from NOD.IgA WT dams varied a lot, with nearly a 5-fold difference between the lowest and highest concentrations (**Fig 4.2.5.2A**). Similar to what I observed with serum and fecal antibody levels, I found that the lack of IgA in NOD.IgA KO breast milk was compensated, showing an average 2.7-fold increase in IgG and 4.6-fold increase in IgM (**Fig 4.2.5.2A**).

Given that each antibody isotype has its own unique specialty with respect to immunological activity, this substantial elevation in IgM and IgG content, in combination with deficiency of IgA, raises numerous questions regarding the physiological impact of breast milk from NOD.IgA KO dams, some of which will be discussed in the following sections.

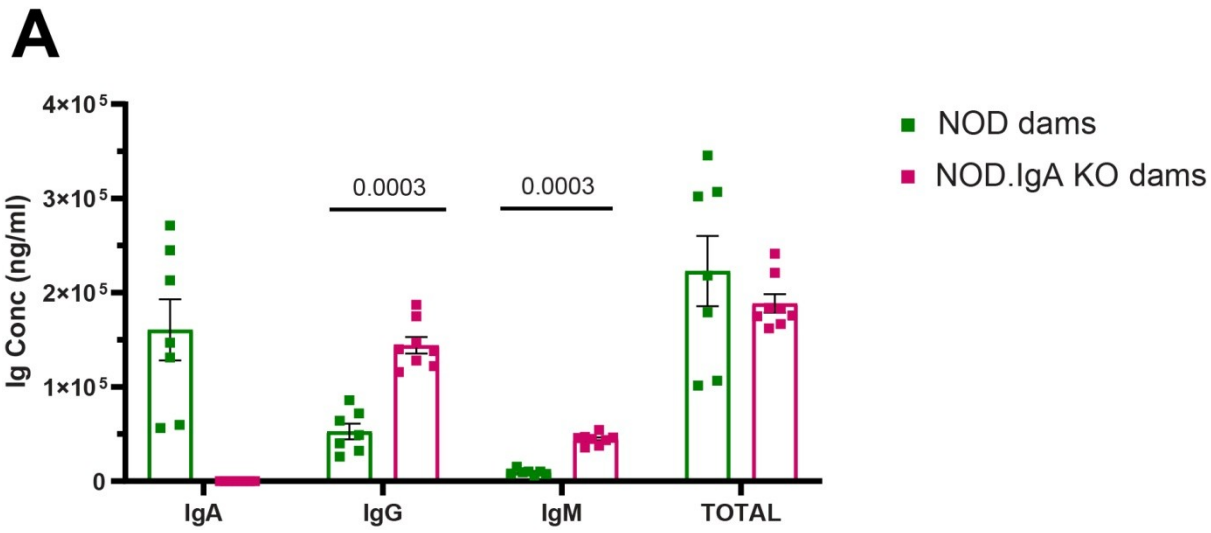


**Figure 4.2.5.2 Antibody concentrations in breast milk from NOD & NOD.IgA KO dams**

Comparison of antibody content (**A**) in breast milk from NOD (green) and NOD.IgA KO (pink) dams. p-values were determined using the Mann-Whitney U test.

### 4.2.5.3 Breast milk from IgA-sufficient and -deficient dams differ substantially in protein composition

Immunoglobulin is only one of many immunomodulatory components in breast milk, and dysbiosis could conceivably have an effect on expression level or secretion of some of these other components into the breast milk. Many milk immunomodulatory factors are proteins, and include antimicrobial factors such as lactoferrin and lysozyme, which neutralize endotoxin activity, degrade proteoglycan matrices in bacterial membranes, and prevent pro-inflammatory cytokine secretion[82]. Growth factors, such as EGF and lactadherin, are also present in breast milk and work to improve gut barrier function by influencing IEC turnover, regulating tight junction protein expression, and increasing mucus production by goblet cells[82]. With this in mind, I decided to perform proteomic analysis on breast milk from the two dam cohorts. Murine milk has high fat content and I was unsure how this might interfere with the analysis. Moreover, the lipid component contains hydrophobic proteins and peptides which I very much

wanted to include in the analysis. I was unable to find an established protocol for extracting protein from murine breast milk, so I contrived a protocol with the goal of removing the cellular and lipid components, while retaining all protein content from both the aqueous and lipid compartments. The proteomic analysis was performed by personnel (Henry Wang) in Dr. Olivier Julien's laboratory at the University of Alberta. Because Dr. Julien's lab had never before analyzed murine breast milk, and I was unsure as to the efficacy of my self-designed protocol, we began by performing the analysis on three milk samples from each of the two types of dams.

The protocol appeared to have worked rather well. Although I was unable to find any publications that provided information on the full protein content of murine breast milk for comparison, our analysis resulted in detection of almost 2000 proteins, with full identification of 1350 proteins and peptides. With one exception, milk total protein content was comparable between the samples (**Figure 4.2.5.3A**). The analysis identified 46 proteins present in decreased abundance and 88 proteins present in increased abundance in the NOD.IgA KO milk (>1.5-fold change, $p<0.05$), as illustrated by a volcano plot (**Figure 4.2.5.3B**). The lack of IgA in the NOD.IgA KO milk was confirmed; when compared to the NOD milk, content of Ig heavy chain $\alpha$ constant region was 66.7-fold lower ($p=0.0002$) and J chain content was 12.5-fold lower ($p=0.0002$) in milk from NOD.IgA KO dams (**Figure 4.2.5.3C**). In accordance with the ELISA data reported above, Ig heavy chain $\mu$ constant region (ie IgM heavy chain) content was 2.8-fold greater in milk from NOD.IgA KO dams (**Figure 4.2.5.3C**). The results regarding IgG content was less clear. Compared to NOD milk, IgG3 in NOD.IgA KO milk was present in lower quantity (3.69-fold lower) but with a significance of $p=0.3$ due to much variation between the samples. IgG2B and IgG1 content was similar between the two groups (1.05-fold & 1.19-fold change, respectively) and IgG2A content was doubled in the KO milk, but with $p=0.19$ again due to variation between samples (**Figure 4.2.5.3D**). The results for Ig light chain expression indicated that the sole $\kappa$ constant region showed a 1.54-fold decrease in NOD.IgA KO milk samples ($p=0.034$), and $\lambda 1$ constant region was present with a 1.89-fold decrease ($p=0.035$). $\lambda 2$ constant region was only modestly elevated (1.34-fold increase, $p=0.42$) (**Figure 4.2.5.3E**), which together suggests that total immunoglobulin content was lower in these NOD.IgA KO milk samples compared to the NOD milk. This was

in contrast to the ELISA results, which indicated no difference in total immunoglobulin content (Section 4.2.5.2). Several variable regions also showed differential expression between the NOD and NOD.IgA KO milk samples, with IgH V2-6 showing the largest increase (12.9-fold, p=0.0003) and IgH V1-18 and V3-6 showing significantly decreased expression (2.94-fold decrease, p=0.04 & 3.57-fold decrease, p=0.004, respectively). Similarly, numerous light chain κ variable regions showed differential expression between the two dam cohorts. This preferential usage of specific light chains and heavy chain variable regions suggests differences in antibody specificity, possibly driven by the presence of certain maternal microbiota-resident species, and warrants future investigation.

Significantly increased levels of other immunomodulatory proteins were indentified in the NOD.IgA KO milk, including prostaglandin E synthase 3, chemerin (RARRES2), H-2K$^{d}$ (MHC I), and CD5 antigen-like (CD5L). Additionally, myeloid-derived growth factor (MYDGF) and chemokine (C-X-C motif) ligand 17 (CXCL17) were found in decreased abundance in NOD.IgA KO milk (**Figure 4.2.5.3B**). All of these proteins are involved in coordinating and modulating inflammatory responses via a variety of mechanisms. Indeed, when up- or down-regulated proteins were grouped according to related function or activity, such as signalling cascades and metabolic pathways, using Enrichr (https://maayanlab.cloud/Enrichr/), results indicated that NOD.IgA KO milk was enriched for proteins involved in several immune signalling cascades, including Type I and III interferon responses, mTORC1 pathway, and Myc pathway targets (**Figure 4.2.5.3F**). Furthermore, NOD.IgA KO milk was significantly down-regulated in proteins involved in extracellular matrix remodelling, which was predicted by Enrichr to strongly affect a process called 'epithelial mesenchymal transition' (**Figure 4.2.5.3G**). This is a process whereby epithelial cells lose their adhesive, non-migratory properties in favor of migration and invasion. Much information is available regarding the role of epithelial mesenchymal transition in cancer and pre-natal development, but its role in post-natal GI development is a topic for future exploration. One could imagine that such a process would be involved in the migration of stem cells from the gut barrier crypts to the villi as they differentiate and replace the various cell types, contributing to the high turnover rate of GI epithelial barrier cells[183].

A considerable number of up-regulated proteins in the NOD.IgA KO milk were identified as various proteasome subunits. Although breast milk is known to include secreted extracellular proteasome components[184], the presence of these proteins was a possible indication of intracellular protein contamination by lysed cells and prompted me to explore how the protocol I devised affected immune cells. Testing the protocol on splenocytes, which involved resuspension in [PBS + 0.28% SDS] followed by centrifugation for 10 min at 14 000g and 4$^{o}$C, resulted in the lysis of 100% of the cells. Thus, the milk protein analysis results included both secreted proteins as well as the intracellular protein components of breast milk cells. Although this was not the initial intention, it does prompt some consideration regarding the cellular component of breast milk and how it is affected by IgA deficiency.

In summary, breast milk protein content differs considerably between the NOD and NOD.IgA KO dams. Not surprisingly, antibody content differs substantially, exhibiting preferential expression of isotypes, light chains, and variable regions. These dissimilarities suggest differences in antigen specificity, leading to the likelihood that each milk modulates the infant microbiome uniquely. Furthermore, the results indicated increased Type I and III interferon, as well as mTORC1, signalling capacity, a clear indication of pro-inflammatory environment promotion in the neonatal GI tract. Moreover, the implications of reduced levels of extracellular matrix components and an apparent promotion of epithelial mesenchymal transition are unclear, although it may suggest maternal support for stem cell migration and IEC turnover in the neonatal gut. Thus, this data set provides me with considerable material to consider and explore as I endeavor to understand the protective mechanisms at work in the mIgA- HET and fostered mIgA+ HET cohorts.

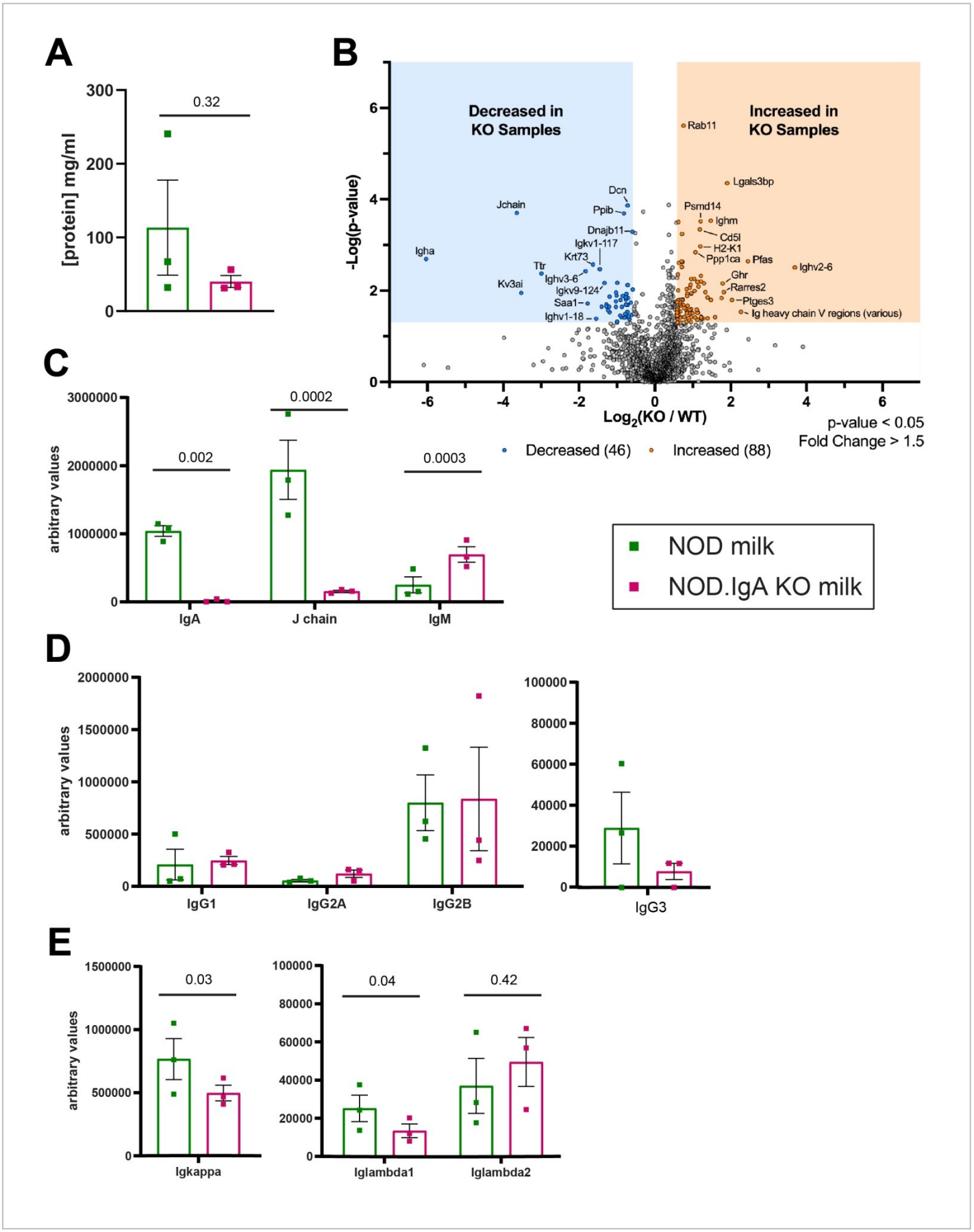
A
[protein] mg/ml
300
200
100
0
0.32
B
Decreased in KO Samples
Increased in KO Samples
-Log(p-value)
Log2(KO / WT)
Rab11
Lgals3bp
Dcn
Jchain
Ppib
Psmd14
Ighm
Dnajb11
Cd5l
Igkv1-117
H2-K1
Igha
Krt73
Ppp1ca
Pfas
Ighv2-6
Ttr
Ighv3-6
Ghr
Kv3ai
Igkv9-124
Rarres2
Saa1
Ptges3
Ighv1-18
Ig heavy chain V regions (various)
p-value < 0.05
Fold Change > 1.5
Decreased (46)
Increased (88)
C
arbitrary values
3000000
2000000
1000000
0
0.002
0.0002
0.0003
IgA
J chain
IgM
NOD milk
NOD.IgA KO milk
D
arbitrary values
2000000
1500000
1000000
500000
0
IgG1
IgG2A
IgG2B
100000
80000
60000
40000
20000
0
IgG3
E
arbitrary values
1500000
1000000
500000
0
0.03
Igkappa
100000
80000
60000
40000
20000
0
0.04
0.42
Iglambda1
Iglambda2

**F**

| Index | Name | P-value | Adjusted p-value | Odds Ratio | Combined score |
|---|---|---|---|---|---|
| 1 | Myc Targets V1 | 2.044e-8 | 6.337e-7 | 13.14 | 232.63 |
| 2 | mTORC1 Signaling | 2.662e-7 | 0.000004125 | 11.62 | 175.84 |
| 3 | Interferon Gamma Response | 0.00003102 | 0.0002404 | 8.72 | 90.54 |
| 4 | Glycolysis | 0.00003102 | 0.0002404 | 8.72 | 90.54 |
| 5 | Hypoxia | 0.0002706 | 0.001678 | 7.35 | 60.35 |
| 6 | Interferon Alpha Response | 0.0009261 | 0.004785 | 10.03 | 70.04 |
| 7 | Xenobiotic Metabolism | 0.01224 | 0.05421 | 4.73 | 20.84 |

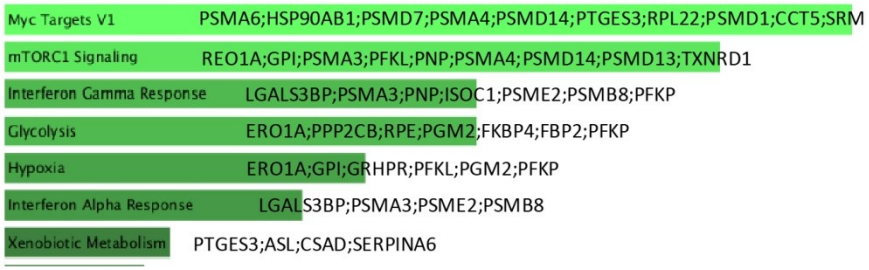


**G**

| Index | Name | P-value | Adjusted p-value | Odds Ratio | Combined score |
|---|---|---|---|---|---|
| 1 | Epithelial Mesenchymal Transition | 0.00005990 | 0.001318 | 13.70 | 133.16 |
| 2 | Pperoxisome | 0.02014 | 0.1696 | 9.73 | 38.01 |
| 3 | Bile Acid Metabolism | 0.02313 | 0.1696 | 9.02 | 33.98 |
| 4 | Apoptosis | 0.04495 | 0.2075 | 6.23 | 19.31 |


**Figure 4.2.5.3 Protein composition of breast milk from NOD & NOD.IgA KO dams**

Proteomic analysis of breast milk from NOD (green) and NOD.IgA KO (pink) dams, showing total protein concentration (**A**), and up- and down-regulated proteins (**B**) visualized in a volcano plot. Comparison of various antibody protein levels (**C-E**), where error bars indicate mean +/- SEM. Up-regulated (**F**) and down-regulated (**G**) proteins in NOD.IgA KO milk grouped according to pathways and biological processes using Enrichr online software. Affected proteins are indicated for each category.

## 4.3 Discussion

Although a deficiency of IgA failed to alter T1D incidence in NOD mice, it had profound effects on disease susceptibility in the following generation. IgA-sufficient offspring from IgA-deficient dams showed reduced T1D incidence over 30 weeks, and this phenotype was replicated in NOD-born IgA-sufficient offspring fostered to IgA-deficient dams. Thus, post-natal factors provided by the IgA-deficient dam resulted in resistance to disease development in offspring. Furthermore, this protection was only perpetuated in the presence of endogenous IgA production, as IgA-deficient pups born to IgA-deficient dams did not show resistance.

I hypothesized that post-natal maternal factors exerted their influence via direct and/or indirect influence of the maternal microbiome, both on her own physiology and that of her offspring. IgA deficiency significantly altered the maternal microbiome, which in turn contributed to changes in breast milk protein composition and strongly influenced the neonatal microbiome composition. Effects of these influences were apparent in the early post-weaning period, evidenced by altered microbial metabolite availability, elevated humoral responses systemically and in the GI tract, and increased immune cell populations in the gut. Long-term effects consisted of sustained elevated serum and lumenal antibody levels, decreased insulitis, subdued immune activity in the PLN, and fewer islet-reactive $CD8^+$ T lymphocytes in the PLN. The GI barrier was affected in adulthood, exhibiting a thicker mucus layer concomitant with increasing gut permeability with age.

The contribution of maternal factors to disease protection is likely multifaceted. The cross-fostering experiments confirmed that the maternal factors at play were largely post-natal. The two most obvious mechanisms for post-natal influences are (1) breast milk ingestion and (2) microbiome seeding. This study demonstrated that elements of the maternal microbiome were mirrored in her offspring, including the presence or absence of specific bacterial species, resulting in progeny microbiota that strongly resembled the maternal microbiome. It may simply have been the presence or absence of specific microbial members in progeny microbiota that drove T1D susceptibility, an hypothesis that could be studied by introducing or removing relevant community members from the early microbiome and observing the effect on disease incidence. Conversely, the maternal microbiome may have influenced the specificity of breast milk antibodies that then either modulated the infant microbiota or

influenced immune development. Indeed, breast milk antibodies have been shown to dampen intestinal $CD4^+$ T lymphocyte activation and GC development during the weaning/early post-weaning period[118,119]. In my hands, the deficiency of breast milk IgA and resulting increase in milk IgG appeared to abolish this dampening effect in 3 week old offspring, as evidenced by higher numbers of activated $CD4^+$ T cells in the bowel and MLN, and increased proportions of MLN-residing $T_{fh}$ cells and GC B lymphocytes in progeny of IgA-deficient dams. This increased activation state may have been a result of changes in the milk antibody repertoire, such that some microorganisms normally bound by sIgA escaped coating by NOD.IgA KO milk antibodies. Indeed, Torow *et al*.[118] proposed that it was the sequestering of microbial antigen by breast milk antibodies in the gut lumen of offspring that allowed for maintained $CD4^+$ T cell naivety. Another possibility is that differences in milk IgG repertoire resulted in FcRn-mediated transfer of unique maternal Ab-Ag complexes having a direct effect on immune development and activation in the neonatal gut. This theory is supported by my finding of significant differences in the early metabolome of the two NOD.IgA HET cohorts, as well as the preferential recombination of certain Ig variable regions in NOD.IgA KO milk. Furthermore, several studies[115,118,119,140,143,185] corroborate this possibility, which could be explored using neonatal FcRn blockade experiments, a future direction of this project. It is also worthwhile to note that while Koch *et al*[119]. observed increased GC activity in 3 week offspring lacking maternal antibodies, the long-term effects on health were left unexplored, prompting questions about whether or not immune regulation is impaired under these conditions.

The heightened GI response in the disease-resistant cohort correlated with a stronger systemic humoral response which was particularly evident at 3 weeks of age. During the weaning period, the introduction of the microbiota has been shown to expand lymphocyte repertoires[73,79,87–89], which could account for the increased serum IgG and IgA. Alternatively, increased serum IgG in mIgA- HET pups at 3 weeks of age may have been of maternal origin, a result of the increased breast milk IgG content and/or enhanced FcRn-mediated maternal IgG transfer. Several studies have shown that cytokine signalling regulates the expression level of FcRn in both neonatal IEC and immune cells, and can enhance the trans-epithelial transport of maternal IgG[186–188]. Indeed, the up-regulated interferon response signalling components and Myc targets are evidence of increased cytokine signalling capacity in

NOD.IgA KO breast milk which may contribute to enhanced FcRn-mediated transport in mIgA- HET offspring.

At 12 weeks, the colonic mucus layer appeared to be superior in the mIgA- HET cohort, at least from an histological viewpoint. The thickness was greater overall, with fewer areas of disrupted mucus and a greater distance between the lumenal contents and epithelial lining. This enhanced barrier is likely attributable to the increased expression of metabolite receptors (AhR, GPR41, GPR43) at 5 weeks of age, enhancing communication between the microbiota and host. It may also be a result of maternally-endorsed IEC turnover arising from milk-derived signals during the pre-weaning period. The interpretation of this phenotype is unclear, however. From a theoretical perspective, a thicker mucus layer would inhibit microbial penetration of the intestinal barrier and prevent translocation, immune activation and inflammation. Considering the theories of autoimmune activation discussed earlier, this would lower susceptibility to T1D. If these differences were evident at a younger age (a future direction of this project), this explanation would be quite conceivable. On the other hand, by 12 weeks of age most of these mice have already developed autoreactive immunity against pancreatic antigens, as evidenced by the presence of NRP-V7$^{+}$ CD8$^{+}$ T cell populations in the PLN, and T1D is well underway so differences in mucus layer integrity at this time point may be a response to changes occurring in the gut or to specific members of the microbiota. Intestinal infections and pathogens have been shown to induce dynamic changes in the mucus layer, in part an effort by the host to restore homeostasis[180,181]. Moreover, various gut microbes are mucin degraders and their over-colonization can erode the colonic mucus layer. One of these species is *Akkermansia muciniphila*[189], which we showed was present at significantly higher proportions in the mIgA+ HET cohort. Moreover, though *A. muciniphila* has been associated with increased mucus layer thickness due to its ability to promote mucus secretion[189], this beneficial aspect may not hold true for compromised gut barriers. Additionally, Lachnospiraceae family members have been found to frequently associate with the mucus layer[189]. This provides an explanation for the observed enrichment of several Lachnospiraceae members in the mIgA- HET cohort, which harbor a thicker mucus layer.

# Chapter 5: Discussion, Conclusion & Future work

In this thesis, I endeavored to explore how various aspects of the GI tract, including microbiome establishment and modulation, as well as host-mediated immune responses, affected the onset and pathogenesis of T1D in a genetically-conducive environment. Using a model of complete IgA deficiency, I investigated how genetic deletion of IgA modulated both the microbiome and mucosal immunity in the GI tract, and how this ultimately affected susceptibility to T1D in our novel NOD.IgA model. Furthermore, I explored how IgA deficiency-induced microbiome changes in breeding dams affected offspring. I showed how maternal dysbiosis contributed to the same in pups, how offspring microbiome compositional changes contributed to functional changes in terms of metabolite production, and how these changes affected the GI environment, shaped early and long-term immunity, and influenced T1D susceptibility in offspring.

## 5.1 Discussion

It has become evident that animal studies using genetic manipulation in order to study the effects of a given gene product or signalling pathway on microbiota composition have historically over-emphasized the role of genetics. Although genotype is a contributor to microbiome composition, it is less of a determinant than initially thought. For example, a 2008 study using a mouse model with defective pattern recognition receptor (PRR) signalling concluded that innate immune signalling is a strong modulator of microbiota composition[190]. A subsequent study proved this conclusion to be over-stated, demonstrating that vertical transmission of the maternal microbiome trumped genetics as a driving force when PRR-deficient and -sufficient littermates were shown to share the same microbiome[191]. Since then, the field has endeavored to provide guidelines for how animal studies should be conducted in order to correctly identify, control for and manipulate the plethora of factors that modulate the microbiome[170].

This thesis has provided new insights into the over-arching question of how the microbiome community affects disease susceptibility. By and large, it is the presence of the microbiome, along with associated metabolites and microbial products, that fuels the immune responses along the GI tract[80,85,86]. In turn, the type of response generated establishes the competence of

the immune system with respect to its ability to distinguish innocuous from threatening entities. When the microbiota is introduced during the aforementioned neonatal window of opportunity, the host immune system responds with tolerance, and adequate immune regulation is the result[79,81]. This tolerogenic response comprises both pro- and anti-inflammatory reactions[79,80], a challenge to the current paradigm that GI inflammation during homeostasis is detrimental to host health. Indeed, in this thesis I provided further evidence that a heightened immune response during the weaning period is in fact favorable, leading to better immune regulation and lowering susceptibility to immuno-dysregulatory diseases. In my study, this bolstered immune response was evidenced at 3-5 weeks by increased ileal cytokine expression, increased $IgA^+$ B cell/PC, $CD4^+$, $CD8^+$ and γδT lymphocyte populations in the GI tract, higher levels of lumenal Lcn-2 and a greater colonic weight:length ratio. Moreover, although Lcn-2 can promote inflammatory responses, there is evidence that intestinal Lcn-2 may act as an anti-inflammatory modulator by enhancing bacterial clearance by macrophages[192]. In the neonate, the effects of this would be two-fold, first increasing antigen presentation to a fledgling immune system in order to drive T lymphocyte repertoire expansion, and secondly enhancing microbiome modulation. Thus, rather than viewing Lcn-2 as an inflammatory marker, perhaps in this context it is a measure of the GI mucosal immune system's response to the developing microbiome, a perspective that underscores the importance of the weaning reaction and is supported by my data.

In my study, the maternal influences on offspring disease incidence was largely mediated by post-natal factors, as shown by the cross-fostering experiments. Initial exploration of breast milk characteristics revealed considerable differences in immunomodulatory factors between milk from NOD vs. NOD.IgA KO dams at 10-11 days postpartum. Differences in proportions of milk antibody isotypes, as well as preferential recombination of specific Ig heavy chain variable regions and light chain combinations, raise the possibility that the milk antibody repertoires are quite different between the two dam cohorts. It has been shown that the maternal microbiome influences the breast milk antibody repertoire[143], and these differences may lead to differential targeting of microbial species in the offspring gut, modifying the newly-colonized microbiome in a divergent manner in the offspring cohorts. This theory is supported by the observation that NOD.IgA HET offspring cohorts harbored enriched bacterial species that were not associated with one dam cohort over the other. A second

possibility is that differences in IgG content and/or antigenic specificity may allow for introduction of unique antigen to their respective progeny cohort via Ab-Ag complexes, thus influencing the establishment of tolerance to different antigens and expanding the lymphocyte repertoire uniquely. Support for this theory can be found in a number of animal studies employing neonatal introduction of foreign antigen, where tolerance and lymphocyte repertoire shaping is the result[140–142,185]. Other up- or down-regulated immunomodulatory factors in the NOD.IgA KO breast milk may have influenced FcRn-mediated transfer of these maternal Ab-Ag complexes, while others may have affected the physiology of the infant gut barrier, such as increasing IEC turnover. Indeed, the capacity for IEC remodelling has been shown for breast milk factors, where initially high levels of milk EGF wane over time, allowing for GAP formation and increasing barrier permeability in the pups[81]. This is an intriguing area of study that provides many possibilities for future directions, some of which will be discussed in Section 5.2.

As discussed throughout this thesis and supported by my data, the maternal microbiome is the initial source of microorganisms colonizing the neonatal GI tract. The ecological term 'priority effect' refers to how a species' timing or order of arrival affects its ability to colonize a particular niche[193]. Thus, these maternally-provided microbes exert priority over microorganisms that are introduced at a later time point, providing a rationale for the strength of maternal transmission in influencing long-term offspring microbiome composition. However, the establishment of the neonatal microbiome is not an immediate event, leaving opportunity for other microorganisms to colonize as well. Alternate sources of microbes include the paternal microbiome, as well as those of littermates. As the offspring age, microorganisms from cagemates can be shared via coprophagy. In this way, any modulatory effects of genetics on the microbiome can be lost through sharing of microorganisms between animals of differing genotype. The terms 'litter effects' and 'cage effects' are used to describe the phenotypic variations seen between litters or cages in animal studies. These effects are thought to be largely due to the microbiota. Littermates or cagemates of the same genotype can show variations in phenotype due to, for example, maternal differences or previous housing with animals of another genotype. Conversely, two cages housing animals of different genotypes can exhibit the same phenotype if they harbor similar microbiomes due to having the same maternal origin or having been housed together at some point. These sorts of

variables have been the source of much frustration in animal studies for decades, producing study results that cannot be replicated in other facilities or at later time points. With all of this in mind, we carefully designed this study to minimize these confounders. Breeding schemes were designed to produce litters of one genotype, and the sire of a new litter was removed from the cage as early as possible to limit his microbial dispersion. After weaning, genotypes were caged separately to prevent microbial transfer via coprophagy, and at no point were animals of differing maternal origin co-housed. All of this was done in order to maximize and exploit cage effects in a disease model that we hypothesized was driven largely by the microbiome, as recommended in the literature[170].

## 5.2 Future work

This thesis project has provided some insights into the largely unknown realm of maternal influences on neonatal immunity in health and disease, helping to discern what exactly constitutes healthy immune development. In doing so, this work has perhaps raised more questions than it has answered. There are a number of directions that this project can take, a few of which are already underway and are discussed below.

### 5.2.1 Continuing cross-fostering experiments

The cross-fostering experiments have provided some very useful data to date, but are still incomplete at this point. A number of the fostered offspring are still being followed for T1D incidence and I anticipate that several of them will become diabetic before 30 weeks of age. Thus, in order to maintain statistical significance, I anticipate the need to follow several more litters of fostered mice. Additionally, I am interested to know if the microbiome of fostered offspring more closely resembles that of their birth or foster dam, or perhaps a melding of the two. I have been collecting fecal material from the fostered pups at weaning (21 days of age) and these are currently being analyzed for bacterial content via 16S rRNA sequencing. Once available, this data will be compared to the microbiota bacterial composition of NOD and NOD.IgA KO adult females. I hope that this will provide insights to several questions, including whether infant microbiome seeding is initiated during gestation and/or the peri-natal period vs. the post-natal period. Moreover, fostered offspring with a microbiome that reflects that of the foster dam will provide support for the hypothesis that maternal microbiome influence on disease incidence in offspring is being conferred via neonatal microbiome

development or modulation. Alternatively, if the fostered offspring harbor a microbiota that more closely resembles that of the birth dam, this would suggest that the protective phenotype is being conferred independently from infant microbiome establishment.

### 5.2.2 Maternal microbiome manipulation (Fecal Microbiota Transfer)

I hypothesized that the protection afforded offspring by IgA-deficient dams involved factors driven by the maternal microbiome. As such, manipulations of the maternal microbiome would be expected to alter disease susceptibility in offspring. I designed a fecal microbiota transfer (FMT) experiment in which the microbiome of NOD adult females were replaced with those of NOD.IgA KO females. These FMT recipient NOD females were then mated to produce NOD.IgA HET offspring, henceforth called $FMT^{KO}$ mIgA+ HET. I reasoned that if the microbiome of the NOD.IgA KO dam is the driver of disease protection in offspring, transferring that microbiome into NOD dams will confer similar protection, and thus similar disease incidence, for the $FMT^{KO}$ mIgA+ HET offspring.

To date, 40 female offspring from this experiment have been weaned and will be followed for T1D incidence until 30 weeks of age. Fecal material was collected from each dam and her litter at weaning and is currently undergoing 16S rRNA sequencing. 16S rRNA sequencing is also being performed on fecal samples taken from NOD females before and after the FMT procedure, as well as on the FMT donation material. The resulting data from these analyses will be used to ascertain (1) whether the FMT procedure was successful at replacing the NOD microbiota; (2) whether the donated microbiota was vertically transmitted to the offspring; (3) how microbiota composition in the $FMT^{KO}$ mIgA+ HET cohort compares to that of the mIgA+ and mIgA- HET cohorts; and (4) whether the donated microbiota is sustained long-term in the NOD dams. As a control, three additional NOD females underwent the same FMT procedure, but received donated microbiota from NOD females. To date, three litters have been born to these females, and the offspring will be followed in a manner identical to that of the $FMT^{KO}$ mIgA+ HET cohort.

I anticipate that the results from this experiment will provide conclusive evidence for the direct influence of the maternal microbiome on offspring disease susceptibility.

### 5.2.3 Further exploration of breast milk

The proteomic analysis of breast milk from NOD and NOD.IgA KO dams presented in this thesis included only three samples from each dam cohort. I would like to expand this analysis to include at least six samples from each cohort. Furthermore, I would like to follow up on some of the immunomodulatory factors that were differentially abundant, particularly those of the type I and III interferon responses and those identified as belonging to the 'epithelial mesenchymal transition' process. Initially, this will require a deep dive into the current literature, as it is currently unclear how delivery of these factors into the neonatal gut lumen would influence gut physiology and immunity. I anticipate these experiments would involve administering down-regulated factors, or conversely blocking the delivery of up-regulated factors, to mIgA- HET neonates during the pre-weaning period to see if this abolishes the protective phenotype.

I have a keen interest in pursuing the theory of an altered breast milk antibody repertoire in the NOD.IgA KO dam. I designed an experiment whereby breast milk from each dam cohort (n=10) was used to coat microorganisms isolated from 3 week NOD.IgA HET feces. The resulting maternal antibody-coated microorganisms were separated from non-coated microbes and collected for taxonomic identification via 16S rRNA sequencing. This analysis is underway, along with sequencing of the initial fecal microbial pool. These results will allow me to determine which bacterial taxa are being bound by milk antibodies, which are escaping, and whether these fractions differ for NOD vs. NOD.IgA KO milk. I would like to design and perform a similar experiment whereby milk antibodies are tested against luminal metabolites, perhaps in a panel format, to determine antigenic specificities for microbial metabolites in each type of milk. As an extension of this, *in vivo* blockade of FcRn could be used to eliminate uptake of maternal Ab-Ag complexes and determine whether this abolishes disease protection in mIgA- HET offspring. Although the execution of such an experiment requires some consideration regarding the timing and route of administration of the blocking agent, this is a future direction we are currently contemplating. Alternately, Ab-Ag complexes identified in NOD.IgA KO milk, but absent from NOD milk, could be administered to mIgA+ HET offspring during the pre-weaning period to determine whether they promote disease resistance.

## 5.3 Conclusion

In conclusion, this thesis provides compelling evidence for the influence of the maternal microbiome on infant microbiome establishment, GI physiology and immune environment, and long-term immune health and regulation. Moreover, protective influences conveyed by a dysbiotic dam primarily during the post-natal period contributed to the strength of both pro- and anti-inflammatory immune responses along the neonatal GI tract that constitute the weaning reaction. In turn, a more robust weaning reaction lessened T1D susceptibility in genetically at-risk offspring, reducing the presence of autoreactive $CD8^+$ T lymphocytes, ameliorating insulitis, and ultimately lowering T1D incidence (**Fig 5.3**). Endogenous production of IgA was, on its own, not sufficient to reduce T1D susceptibility, but played an essential role in maintaining the maternally-provided protective phenotype introduced during the neonatal period. The conclusion of heightened GI inflammatory processes contributing to greater immune regulation and improved health outcomes in adulthood is a challenge to the current paradigm, and presents an opportunity to revisit this subject with a fresh perspective.

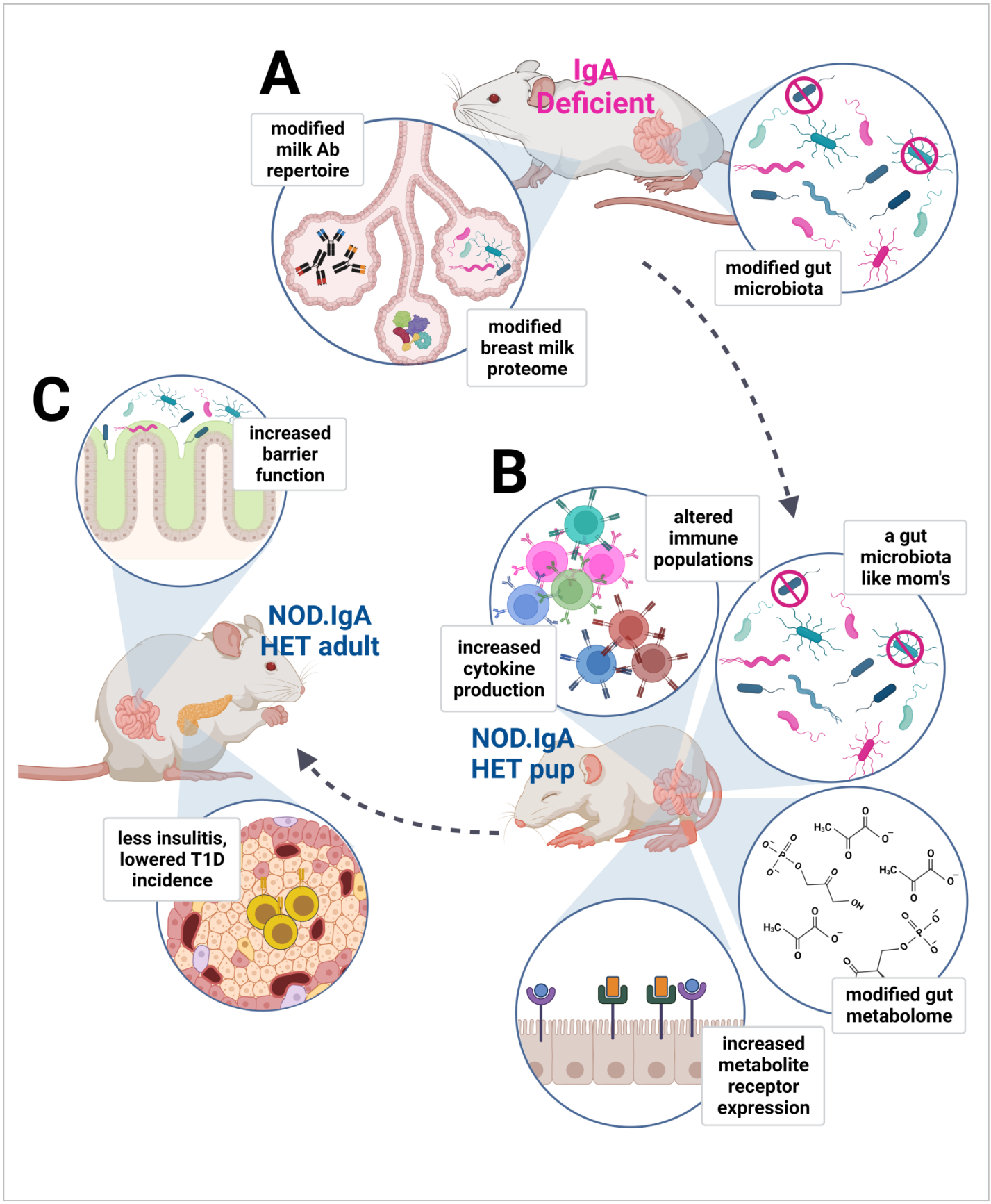
A
IgA Deficient
modified milk Ab repertoire
modified breast milk proteome
modified gut microbiota
B
altered immune populations
increased cytokine production
a gut microbiota like mom's
NOD.IgA HET pup
modified gut metabolome
increased metabolite receptor expression
C
increased barrier function
NOD.IgA HET adult
less insulitis, lowered T1D incidence

**Figure 5.3 The effects of maternal IgA deficiency on T1D incidence in offspring**

(**A**) Complete IgA deficiency in NOD female mice results in microbiome alterations that persist into adulthood. Postpartum, a dysbiotic microbiome and lack of IgA contribute to changes in the breast milk proteome, including altered levels of IgG & IgM as well as antibody repertoire. (**B**) Influences from a dysbiotic dam, likely mediated by both breast milk and maternal microbiome, modulate immune development and microbiome establishment in IgA-sufficient offspring during the post-weaning period. The dysbiotic maternal microbiota is mirrored in the microbiota of offspring and contributes to an altered metabolome, including decreased SCFA levels and altered amino acid & folate metabolism. Immune cell population numbers, activation state and cytokine production are elevated, and metabolite receptor expression is boosted. (**C**) In adulthood, these offspring exhibit greater gut barrier function in the form of a thicker mucus layer. Concurrently, immune activity involving the pancreas is subdued, showing less insulitis and fewer autoreactive $CD8^+$ T lymphocytes in the draining lymph nodes. By 30 weeks of age, IgA-sufficient offspring born to, or fostered to, IgA-deficient dams have reduced T1D incidence.

Figure created with BioRender.com

# Bibliography


1. Pugliese A. The multiple origins of Type 1 diabetes. *Diabetic Medicine*. 2013;30(2):135-146. doi:10.1111/dme.12081

2. Gregory GA, Robinson TIG, Linklater SE, et al. Global incidence, prevalence, and mortality of type 1 diabetes in 2021 with projection to 2040: a modelling study. *Lancet Diabetes Endocrinol*. 2022;10(10):741-760. doi:10.1016/S2213-8587(22)00218-2

3. Ilonen J, Lempainen J, Veijola R. The heterogeneous pathogenesis of type 1 diabetes mellitus. *Nat Rev Endocrinol*. 2019;15(11):635-650. doi:10.1038/s41574-019-0254-y

4. Insel R, Knip M. Prospects for primary prevention of type 1 diabetes by restoring a disappearing microbe. *Pediatr Diabetes*. 2018;19(8):1400-1406. doi:10.1111/pedi.12756

5. Stanley HM, Norris JM, Barriga K, et al. Is presence of islet autoantibodies at birth associated with development of persistent islet autoimmunity? The Diabetes Autoimmunity Study in the Young (DAISY). *Diabetes Care*. 2004;27(2):497-502. doi:10.2337/diacare.27.2.497

6. Roll U, Christie MR, Füchtenbusch M, Payton MA, Hawkes CJ, Ziegler AG. Perinatal autoimmunity in offspring of diabetic parents. The German Multicenter BABY-DIAB study: detection of humoral immune responses to islet antigens in early childhood. *Diabetes*. 1996;45(7):967-973. doi:10.2337/diab.45.7.967

7. Fousteri G, Ippolito E, Ahmed R, Hamad ARA. Beta-cell Specific Autoantibodies: Are they Just an Indicator of Type 1 Diabetes? *Curr Diabetes Rev*. 2017;13(3):322-329. doi:10.2174/1573399812666160427104157

8. Pescovitz MD, Greenbaum CJ, Bundy B, et al. B-lymphocyte depletion with rituximab and β-cell function: two-year results. *Diabetes Care*. 2014;37(2):453-459. doi:10.2337/dc13-0626

9. Vendrame F, Pileggi A, Laughlin E, et al. Recurrence of type 1 diabetes after simultaneous pancreas-kidney transplantation, despite immunosuppression, is associated with autoantibodies and pathogenic autoreactive CD4 T-cells. *Diabetes*. 2010;59(4):947-957. doi:10.2337/db09-0498

10. Coppieters KT, Dotta F, Amirian N, et al. Demonstration of islet-autoreactive CD8 T cells in insulitic lesions from recent onset and long-term type 1 diabetes patients. *J Exp Med*. 2012;209(1):51-60. doi:10.1084/jem.20111187

11. Skowera A, Ellis RJ, Varela-Calviño R, et al. CTLs are targeted to kill beta cells in patients with type 1 diabetes through recognition of a glucose-regulated preproinsulin epitope. *J Clin Invest*. 2008;118(10):3390-3402. doi:10.1172/JCI35449

12. Radenkovic M, Uvebrant K, Skog O, et al. Characterization of resident lymphocytes in human pancreatic islets. *Clin Exp Immunol*. 2017;187(3):418-427. doi:10.1111/cei.12892

13. Richardson SJ, Rodriguez-Calvo T, Gerling IC, et al. Islet cell hyperexpression of HLA class I antigens: a defining feature in type 1 diabetes. *Diabetologia*. 2016;59(11):2448-2458. doi:10.1007/s00125-016-4067-4

14. Christoffersson G, Flodström-Tullberg M. Mouse Models of Virus-Induced Type 1 Diabetes. *Methods Mol Biol*. 2020;2128:93-105. doi:10.1007/978-1-0716-0385-7_7

15. Al-Awar A, Kupai K, Veszelka M, et al. Experimental Diabetes Mellitus in Different Animal Models. *J Diabetes Res*. 2016;2016:9051426. doi:10.1155/2016/9051426

16. Pandey S, Dvorakova MC. Future Perspective of Diabetic Animal Models. *Endocr Metab Immune Disord Drug Targets*. 2020;20(1):25-38. doi:10.2174/1871530319666190626143832

17. Tatti P, Pavandeep S. Gender Difference in Type 1 Diabetes: An Underevaluated Dimension of the Disease. *Diabetology*. 2022;3(2):364-368. doi:10.3390/diabetology3020027

18. Lynch KF, Lee HS, Törn C, et al. Gestational respiratory infections interacting with offspring HLA and CTLA-4 modifies incident β-cell autoantibodies. *J Autoimmun*. 2018;86:93-103. doi:10.1016/j.jaut.2017.09.005

19. Craig ME, Kim KW, Isaacs SR, et al. Early-life factors contributing to type 1 diabetes. *Diabetologia*. 2019;62(10):1823-1834. doi:10.1007/s00125-019-4942-x

20. Noble JA, Valdes AM. Genetics of the HLA region in the prediction of type 1 diabetes. *Curr Diab Rep*. 2011;11(6):533-542. doi:10.1007/s11892-011-0223-x

21. Tsai S, Serra P, Clemente-Casares X, et al. Antidiabetogenic MHC class II promotes the differentiation of MHC-promiscuous autoreactive T cells into FOXP3+ regulatory T cells. *Proc Natl Acad Sci U S A*. 2013;110(9):3471-3476. doi:10.1073/pnas.1211391110

22. Tsai S, Santamaria P. MHC Class II Polymorphisms, Autoreactive T-Cells, and Autoimmunity. *Front Immunol*. 2013;4:321. doi:10.3389/fimmu.2013.00321

23. Tsai S, Serra P, Clemente-Casares X, Slattery RM, Santamaria P. Dendritic cell-dependent in vivo generation of autoregulatory T cells by antidiabetogenic MHC class II. *J Immunol*. 2013;191(1):70-82. doi:10.4049/jimmunol.1300168

24. Rich SS, Akolkar B, Concannon P, et al. Overview of the Type I Diabetes Genetics Consortium. *Genes Immun*. 2009;10 Suppl 1:S1-4. doi:10.1038/gene.2009.84

25. Bonifacio E, Beyerlein A, Hippich M, et al. Genetic scores to stratify risk of developing multiple islet autoantibodies and type 1 diabetes: A prospective study in children. *PLoS Med*. 2018;15(4):e1002548. doi:10.1371/journal.pmed.1002548

26. Barrett JC, Clayton DG, Concannon P, et al. Genome-wide association study and meta-analysis find that over 40 loci affect risk of type 1 diabetes. *Nat Genet*. 2009;41(6):703-707. doi:10.1038/ng.381

27. Pugliese A, Zeller M, Fernandez A, et al. The insulin gene is transcribed in the human thymus and transcription levels correlated with allelic variation at the INS VNTR-IDDM2 susceptibility locus for type 1 diabetes. *Nat Genet*. 1997;15(3):293-297. doi:10.1038/ng0397-293

28. Atkinson MA, Eisenbarth GS, Michels AW. Type 1 diabetes. *Lancet*. 2014;383(9911):69-82. doi:10.1016/S0140-6736(13)60591-7

29. Clausen TD, Bergholt T, Bouaziz O, et al. Broad-Spectrum Antibiotic Treatment and Subsequent Childhood Type 1 Diabetes: A Nationwide Danish Cohort Study. *PLoS One*. 2016;11(8):e0161654. doi:10.1371/journal.pone.0161654

30. Rutayisire E, Huang K, Liu Y, Tao F. The mode of delivery affects the diversity and colonization pattern of the gut microbiota during the first year of infants' life: a systematic review. *BMC Gastroenterol*. 2016;16(1):86. doi:10.1186/s12876-016-0498-0

31. Quinn LM, Wong FS, Narendran P. Environmental Determinants of Type 1 Diabetes: From Association to Proving Causality. *Front Immunol*. 2021;12:737964. doi:10.3389/fimmu.2021.737964

32. Yeung WCG, Rawlinson WD, Craig ME. Enterovirus infection and type 1 diabetes mellitus: systematic review and meta-analysis of observational molecular studies. *BMJ*. 2011;342:d35. doi:10.1136/bmj.d35

33. Bonifacio E, Pflüger M, Marienfeld S, Winkler C, Hummel M, Ziegler AG. Maternal type 1 diabetes reduces the risk of islet autoantibodies: relationships with birthweight and maternal HbA(1c). *Diabetologia*. 2008;51(7):1245-1252. doi:10.1007/s00125-008-1022-z

34. Warram JH, Krolewski AS, Gottlieb MS, Kahn CR. Differences in risk of insulin-dependent diabetes in offspring of diabetic mothers and diabetic fathers. *N Engl J Med*. 1984;311(3):149-152. doi:10.1056/NEJM198407193110304

35. Familial risk of type I diabetes in European children. The Eurodiab Ace Study Group and The Eurodiab Ace Substudy 2 Study Group. *Diabetologia*. 1998;41(10):1151-1156. doi:10.1007/s001250051044

36. Harjutsalo V, Reunanen A, Tuomilehto J. Differential transmission of type 1 diabetes from diabetic fathers and mothers to their offspring. *Diabetes*. 2006;55(5):1517-1524. doi:10.2337/db05-1296

37. Turtinen M, Härkönen T, Parkkola A, Ilonen J, Knip M, Finnish Pediatric Diabetes Register. Characteristics of familial type 1 diabetes: effects of the relationship to the affected family member on phenotype and genotype at diagnosis. *Diabetologia*. 2019;62(11):2025-2039. doi:10.1007/s00125-019-4952-8

38. Pacaud D, Nucci AM, Cuthbertson D, et al. Association between family history, early growth and the risk of beta cell autoimmunity in children at risk for type 1 diabetes. *Diabetologia*. 2021;64(1):119-128. doi:10.1007/s00125-020-05287-1

39. Degnbol B, Green A. Diabetes mellitus among first- and second-degree relatives of early onset diabetics. *Ann Hum Genet*. 1978;42(1):25-47. doi:10.1111/j.1469-1809.1978.tb00929.x

40. Simpson NE. Heritabilities of liability to diabetes when sex and age at onset are considered. *Ann Hum Genet*. 1969;32(3):283-303. doi:10.1111/j.1469-1809.1969.tb00077.x

41. Wagener DK, Sacks JM, LaPorte RE, Macgregor JM. The Pittsburgh study of insulin-dependent diabetes mellitus. Risk for diabetes among relatives of IDDM. *Diabetes*. 1982;31(2):136-144. doi:10.2337/diab.31.2.136

42. Dahlquist G, Gustavsson KH, Holmgren G, et al. The incidence of diabetes mellitus in Swedish children 0-14 years of age. A prospective study 1977-1980. *Acta Paediatr Scand*. 1982;71(1):7-14. doi:10.1111/j.1651-2227.1982.tb09364.x

43. Waldhör T, Schober E, Rami B, Tuomilehto J. The prevalence of IDDM in the first degree relatives of children newly diagnosed with IDDM in Austria--a population-based study. Austrian Diabetes Incidence Study Group. *Exp Clin Endocrinol Diabetes*. 1999;107(5):323-327. doi:10.1055/s-0029-1212120

44. Colman PG, Steele C, Couper JJ, et al. Islet autoimmunity in infants with a Type I diabetic relative is common but is frequently restricted to one autoantibody. *Diabetologia*. 2000;43(2):203-209. doi:10.1007/s001250050030

45. Naserke HE, Bonifacio E, Ziegler AG. Prevalence, characteristics and diabetes risk associated with transient maternally acquired islet antibodies and persistent islet antibodies in offspring of parents with type 1 diabetes. *J Clin Endocrinol Metab*. 2001;86(10):4826-4833. doi:10.1210/jcem.86.10.7931

46. Hämäläinen AM, Savola K, Kulmala PK, et al. Disease-associated autoantibodies during pregnancy and at birth in families affected by type 1 diabetes. *Clin Exp Immunol*. 2001;126(2):230-235. doi:10.1046/j.1365-2249.2001.01676.x

47. Greeley SAW, Katsumata M, Yu L, et al. Elimination of maternally transmitted autoantibodies prevents diabetes in nonobese diabetic mice. *Nat Med*. 2002;8(4):399-402. doi:10.1038/nm0402-399

48. Koczwara K, Ziegler AG, Bonifacio E. Maternal immunity to insulin does not affect diabetes risk in progeny of non obese diabetic mice. *Clin Exp Immunol*. 2004;136(1):56-59. doi:10.1111/j.1365-2249.2004.02406.x

49. Patelarou E, Girvalaki C, Brokalaki H, Patelarou A, Androulaki Z, Vardavas C. Current evidence on the associations of breastfeeding, infant formula, and cow's milk introduction with type 1 diabetes mellitus: a systematic review. *Nutr Rev*. 2012;70(9):509-519. doi:10.1111/j.1753-4887.2012.00513.x

50. Lampousi AM, Carlsson S, Löfvenborg JE. Dietary factors and risk of islet autoimmunity and type 1 diabetes: a systematic review and meta-analysis. *EBioMedicine*. 2021;72:103633. doi:10.1016/j.ebiom.2021.103633

51. CDC. Type 1 Diabetes and Pregnancy. Centers for Disease Control and Prevention. Published March 30, 2021. Accessed September 12, 2022. https://www.cdc.gov/diabetes/library/features/type-1-and-pregnancy.html

52. Diabetes and Breastfeeding | ADA. Accessed September 12, 2022. https://diabetes.org/diabetes/gestational-diabetes/diabetes-breastfeeding

53. Breastfeeding and Diabetes - Type 1, Type 2 and Gestational diabetes | Australian Breastfeeding Association. Accessed September 12, 2022. https://www.breastfeeding.asn.au/resources/breastfeeding-and-diabetes-type-1-type-2-and-gestational-diabetes

54. Jamshidi P, Hasanzadeh S, Tahvildari A, et al. Is there any association between gut microbiota and type 1 diabetes? A systematic review. *Gut Pathog*. 2019;11:49. doi:10.1186/s13099-019-0332-7

55. Stewart CJ, Ajami NJ, O'Brien JL, et al. Temporal development of the gut microbiome in early childhood from the TEDDY study. *Nature*. 2018;562(7728):583-588. doi:10.1038/s41586-018-0617-x

56. de Goffau MC, Fuentes S, van den Bogert B, et al. Aberrant gut microbiota composition at the onset of type 1 diabetes in young children. *Diabetologia*. 2014;57(8):1569-1577. doi:10.1007/s00125-014-3274-0

57. Kostic AD, Gevers D, Siljander H, et al. The dynamics of the human infant gut microbiome in development and in progression toward type 1 diabetes. *Cell Host Microbe*. 2015;17(2):260-273. doi:10.1016/j.chom.2015.01.001

58. Maffeis C, Martina A, Corradi M, et al. Association between intestinal permeability and faecal microbiota composition in Italian children with beta cell autoimmunity at risk for type 1 diabetes. *Diabetes Metab Res Rev*. 2016;32(7):700-709. doi:10.1002/dmrr.2790

59. de Goffau MC, Luopajärvi K, Knip M, et al. Fecal microbiota composition differs between children with β-cell autoimmunity and those without. *Diabetes*. 2013;62(4):1238-1244. doi:10.2337/db12-0526

60. Brown CT, Davis-Richardson AG, Giongo A, et al. Gut microbiome metagenomics analysis suggests a functional model for the development of autoimmunity for type 1 diabetes. *PLoS One*. 2011;6(10):e25792. doi:10.1371/journal.pone.0025792

61. Huang J, Pearson JA, Peng J, et al. Gut microbial metabolites alter IgA immunity in type 1 diabetes. *JCI Insight*. 2020;5(10):e135718, 135718. doi:10.1172/jci.insight.135718

62. Sorini C, Cosorich I, Lo Conte M, et al. Loss of gut barrier integrity triggers activation of islet-reactive T cells and autoimmune diabetes. *Proc Natl Acad Sci U S A*. 2019;116(30):15140-15149. doi:10.1073/pnas.1814558116

63. Costa FRC, Françozo MCS, de Oliveira GG, et al. Gut microbiota translocation to the pancreatic lymph nodes triggers NOD2 activation and contributes to T1D onset. *J Exp Med*. 2016;213(7):1223-1239. doi:10.1084/jem.20150744

64. Vaarala O, Atkinson MA, Neu J. The "perfect storm" for type 1 diabetes: the complex interplay between intestinal microbiota, gut permeability, and mucosal immunity. *Diabetes*. 2008;57(10):2555-2562. doi:10.2337/db08-0331

65. Mønsted MØ, Falck ND, Pedersen K, Buschard K, Holm LJ, Haupt-Jorgensen M. Intestinal permeability in type 1 diabetes: An updated comprehensive overview. *J Autoimmun*. 2021;122:102674. doi:10.1016/j.jaut.2021.102674

66. Pietrzak B, Tomela K, Olejnik-Schmidt A, Mackiewicz A, Schmidt M. Secretory IgA in Intestinal Mucosal Secretions as an Adaptive Barrier against Microbial Cells. *Int J Mol Sci*. 2020;21(23):9254. doi:10.3390/ijms21239254

67. Macpherson AJ, McCoy KD, Johansen FE, Brandtzaeg P. The immune geography of IgA induction and function. *Mucosal Immunol*. 2008;1(1):11-22. doi:10.1038/mi.2007.6

68. Sonoda E, Hitoshi Y, Yamaguchi N, et al. Differential regulation of IgA production by TGF-beta and IL-5: TGF-beta induces surface IgA-positive cells bearing IL-5 receptor, whereas IL-5 promotes their survival and maturation into IgA-secreting cells. *Cell Immunol*. 1992;140(1):158-172. doi:10.1016/0008-8749(92)90184-q

69. Mora JR, Iwata M, Eksteen B, et al. Generation of gut-homing IgA-secreting B cells by intestinal dendritic cells. *Science*. 2006;314(5802):1157-1160. doi:10.1126/science.1132742

70. Macpherson AJ, Gatto D, Sainsbury E, Harriman GR, Hengartner H, Zinkernagel RM. A primitive T cell-independent mechanism of intestinal mucosal IgA responses to commensal bacteria. *Science*. 2000;288(5474):2222-2226. doi:10.1126/science.288.5474.2222

71. Stoel M, Jiang HQ, van Diemen CC, et al. Restricted IgA repertoire in both B-1 and B-2 cell-derived gut plasmablasts. *J Immunol*. 2005;174(2):1046-1054. doi:10.4049/jimmunol.174.2.1046

72. Pabst O, Slack E. IgA and the intestinal microbiota: the importance of being specific. *Mucosal Immunol*. 2020;13(1):12-21. doi:10.1038/s41385-019-0227-4

73. Vergani S, Muleta KG, Da Silva C, et al. A self-sustaining layer of early-life-origin B cells drives steady-state IgA responses in the adult gut. *Immunity*. 2022;55(10):1829-1842.e6. doi:10.1016/j.immuni.2022.08.018

74. Paun A, Yau C, Meshkibaf S, et al. Association of HLA-dependent islet autoimmunity with systemic antibody responses to intestinal commensal bacteria in children. *Science Immunology*. 2019;4(32):eaau8125. doi:10.1126/sciimmunol.aau8125

75. Yazdani R, Azizi G, Abolhassani H, Aghamohammadi A. Selective IgA Deficiency: Epidemiology, Pathogenesis, Clinical Phenotype, Diagnosis, Prognosis and Management. *Scand J Immunol*. 2017;85(1):3-12. doi:10.1111/sji.12499

76. Simon AK, Hollander GA, McMichael A. Evolution of the immune system in humans from infancy to old age. *Proc Biol Sci*. 2015;282(1821):20143085. doi:10.1098/rspb.2014.3085

77. Gonzalez CA, Gonzalez S. Fetal and neonatal allo-immune response. *Transfus Apher Sci*. 2020;59(5):102945. doi:10.1016/j.transci.2020.102945

78. Rackaityte E, Halkias J. Mechanisms of Fetal T Cell Tolerance and Immune Regulation. *Front Immunol*. 2020;11:588. doi:10.3389/fimmu.2020.00588

79. Al Nabhani Z, Dulauroy S, Marques R, et al. A Weaning Reaction to Microbiota Is Required for Resistance to Immunopathologies in the Adult. *Immunity*. 2019;50(5):1276-1288.e5. doi:10.1016/j.immuni.2019.02.014

80. El Aidy S, van Baarlen P, Derrien M, et al. Temporal and spatial interplay of microbiota and intestinal mucosa drive establishment of immune homeostasis in conventionalized mice. *Mucosal Immunol*. 2012;5(5):567-579. doi:10.1038/mi.2012.32

81. Knoop KA, Gustafsson JK, McDonald KG, et al. Microbial Antigen Encounter During a Pre-weaning Interval is Critical for Tolerance to Gut Bacteria. *Sci Immunol*. 2017;2(18):eaao1314. doi:10.1126/sciimmunol.aao1314

82. Nolan LS, Parks OB, Good M. A Review of the Immunomodulating Components of Maternal Breast Milk and Protection Against Necrotizing Enterocolitis. *Nutrients*. 2019;12(1):E14. doi:10.3390/nu12010014

83. Ballard O, Morrow AL. Human milk composition: nutrients and bioactive factors. *Pediatr Clin North Am*. 2013;60(1):49-74. doi:10.1016/j.pcl.2012.10.002

84. Toscano M, De Grandi R, Grossi E, Drago L. Role of the Human Breast Milk-Associated Microbiota on the Newborns' Immune System: A Mini Review. *Front Microbiol*. 2017;8:2100. doi:10.3389/fmicb.2017.02100

85. Fink LN, Metzdorff SB, Zeuthen LH, et al. Establishment of tolerance to commensal bacteria requires a complex microbiota and is accompanied by decreased intestinal chemokine expression. *Am J Physiol Gastrointest Liver Physiol*. 2012;302(1):G55-65. doi:10.1152/ajpgi.00428.2010

86. Gomez de Agüero M, Ganal-Vonarburg SC, Fuhrer T, et al. The maternal microbiota drives early postnatal innate immune development. *Science*. 2016;351(6279):1296-1302. doi:10.1126/science.aad2571

87. Li H, Limenitakis JP, Greiff V, et al. Mucosal or systemic microbiota exposures shape the B cell repertoire. *Nature*. 2020;584(7820):274-278. doi:10.1038/s41586-020-2564-6

88. Zegarra-Ruiz DF, Kim DV, Norwood K, et al. Thymic development of gut-microbiota-specific T cells. *Nature*. 2021;594(7863):413-417. doi:10.1038/s41586-021-03531-1

89. Cebula A, Seweryn M, Rempala GA, et al. Thymus-derived regulatory T cells contribute to tolerance to commensal microbiota. *Nature*. 2013;497(7448):258-262. doi:10.1038/nature12079

90. Wood H, Acharjee A, Pearce H, et al. Breastfeeding promotes early neonatal regulatory T-cell expansion and immune tolerance of non-inherited maternal antigens. *Allergy*. 2021;76(8):2447-2460. doi:10.1111/all.14736

91. Yu JC, Khodadadi H, Malik A, et al. Innate Immunity of Neonates and Infants. *Front Immunol*. 2018;9:1759. doi:10.3389/fimmu.2018.01759

92. Sefik E, Geva-Zatorsky N, Oh S, et al. Individual intestinal symbionts induce a distinct population of RORγ+ regulatory T cells. *Science*. 2015;349(6251):993-997. doi:10.1126/science.aaa9420

93. Zhang X, Borbet TC, Fallegger A, Wipperman MF, Blaser MJ, Müller A. An Antibiotic-Impacted Microbiota Compromises the Development of Colonic Regulatory T Cells and Predisposes to Dysregulated Immune Responses. *mBio*. 2021;12(1):e03335-20. doi:10.1128/mBio.03335-20

94. Strachan E, Clemente-Casares X, Tsai S. Maternal provisions in type 1 diabetes: Evidence for both protective & pathogenic potential. *Frontiers in Immunology*. 2023;14. Accessed March 29, 2023. https://www.frontiersin.org/articles/10.3389/fimmu.2023.1146082

95. Perez-Muñoz ME, Arrieta MC, Ramer-Tait AE, Walter J. A critical assessment of the "sterile womb" and "in utero colonization" hypotheses: implications for research on the pioneer infant microbiome. *Microbiome*. 2017;5(1):48. doi:10.1186/s40168-017-0268-4

96. Azad MB, Konya T, Maughan H, et al. Gut microbiota of healthy Canadian infants: profiles by mode of delivery and infant diet at 4 months. *CMAJ*. 2013;185(5):385-394. doi:10.1503/cmaj.121189

97. Montoya-Williams D, Lemas DJ, Spiryda L, et al. The Neonatal Microbiome and Its Partial Role in Mediating the Association between Birth by Cesarean Section and Adverse Pediatric Outcomes. *Neonatology*. 2018;114(2):103-111. doi:10.1159/000487102

98. Daft JG, Ptacek T, Kumar R, Morrow C, Lorenz RG. Cross-fostering immediately after birth induces a permanent microbiota shift that is shaped by the nursing mother. *Microbiome*. 2015;3:17. doi:10.1186/s40168-015-0080-y

99. Fehr K, Moossavi S, Sbihi H, et al. Breastmilk Feeding Practices Are Associated with the Co-Occurrence of Bacteria in Mothers' Milk and the Infant Gut: the CHILD Cohort Study. *Cell Host Microbe*. 2020;28(2):285-297.e4. doi:10.1016/j.chom.2020.06.009

100. Lackey KA, Williams JE, Meehan CL, et al. What's Normal? Microbiomes in Human Milk and Infant Feces Are Related to Each Other but Vary Geographically: The INSPIRE Study. *Front Nutr*. 2019;6:45. doi:10.3389/fnut.2019.00045

101. Solís G, de Los Reyes-Gavilan CG, Fernández N, Margolles A, Gueimonde M. Establishment and development of lactic acid bacteria and bifidobacteria microbiota in breast-milk and the infant gut. *Anaerobe*. 2010;16(3):307-310. doi:10.1016/j.anaerobe.2010.02.004

102. Muñoz JAM, Chenoll E, Casinos B, et al. Novel probiotic Bifidobacterium longum subsp. infantis CECT 7210 strain active against rotavirus infections. *Appl Environ Microbiol*. 2011;77(24):8775-8783. doi:10.1128/AEM.05548-11

103. Beghetti I, Panizza D, Lenzi J, et al. Probiotics for Preventing Necrotizing Enterocolitis in Preterm Infants: A Network Meta-Analysis. *Nutrients*. 2021;13(1):192. doi:10.3390/nu13010192

104. Sonnenburg JL, Chen CTL, Gordon JI. Genomic and metabolic studies of the impact of probiotics on a model gut symbiont and host. *PLoS Biol*. 2006;4(12):e413. doi:10.1371/journal.pbio.0040413

105. Moens F, Verce M, De Vuyst L. Lactate- and acetate-based cross-feeding interactions between selected strains of lactobacilli, bifidobacteria and colon bacteria in the presence of inulin-type fructans. *Int J Food Microbiol*. 2017;241:225-236. doi:10.1016/j.ijfoodmicro.2016.10.019

106. Hidalgo-Cantabrana C, Delgado S, Ruiz L, Ruas-Madiedo P, Sánchez B, Margolles A. Bifidobacteria and Their Health-Promoting Effects. *Microbiol Spectr*. 2017;5(3). doi:10.1128/microbiolspec.BAD-0010-2016

107. Thananimit S, Pahumunto N, Teanpaisan R. Characterization of Short Chain Fatty Acids Produced by Selected Potential Probiotic Lactobacillus Strains. *Biomolecules*. 2022;12(12):1829. doi:10.3390/biom12121829

108. Tamburini S, Shen N, Wu HC, Clemente JC. The microbiome in early life: implications for health outcomes. *Nat Med*. 2016;22(7):713-722. doi:10.1038/nm.4142

109. Harbison JE, Roth-Schulze AJ, Giles LC, et al. Gut microbiome dysbiosis and increased intestinal permeability in children with islet autoimmunity and type 1 diabetes: A prospective cohort study. *Pediatr Diabetes*. 2019;20(5):574-583. doi:10.1111/pedi.12865

110. Zhao G, Vatanen T, Droit L, et al. Intestinal virome changes precede autoimmunity in type I diabetes-susceptible children. *Proc Natl Acad Sci U S A*. 2017;114(30):E6166-E6175. doi:10.1073/pnas.1706359114

111. van Heck JIP, Gacesa R, Stienstra R, et al. The Gut Microbiome Composition Is Altered in Long-standing Type 1 Diabetes and Associates With Glycemic Control and Disease-Related Complications. *Diabetes Care*. 2022;45(9):2084-2094. doi:10.2337/dc21-2225

112. Vatanen T, Franzosa EA, Schwager R, et al. The human gut microbiome in early-onset type 1 diabetes from the TEDDY study. *Nature*. 2018;562(7728):589-594. doi:10.1038/s41586-018-0620-2

113. Maruyama K, Hida M, Kohgo T, Fukunaga Y. Changes in salivary and fecal secretory IgA in infants under different feeding regimens. *Pediatr Int*. 2009;51(3):342-345. doi:10.1111/j.1442-200X.2008.02748.x

114. Bridgman SL, Konya T, Azad MB, et al. Infant gut immunity: a preliminary study of IgA associations with breastfeeding. *J Dev Orig Health Dis*. 2016;7(1):68-72. doi:10.1017/S2040174415007862

115. Zheng W, Zhao W, Wu M, et al. Microbiota-targeted maternal antibodies protect neonates from enteric infection. *Nature*. 2020;577(7791):543-548. doi:10.1038/s41586-019-1898-4

116. Caballero-Flores G, Sakamoto K, Zeng MY, et al. Maternal Immunization Confers Protection to the Offspring against an Attaching and Effacing Pathogen through Delivery of IgG in Breast Milk. *Cell Host Microbe*. 2019;25(2):313-323.e4. doi:10.1016/j.chom.2018.12.015

117. Rogier EW, Frantz AL, Bruno MEC, Kaetzel CS. Secretory IgA is Concentrated in the Outer Layer of Colonic Mucus along with Gut Bacteria. *Pathogens*. 2014;3(2):390-403. doi:10.3390/pathogens3020390

118. Torow N, Yu K, Hassani K, et al. Active suppression of intestinal CD4(+)TCRαβ(+) T-lymphocyte maturation during the postnatal period. *Nat Commun*. 2015;6:7725. doi:10.1038/ncomms8725

119. Koch MA, Reiner GL, Lugo KA, et al. Maternal IgG and IgA Antibodies Dampen Mucosal T Helper Cell Responses in Early Life. *Cell*. 2016;165(4):827-841. doi:10.1016/j.cell.2016.04.055

120. França EL, Morceli G, Fagundes DLG, Rudge MVC, Calderon IDMP, Honorio-França AC. Secretory IgA-Fcα receptor interaction modulating phagocytosis and microbicidal activity by phagocytes in human colostrum of diabetics. *APMIS*. 2011;119(10):710-719. doi:10.1111/j.1600-0463.2011.02789.x

121. Monteiro RC, Van De Winkel JGJ. IgA Fc receptors. *Annu Rev Immunol*. 2003;21:177-204. doi:10.1146/annurev.immunol.21.120601.141011

122. Bentley JP, Simpson JM, Bowen JR, Morris JM, Roberts CL, Nassar N. Gestational age, mode of birth and breastmilk feeding all influence acute early childhood gastroenteritis: a record-linkage cohort study. *BMC Pediatr*. 2016;16:55. doi:10.1186/s12887-016-0591-0

123. Le Doare K, Bellis K, Faal A, et al. SIgA, TGF-β1, IL-10, and TNFα in Colostrum Are Associated with Infant Group B Streptococcus Colonization. *Front Immunol*. 2017;8:1269. doi:10.3389/fimmu.2017.01269

124. Ahouse JJ, Hagerman CL, Mittal P, et al. Mouse MHC class I-like Fc receptor encoded outside the MHC. *J Immunol*. 1993;151(11):6076-6088.

125. Latvala S, Jacobsen B, Otteneder MB, Herrmann A, Kronenberg S. Distribution of FcRn Across Species and Tissues. *J Histochem Cytochem*. 2017;65(6):321-333. doi:10.1369/0022155417705095

126. Appleby P, Catty D. Transmission of immunoglobulin to foetal and neonatal mice. *J Reprod Immunol*. 1983;5(4):203-213. doi:10.1016/0165-0378(83)90236-x

127. Kristoffersen EK, Matre R. Co-localization of the neonatal Fc gamma receptor and IgG in human placental term syncytiotrophoblasts. *Eur J Immunol*. 1996;26(7):1668-1671. doi:10.1002/eji.1830260741

128. Leach JL, Sedmak DD, Osborne JM, Rahill B, Lairmore MD, Anderson CL. Isolation from human placenta of the IgG transporter, FcRn, and localization to the syncytiotrophoblast: implications for maternal-fetal antibody transport. *J Immunol*. 1996;157(8):3317-3322.

129. Antohe F, Rădulescu L, Gafencu A, Gheţie V, Simionescu M. Expression of functionally active FcRn and the differentiated bidirectional transport of IgG in human placental endothelial cells. *Hum Immunol*. 2001;62(2):93-105. doi:10.1016/s0198-8859(00)00244-5

130. Kiskova T, Mytsko Y, Schepelmann M, et al. Expression of the neonatal Fc-receptor in placental-fetal endothelium and in cells of the placental immune system. *Placenta*. 2019;78:36-43. doi:10.1016/j.placenta.2019.02.012

131. Simister NE, Story C, Chen H, Hunt H. An IgG-transporting Fc receptor expressed in the syncytiotrophoblast of human placenta. *European journal of immunology*. 1996;26(7). doi:10.1002/eji.1830260718

132. Kohler PF, Farr RS. Elevation of cord over maternal IgG immunoglobulin: evidence for an active placental IgG transport. *Nature*. 1966;210(5040):1070-1071. doi:10.1038/2101070a0

133. Malek A, Sager R, Schneider H. Maternal-fetal transport of immunoglobulin G and its subclasses during the third trimester of human pregnancy. *Am J Reprod Immunol*. 1994;32(1):8-14. doi:10.1111/j.1600-0897.1994.tb00873.x

134. Malek A, Sager R, Kuhn P, Nicolaides KH, Schneider H. Evolution of maternofetal transport of immunoglobulins during human pregnancy. *Am J Reprod Immunol*. 1996;36(5):248-255. doi:10.1111/j.1600-0897.1996.tb00172.x

135. Montoyo HP, Vaccaro C, Hafner M, Ober RJ, Mueller W, Ward ES. Conditional deletion of the MHC class I-related receptor FcRn reveals the sites of IgG homeostasis in mice. *Proc Natl Acad Sci U S A*. 2009;106(8):2788-2793. doi:10.1073/pnas.0810796106

136. Zhu X, Meng G, Dickinson BL, et al. MHC class I-related neonatal Fc receptor for IgG is functionally expressed in monocytes, intestinal macrophages, and dendritic cells. *J Immunol*. 2001;166(5):3266-3276. doi:10.4049/jimmunol.166.5.3266

137. Vidarsson G, Stemerding AM, Stapleton NM, et al. FcRn: an IgG receptor on phagocytes with a novel role in phagocytosis. *Blood*. 2006;108(10):3573-3579. doi:10.1182/blood-2006-05-024539

138. Mimoun A, Delignat S, Peyron I, et al. Relevance of the Materno-Fetal Interface for the Induction of Antigen-Specific Immune Tolerance. *Front Immunol*. 2020;11:810. doi:10.3389/fimmu.2020.00810

139. Giacoia GP. Transplacentally transmitted autoimmune disorders of the fetus and newborn: pathogenic considerations. *South Med J*. 1992;85(2):139-145. doi:10.1097/00007611-199202000-00006

140. Ohsaki A, Venturelli N, Buccigrosso TM, et al. Maternal IgG immune complexes induce food allergen-specific tolerance in offspring. *J Exp Med*. 2018;215(1):91-113. doi:10.1084/jem.20171163

141. Polte T, Hansen G. Maternal tolerance achieved during pregnancy is transferred to the offspring via breast milk and persistently protects the offspring from allergic asthma. *Clin Exp Allergy*. 2008;38(12):1950-1958. doi:10.1111/j.1365-2222.2008.03096.x

142. Mosconi E, Rekima A, Seitz-Polski B, et al. Breast milk immune complexes are potent inducers of oral tolerance in neonates and prevent asthma development. *Mucosal Immunol*. 2010;3(5):461-474. doi:10.1038/mi.2010.23

143. Usami K, Niimi K, Matsuo A, et al. The gut microbiota induces Peyer's-patch-dependent secretion of maternal IgA into milk. *Cell Rep*. 2021;36(10):109655. doi:10.1016/j.celrep.2021.109655

144. Bulek AM, Cole DK, Skowera A, et al. Structural basis for the killing of human beta cells by CD8(+) T cells in type 1 diabetes. *Nat Immunol*. 2012;13(3):283-289. doi:10.1038/ni.2206

145. Qiao YC, Shen J, Hong XZ, et al. Changes of regulatory T cells, transforming growth factor-beta and interleukin-10 in patients with type 1 diabetes mellitus: A systematic review and meta-analysis. *Clin Immunol*. 2016;170:61-69. doi:10.1016/j.clim.2016.08.004

146. Grupillo M, Gualtierotti G, He J, et al. Essential roles of insulin expression in Aire+ tolerogenic dendritic cells in maintaining peripheral self-tolerance of islet β-cells. *Cell Immunol*. 2012;273(2):115-123. doi:10.1016/j.cellimm.2011.12.010

147. Gardner JM, Devoss JJ, Friedman RS, et al. Deletional tolerance mediated by extrathymic Aire-expressing cells. *Science*. 2008;321(5890):843-847. doi:10.1126/science.1159407

148. Kodama K, Butte AJ, Creusot RJ, et al. Tissue- and age-specific changes in gene expression during disease induction and progression in NOD mice. *Clin Immunol*. 2008;129(2):195-201. doi:10.1016/j.clim.2008.07.028

149. Ylipaasto P, Klingel K, Lindberg AM, et al. Enterovirus infection in human pancreatic islet cells, islet tropism in vivo and receptor involvement in cultured islet beta cells. *Diabetologia*. 2004;47(2):225-239. doi:10.1007/s00125-003-1297-z

150. Piganelli JD, Mamula MJ, James EA. The Role of β Cell Stress and Neo-Epitopes in the Immunopathology of Type 1 Diabetes. *Front Endocrinol (Lausanne)*. 2020;11:624590. doi:10.3389/fendo.2020.624590

151. Jalonen T, Isolauri E, Heyman M, Crain-Denoyelle AM, Sillanaukee P, Koivula T. Increased beta-lactoglobulin absorption during rotavirus enteritis in infants: relationship to sugar permeability. *Pediatr Res*. 1991;30(3):290-293. doi:10.1203/00006450-199109000-00019

152. Härkönen T, Paananen A, Lankinen H, Hovi T, Vaarala O, Roivainen M. Enterovirus infection may induce humoral immune response reacting with islet cell autoantigens in humans. *J Med Virol*. 2003;69(3):426-440. doi:10.1002/jmv.10306

153. Honeyman MC, Stone NL, Falk BA, Nepom G, Harrison LC. Evidence for molecular mimicry between human T cell epitopes in rotavirus and pancreatic islet autoantigens. *J Immunol*. 2010;184(4):2204-2210. doi:10.4049/jimmunol.0900709

154. Tan J, McKenzie C, Potamitis M, Thorburn AN, Mackay CR, Macia L. The role of short-chain fatty acids in health and disease. *Adv Immunol*. 2014;121:91-119. doi:10.1016/B978-0-12-800100-4.00003-9

155. Hänninen A, Toivonen R, Pöysti S, et al. Akkermansia muciniphila induces gut microbiota remodelling and controls islet autoimmunity in NOD mice. *Gut*. 2018;67(8):1445-1453. doi:10.1136/gutjnl-2017-314508

156. Markle JGM, Frank DN, Mortin-Toth S, et al. Sex differences in the gut microbiome drive hormone-dependent regulation of autoimmunity. *Science*. 2013;339(6123):1084-1088. doi:10.1126/science.1233521

157. de Groot P, Nikolic T, Pellegrini S, et al. Faecal microbiota transplantation halts progression of human new-onset type 1 diabetes in a randomised controlled trial. *Gut*. 2021;70(1):92-105. doi:10.1136/gutjnl-2020-322630

158. Oksana Boyarchuk, Lesya Dobrovolska, Halyna Svystunovych. Selective immunoglobulin A deficiency in children with diabetes mellitus: Data from a medical center in Ukraine. *PLoS ONE*. 2022;17(11):e0277273-e0277273. doi:10.1371/journal.pone.0277273

159. Elsayed HM, Ali FHA, Sheha DS, Ibrahim NA, Sharawy YS, Kamal ST. Prevalence of Selective IgA Deficiency in a Sample of Egyptian Patients with Type1 Diabetes Mellitus. *Egyptian Journal of Hospital Medicine*. 2022;86:17-21.

160. Greco D, Maggio F. Selective Immunoglobulin A Deficiency in Type 1 Diabetes Mellitus: A Prevalence Study in Western Sicily (Italy). *Diabetes Metab J*. 2015;39(2):132-136. doi:10.4093/dmj.2015.39.2.132

161. Lo Conte M, Cosorich I, Ferrarese R, et al. Alterations of the intestinal mucus layer correlate with dysbiosis and immune dysregulation in human Type 1 Diabetes. *EBioMedicine*. 2023;91:104567. doi:10.1016/j.ebiom.2023.104567

162. Miranda MCG, Oliveira RP, Torres L, et al. Frontline Science: Abnormalities in the gut mucosa of non-obese diabetic mice precede the onset of type 1 diabetes. *J Leukoc Biol*. 2019;106(3):513-529. doi:10.1002/JLB.3HI0119-024RR

163. Zhang J, van Oostrom D, Li J, Savelkoul HFJ. Innate Mechanisms in Selective IgA Deficiency. *Front Immunol*. 2021;12:649112. doi:10.3389/fimmu.2021.649112

164. Nagaishi T, Watabe T, Kotake K, et al. Immunoglobulin A-specific deficiency induces spontaneous inflammation specifically in the ileum. *Gut*. 2022;71(3):487-496. doi:10.1136/gutjnl-2020-322873

165. Hu J, Nomura Y, Bashir A, et al. Diversified microbiota of meconium is affected by maternal diabetes status. *PLoS One*. 2013;8(11):e78257. doi:10.1371/journal.pone.0078257

166. Wang J, Zheng J, Shi W, et al. Dysbiosis of maternal and neonatal microbiota associated with gestational diabetes mellitus. *Gut*. 2018;67(9):1614-1625. doi:10.1136/gutjnl-2018-315988

167. Su M, Nie Y, Shao R, et al. Diversified gut microbiota in newborns of mothers with gestational diabetes mellitus. *PLoS One*. 2018;13(10):e0205695. doi:10.1371/journal.pone.0205695

168. Zhao C, Ge J, Li X, et al. Integrated metabolome analysis reveals novel connections between maternal fecal metabolome and the neonatal blood metabolome in women with gestational diabetes mellitus. *Sci Rep*. 2020;10(1):3660. doi:10.1038/s41598-020-60540-2

169. Harriman GR, Bogue M, Rogers P, et al. Targeted Deletion of the IgA Constant Region in Mice Leads to IgA Deficiency with Alterations in Expression of Other Ig Isotypes1. *The Journal of Immunology*. 1999;162(5):2521-2529. doi:10.4049/jimmunol.162.5.2521

170. McCoy KD, Geuking MB, Ronchi F. Gut Microbiome Standardization in Control and Experimental Mice. *Curr Protoc Immunol*. 2017;117:23.1.1-23.1.13. doi:10.1002/cpim.25

171. Hartmann PE, Cregan MD, Mitoulas LR. Maternal modulation of specific and non-specific immune components of colostrum and mature milk. *Adv Nutr Res*. 2001;10:365-387. doi:10.1007/978-1-4615-0661-4_18

172. França EL, Calderon I de MP, Vieira EL, Morceli G, Honorio-França AC. Transfer of maternal immunity to newborns of diabetic mothers. *Clin Dev Immunol*. 2012;2012:928187. doi:10.1155/2012/928187

173. Chakraborty S, Kaur S, Guha S, Batra SK. The multifaceted roles of neutrophil gelatinase associated lipocalin (NGAL) in inflammation and cancer. *Biochim Biophys Acta*. 2012;1826(1):129-169. doi:10.1016/j.bbcan.2012.03.008

174. Rojas OL, Pröbstel AK, Porfilio EA, et al. Recirculating Intestinal IgA-Producing Cells Regulate Neuroinflammation via IL-10. *Cell*. 2019;176(3):610-624.e18. doi:10.1016/j.cell.2018.11.035

175. Oliphant K, Allen-Vercoe E. Macronutrient metabolism by the human gut microbiome: major fermentation by-products and their impact on host health. *Microbiome*. 2019;7:91. doi:10.1186/s40168-019-0704-8

176. Verbeke KA, Boobis AR, Chiodini A, et al. Towards microbial fermentation metabolites as markers for health benefits of prebiotics. *Nutr Res Rev*. 2015;28(1):42-66. doi:10.1017/S0954422415000037

177. Ducker GS, Rabinowitz JD. One-Carbon Metabolism in Health and Disease. *Cell Metab*. 2017;25(1):27-42. doi:10.1016/j.cmet.2016.08.009

178. Garcia-Hernandez V, Quiros M, Nusrat A. Intestinal epithelial claudins: expression and regulation in homeostasis and inflammation. *Ann N Y Acad Sci*. 2017;1397(1):66-79. doi:10.1111/nyas.13360

179. Camilleri M. Leaky gut: mechanisms, measurement and clinical implications in humans. *Gut*. 2019;68(8):1516-1526. doi:10.1136/gutjnl-2019-318427

180. Gustafsson JK, Navabi N, Rodriguez-Piñeiro AM, et al. Dynamic changes in mucus thickness and ion secretion during Citrobacter rodentium infection and clearance. *PLoS One*. 2013;8(12):e84430. doi:10.1371/journal.pone.0084430

181. Oderda G, D'Alessandro M, Mariani P, et al. Prostaglandin E2 in gastric mucosa of children with Helicobacter pylori gastritis: relation to thickness of mucus gel layer. *J Clin Pathol*. 1993;46(9):836-839. doi:10.1136/jcp.46.9.836

182. Pullan RD, Thomas GA, Rhodes M, et al. Thickness of adherent mucus gel on colonic mucosa in humans and its relevance to colitis. *Gut*. 1994;35(3):353-359. doi:10.1136/gut.35.3.353

183. Gehart H, Clevers H. Tales from the crypt: new insights into intestinal stem cells. *Nat Rev Gastroenterol Hepatol*. 2019;16(1):19-34. doi:10.1038/s41575-018-0081-y

184. Ben-Nissan G, Katzir N, Füzesi-Levi MG, Sharon M. Biology of the Extracellular Proteasome. *Biomolecules*. 2022;12(5):619. doi:10.3390/biom12050619

185. Culina S, Gupta N, Boisgard R, et al. Materno-Fetal Transfer of Preproinsulin Through the Neonatal Fc Receptor Prevents Autoimmune Diabetes. *Diabetes*. 2015;64(10):3532-3542. doi:10.2337/db15-0024

186. Liu X, Ye L, Christianson GJ, Yang JQ, Roopenian DC, Zhu X. NF-kappaB signaling regulates functional expression of the MHC class I-related neonatal Fc receptor for IgG via intronic binding sequences. *J Immunol*. 2007;179(5):2999-3011. doi:10.4049/jimmunol.179.5.2999

187. Liu X, Ye L, Bai Y, Mojidi H, Simister NE, Zhu X. Activation of the JAK/STAT-1 signaling pathway by IFN-gamma can down-regulate functional expression of the MHC class I-related neonatal Fc receptor for IgG. *J Immunol*. 2008;181(1):449-463. doi:10.4049/jimmunol.181.1.449

188. Qian S, Li C, Liu X, Jia X, Xiao Y, Li Z. Activation of the JNK/MAPK Signaling Pathway by TGF-β1 Enhances Neonatal Fc Receptor Expression and IgG Transcytosis. *Microorganisms*. 2021;9(4):879. doi:10.3390/microorganisms9040879

189. Paone P, Cani PD. Mucus barrier, mucins and gut microbiota: the expected slimy partners? *Gut*. 2020;69(12):2232-2243. doi:10.1136/gutjnl-2020-322260

190. Wen L, Ley RE, Volchkov PY, et al. Innate immunity and intestinal microbiota in the development of Type 1 diabetes. *Nature*. 2008;455(7216):1109-1113. doi:10.1038/nature07336

191. Ubeda C, Lipuma L, Gobourne A, et al. Familial transmission rather than defective innate immunity shapes the distinct intestinal microbiota of TLR-deficient mice. *J Exp Med*. 2012;209(8):1445-1456. doi:10.1084/jem.20120504

192. Toyonaga T, Matsuura M, Mori K, et al. Lipocalin 2 prevents intestinal inflammation by enhancing phagocytic bacterial clearance in macrophages. *Sci Rep*. 2016;6:35014. doi:10.1038/srep35014

193. Debray R, Herbert RA, Jaffe AL, Crits-Christoph A, Power ME, Koskella B. Priority effects in microbiome assembly. *Nat Rev Microbiol*. 2022;20(2):109-121. doi:10.1038/s41579-021-00604-w